University College Cork, Ireland
Coláiste na hOllscoile Corcaigh

Energy Engineering
School of Engineering
& Environmental Research Institute
University College Cork

Integrated Biogas Systems

Markus Voelklein MSc

Thesis submitted for the degree of Doctor of Philosophy to the National University of Ireland, Cork

Supervisors: Professor Jerry Murphy & Dr. Paul Leahy

Head of School: Professor Liam Marnane

June 2019

Once delicious food,
then just refuse(d).
Left over and waste(d),
digested to gases.
Ingenious like Boole,
reborn as fuel.

Circle of biogas

Table of contents

Declaration

I hereby declare that this thesis is my own work and effort and that it has not been submitted anywhere for any award. Only the sources cited have been used in this draft.

Signature: *Markus Völklein*

Date: 24th June 2019

List of figures

List of tables

Acknowledgements

The past few years in Ireland have been a refreshing and fulfilling experience, reshaping both my academic and personal life. A change I fully embrace! An exploration and opportunity beyond measure.

First, I would like to thank my supervisor, Professor Jerry D. Murphy, for giving me this unique and fruitful opportunity. I am incredibly grateful to have benefitted from his guidance. The genuine support and encouragement he has given me throughout the course of my research was inspiring! His sharing of excitement about science and my research induced motivation to bring this doctoral journey to completion.

I would like to express my gratitude to my co-supervisor Dr. Paul Leahy for his supervision and counsel.

None of this work would have been possible without the Marie-Curie Initial Training Network funding my research and allowing me the opportunity to undertake this fellowship as part of ATBEST (Advanced Technologies for Biogas Efficiency, Sustainability and Transport). The collaboration within an international group of fellows all among Europe has added unique value to my doctoral program. A place for priceless scientific, personal and cultural exchange.

I would like to thank Professor Sarah Culloty, director of the Environmental Research Institute for providing the facilities to conduct this research and Science Foundation Ireland for co-funding my work through the MaREI centre.

A great thank to my colleagues and friends in the Bioenergy Research Group Magdalena, Amita, Richie, Christiane, Davis, Enrique, Truc, David, Aoife, Shane, Chen, Richen and Karthik for shared discussions, support and great company. Special thanks to my friend Alesia for sharing tea breaks and spreading enthusiasm.

Thanks to my friends and fellows from the Marie Curie ATBEST fellowship for sharing knowledge, travel, joy and PhD trouble. In particular Nikoletta, Paz and Himanshu for making this fellowship a time to remember.

On a more personal note I am deeply grateful to my parents and my brothers for making this journey at all possible.

A journey to be continued. It took longer than anticipated, it took time to grow.

Abstract

An integrated biogas system is a synergistic cycle of processes sustainably recovering energy and nutrients by anaerobic digestion systems. It is a value adding sequence managing waste and biomass with a final gaseous by-product biogas or biomethane (a natural gas substitute). This thesis explored its core process, technology and strategies of biogas production and upgrading to biomethane.

Various studies of this thesis highlight pathways to conduct and optimise anaerobic digestion at intensified conditions while improving reactor utilisation. An increase in substrate throughput and loading was attained by a pre-treating first stage hydrolysis reactor. The solubilisation of substrate provided upstream carbon dioxide segregation and high quantities of readily available liquid fermentation products. A downstream digester increased methane yields and enriched the methane content to levels of 71% of the biogas composition. Intensified conditions and mono-digestion of a single substrate such as food waste can exhibit deficiencies in essential nutrients and inhibition of methanogenic activity. Supplementation of undersupplied trace elements induced immediate recovery allowing stable digestion at loading rates as high as 5 g VS L^{-1} d^{-1} at mesophilic temperatures. An increase in temperature further improved degradation kinetics and stimulated higher biomethane yields at shorter substrate retention in grass digestion.

In an integrated biogas system, biogas may be upgraded in conjunction with in-situ and ex-situ biological methanation strategies. The addition of hydrogen revealed positive effects on the methanogenic process. Adverse effects of elevated dissolved hydrogen concentrations on acetogenesis became evident in-situ. A biomethane with methane concentrations in excess of 96% successfully demonstrated the potential for gas grid injection at methane formation rates of 3.7 L per litre reactor volume per day. An approach, supplying gases continuously into a sequential ex-situ reactor system and steadily displacing the upgraded biogas, confirmed similar methane formation yields. A hybrid model, where an in-situ grass digester is followed by an ex-situ reactor suggested an alternative approach to conventional biogas upgrading.

The contribution of this thesis is the successful demonstration of optimisation potential in novel and existing digestion systems. The employed biogas upgrading strategies proved to be efficient and suitable for gas grid injection.

Thesis output

Chapters published as papers or currently under review in peer-reviewed journals:

Chapter 3:

Voelklein, M. A., A. Jacob, R. O' Shea and J. D. Murphy (2016). Assessment of increasing loading rate on two-stage digestion of food waste. Bioresource Technology 202: 172-180. (published)

Chapter 4:

Voelklein, M. A., R. O' Shea, A. Jacob and J. D. Murphy (2017). Role of trace elements in single and two-stage digestion of food waste at high organic loading rates. Energy 121: 185-192. (published)

Chapter 5:

Voelklein, M. A., D. Rusmanis and J. D. Murphy (2016). Increased loading rates and specific methane yields facilitated by digesting grass silage at thermophilic rather than mesophilic temperatures. Bioresource Technology 216: 486-493. (published)

Chapter 6:

Voelklein, M. A., D. Rusmanis, J. D. Murphy (2018). Biological methanation: Strategies for in-situ and ex-situ upgrading in anaerobic digestion. Applied Energy. (in review)

Contribution to the papers

Chapter 3

I was the first author of the paper and principally responsible for the decision making in the approach of the study. I was responsible for the experimental design, undertaking of laboratory work and data analysis.

Chapter 4

I was the first author of the paper and was responsible for the planning, data collection, processing, and interpretation of the results.

Chapter 5

I was the first author of the paper. I proposed the study and was responsible for data collection. I carried out the assessment and interpretation of the results.

Chapter 6

I was the first author of the paper. I was responsible for the associated thought process, developing the reactor and experimental design. I operated the laboratory trials. I proposed and implemented upgrading strategies to facilitate biomethane production in lab scale. I analysed and interpreted the results.

Nomenclature

Δ	lag phase
AD	anaerobic digestion
ADF	acid detergent fibre
BIS	batch in-situ (reactor name in chapter 6)
BES	batch ex-situ (reactor name in chapter 6)
BMP	biomethane potential assay
BMP_{th}	theoretical maximum biomethane potential
Ca	calcium
CES	continuous ex-situ (reactor name in chapter 6)
c_G	gas concentrations in the headspace of a reactor
$c_{H_2,G}$	gaseous hydrogen concentration in the headspace of a reactor
$c_{H_2,L}$	dissolved hydrogen concentration in the liquid phase of a reactor
CH_4	methane gas
CHP	combined heat and power
c_L	dissolved gas concentrations in the liquid phase of a reactor
C:N	carbon to nitrogen (ratio)
CO_2	carbon dioxide gas
Cd	cadmium
Co	cobalt
COD	chemical oxygen demand
COD_{th}	theoretical chemical oxygen demand
CSTR	continuously stirred tank reactor
Cu	copper
DS	dry solids
DSD	dry solids digestibility
ET	ethanol
EU	European Union
$F_{CH_4\ in}$	volumetric methane flow rate entering the digester
$F_{CH_4\ out}$	volumetric methane flow rate leaving the digester
Fe	iron
$F_{gas\ in}$	gas flow entering the reactor
$F_{gas\ out}$	gas flow leaving the reactor

$F_{H_2\ in}$	volumetric hydrogen flow entering the reactor
$F_{H_2\ out}$	volumetric hydrogen flow leaving the reactor
FID	flame ionization detector
H1	hydrolysis 1 (reactor name in two-stage system chapter 3)
H2	hydrolysis 2 (reactor name in two-stage system chapter 3)
H_2	hydrogen gas
H_2S	hydrogen sulphide gas
HPLC	high performance liquid chromatography
HRT	hydraulic retention time
ICP-MS	inductively coupled plasma mass spectrometry
ICP-OES	inductively coupled plasma optical emission spectrometry
k	decay constant
K	potassium
k_La	volumetric mass transfer coefficient
LA	lactic acid
M1	methane 1 (reactor name in two-stage system chapter 3)
M2	methane 2 (reactor name in two-stage system chapter 3)
M3	methane 3 (reactor name in single-stage system chapter 3)
Mb	molybdenum
MFR	methane formation rate
Mg	magnesium
Mn	manganese
M(t)	cumulative methane yield
N	nitrogen
Na	sodium
NDF	neutral detergent fibre
NH_3	ammonia
NH_4	ammonium
Ni	nickel
OFMSW	organic fraction of municipal solid waste
OLR	organic loading rate
ORP	oxidation reduction potential
P	phosphorus

P	maximum methane production potential (established in a BMP)
P2G	power to gas
R1	reactor 1 (reactor name in experiment chapter 5)
R2	reactor 2 (reactor name in experiment chapter 5)
R3	reactor 3 (reactor name in experiment chapter 5)
R_{H_2}	volumetric hydrogen mass transfer rate
R_{max}	maximum methane production rate
RT	gas retention time
S	sulphur
Se	selenium
SHY	specific hydrogen yield
SMY	specific methane yield
sCOD	soluble chemical oxygen demand
S_i	initial total COD (tCODi)
S_S	soluble chemical oxygen demand (sCOD)
S_{tVFA}	total volatile fatty acids
$S_{t(VFA,La,Et)}$	total of volatile fatty acids, lactic acid and ethanol
t	time
T_{50}	half-life
TAN	total ammoniacal nitrogen
TCD	thermal conductivity detector
TE	trace element
tCODi	initial total COD
TS	total solids
VFA	volatile fatty acids
VFA/TIC	ratio of VFA to alkalinity
VMP	volumetric methane production
VR	reactor volume
VS	volatile solids
VDI	association of German engineers
W	tungsten
Ww	wet weight
$X_{CO_2+H_2 \rightarrow CH_4}$	methane formation derived from carbon dioxide and hydrogen

$X_{Grass+H_2 \rightarrow CH_4}$	methane formation derived from grass and hydrogen
X_i	gas conversions (CO_2 to CH_4)
Y(t)	cumulative methane yield
Y_m	maximum methane potential
Zn	zinc

Chapter 1: Introduction

1.1 Introduction and background to thesis

"The ultimate test of man's conscience may be his willingness to sacrifice something today for future generations whose words of thanks will not be heard" Gaylord Nelson.

The fundamental, possibly unheard sacrifice of our generation will be the transition from a fossil fuel based society to a society driven by renewable decarbonised sustainable energy. The decarbonisation of the economic sectors associated with electricity, heat and transport, together with a responsible use of resources will play a key role in offsetting the worst effects of climate change and reducing environmental pollution. The European Union (EU) has set ambitious greenhouse gas emission targets aiming at 20% reduction by 2020 (EC, 2009). A crucial element to advance towards the proposed targets is the introduction of a circular economy (European Commission, 2015). The Zero Waste Programme for Europe promotes sustainable waste treatment with effective nutrient and energy recovery. Anaerobic digestion (AD) may be considered a beneficial treatment system due to its direct conversion to biogas whilst simultaneously retaining nutrients in the digestate (Murphy & McKeogh, 2004).

The technology of anaerobic digestion has advanced continuously over the course of the last decades as the possible treatment and substrate spectrum broadened. The initial digestion of waste water or manure was rapidly complemented by slurries and residues. In the last decade the range of substrates expanded and included for more complex resources such as energy crops (for example maize and grass) with focus partially shifting from waste management to energy recovery and renewable energy production. Food waste (as it has a gate fee associated with its treatment) can provide the most economic source of biogas production (Murphy & Power, 2006). Manures and energy crops usually require further subsidies to provide an economic basis. However, they drastically increase the potential resources for biogas production. The

technology to co- or mono-digest energy crops emerged in the early 2000s with research still exploring and optimising its full potential.

Foremost, the produced biogas is used in onside combined heat and power (CHP) applications. The electricity is usually injected into the electricity grid, while complete utilisation of heat remains challenging. The installation of remote biogas powered CHP units at a local heat sink can provide a solution to exploit the full energy potential. Another approach to increase the utilisation and distribution range of biogas powered CHP units is gas grid injection. Upgrading technologies to convert biogas to biomethane and inject to the gas grid has undergone exponential growth rates in the last decade in some European countries. After removing the carbon dioxide (CO_2) fraction in the biogas, the remaining methane (CH_4) can be injected to the gas grid and withdrawn for CHP use (or for transport use in natural gas vehicles) at any location along the gas grid.

Rather than removing the CO_2, a novel approach of biogas upgrading by methanation has become the latest focus of attention in biogas research and is implemented in a number of industrial applications. CO_2 is coupled with externally added hydrogen (H_2) to form methane typically via a process stoichiometrically explained by the Sabatier Equation ($4H_2 + CO_2 \rightarrow CH_4 + 2\ H_2O$). The process may be catalysed by microbes (hydrogenotrophic methanogenic archaea) and can provide a biomethane of natural gas quality.

The innovation in anaerobic digestion has facilitated significant progress in optimizing design and operation of biogas technology in the last decades. This has been the foundation of a dynamic and booming biogas industry in Europe contributing substantially to greenhouse gas emission reduction and the stimulation of a more circular economy.

1.2 Rationale for the thesis

The theme of the thesis aspires to explore and advance biogas technology and anaerobic digestion concepts. The rational of this thesis is moved by the idea of integrated biogas systems and its implementation into existing infrastructure. An integrated biogas system is essentially a synergistic cycle of processes sustainably recovering energy and nutrients with an anaerobic digestion system at the centre of

the circular economy system. It is a value adding sequence managing waste and resources with a final gaseous by-product biomethane (natural gas). Figure 1.1 reveals the bigger picture of integrated biogas systems where biogas technology is the central element interconnecting waste and energy management with biological power to gas applications. The interconnection of biogas and biological power to gas into existing energy systems facilitates a higher penetration of variable renewable energy. It allows a change in energy vector from electricity to renewable green decarbonised gas and provides storage capacity for intermittent renewable energies such as wind or photovoltaic (PV).

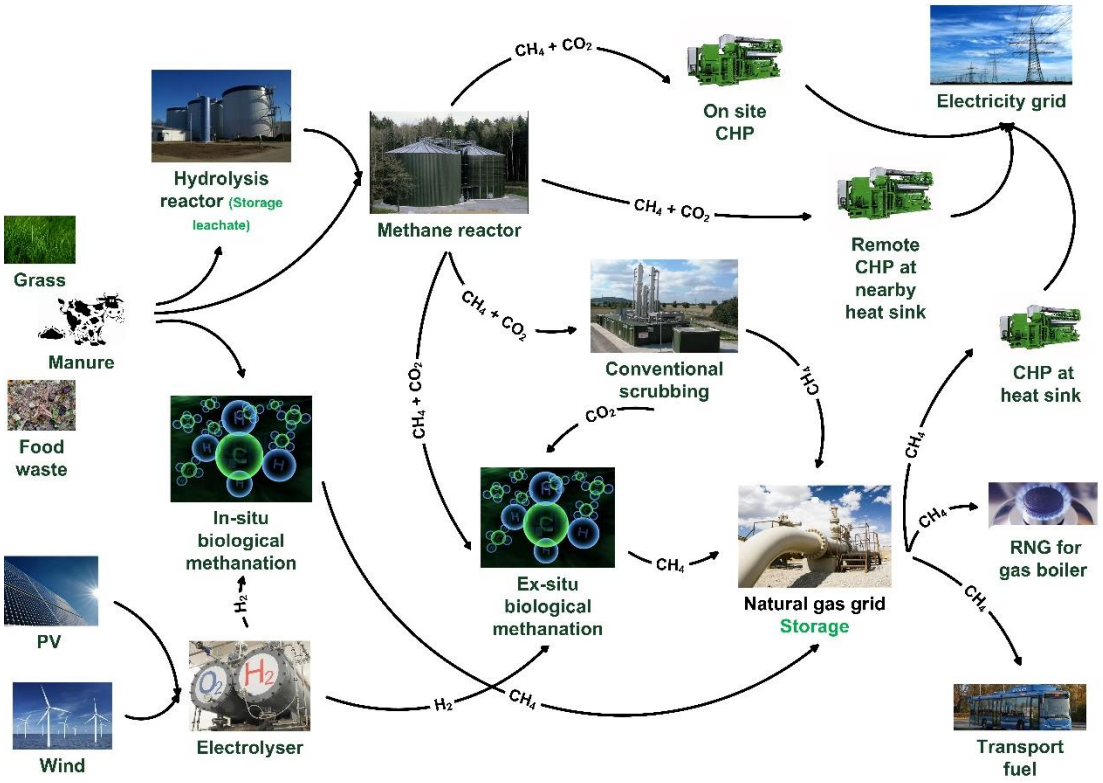

Fig. 1.1 Integrated biogas systems.

In this example of an integrated biogas system the substrate (grass, food waste or manure) is treated in an anaerobic digestion system and may include for upstream hydrolysis. The methane produced in the methane reactor can instantly be utilised in an onsite CHP or forwarded to a remote CHP at a heat sink. Optionally the biogas can be purified by a gas scrubber and injected into the gas grid. The biological power to gas process involves the addition of hydrogen to biogas from an electrolyser, ideally powered by curtailed wind or PV. The actual methanation employs the

Sabatier reaction either in-situ within the anaerobic digestion process or ex-situ in an external vessel. The ex-situ process may avail of exogenous carbon dioxide from conventional upgrading systems or is directly fed with biogas from the methane reactor. In all scenarios the upgraded biogas can be stored and withdrawn from the gas grid and utilised for heat, transport and electricity applications.

1.3 Thesis aims and objectives

The thesis aims to optimise the technology of biogas production and upgrading in integrated biogas systems by investigating and providing solutions on how to:

- maximise possible biogas quantities per input (specific methane yield).
- improve reactor utilisation (volumetric methane production).
- elevate loading (organic loading rate).
- reduce necessary retention time (hydraulic retention time).
- attain methane concentrations meeting gas grid injection standards.

The detailed aims and objectives of the thesis were as follows:

- Assess a two-stage fermentation system through quantification of performance parameters.
- Investigate hydrolysis efficiency and specific hydrogen yield of a hydrolysis reactor.
- Evaluate overall energy yield of two-stage digestion at increasing organic loading rate and contrast with a similar single-stage system.
- Assess the effect of trace elements (TE) on mono-digestion of source segregated food waste in single and two-stage systems.
- Determine the impact of trace element deficiency and its response after supplementation.
- Assess performance of thermophilic digestion at increasing loading rates.
- Compare mesophilic and thermophilic grass digestion.
- Investigate in-situ and ex-situ methanation.
- Outline and contrast performance characteristics of lab scale methanation systems.
- Propose upgrading strategies based on lab scale findings.

1.4 Thesis outline and link between chapters

The thesis is comprised of 7 chapters and investigates opportunities to make advancements in anaerobic digestion. Chapter 1 introduces the thesis. It expands on background and expresses the rationale for the thesis. The chapter closes with the objectives, outline of the thesis and link between chapters. Chapter 2 provides a review of anaerobic digestion technologies and scientific literature relevant to the thesis. Chapters 3 to 6 of the thesis represent the core work carried out during the course of the research programme. These are original manuscripts of journal papers comprising individual sections of introduction, material and methods, results, discussion and conclusions. Each paper can be read in isolation while also contributing to the main theme of the thesis. Chapters 3 to 5 are published in scientific journals. Chapter 6 is currently under review. Chapter 7 completes the thesis with conclusions, recommendations, final remarks, future research and developments. The link between each chapter and a summary of chapters 2 to 6 are given as follows:

Chapter 2: Review of anaerobic digestion technology and systems

The aim of this chapter is to provide background for this thesis. It focuses on a review of knowledge, research and studies previously published on relevant topics to the thesis. A perspective on potential optimisation in anaerobic digestion opens this chapter. It elaborates on key parameters and possible digestion systems. Special attention is given to the digestion of food waste. Single and two-stage systems are contrasted, and major findings are outlined. An overview of trace element supplementation provides guidelines for optimum addition and stable fermentation. Challenges in digesting grass are emphasised. The advantages of elevated process temperature are discussed in the context of intensified reactor loading. The addition of exogenous hydrogen to a digester (in-situ methanation) or the injection into an individual upgrading unit (ex-situ methanation) is explained and reviewed.

Chapter 3: Assessment of increasing loading rate on two-stage digestion of food waste

This chapter sets out to tackle the optimisation of anaerobic digestion systems. The objective was set to answer the question if the benefits of a two-stage food waste digestion system could outperform a single-stage system under similar conditions. The two-stage system comprised a first stage hydrolysis reactor followed by a second stage methanogenic reactor. At increasing organic loading rates, the performance was investigated to establish specific methane yields (SMY) and methane concentrations. An assessment of the first stage hydrolysis reactor was conducted to provide insights into produced liquid fermentation products. The challenges faced in this experiment let to chapter 4.

Chapter 4: Role of trace elements in single and two-stage digestion of food waste at high organic loading rates

The anaerobic digestion process in chapter 3 revealed a deficiency in essential trace elements. It was assumed that the advantages of two-stage digestion systems potentially facilitate an increased resilience towards a deficiency of trace elements. Thus, the impact of trace element deficiency and its response after supplementation was documented and discussed in this chapter. Besides the addition of trace elements, further potential to optimise anaerobic digestion was seen in higher temperature levels.

Chapter 5: Increased loading rates and specific methane yields facilitated by digesting grass silage at thermophilic temperatures rather than mesophilic

This study was conducted to advance the understanding of grass digestion at higher temperature levels. It was of particular interest as Ireland possesses an abundant resource of grass. Late harvested grass silage was fermented at thermophilic conditions. The addition of trace elements previously proved to have beneficial effects and was therefore thought to facilitate an increase in loading. The overall performance was assessed and compared to mesophilic digestion. Besides increasing the methane yield, the ultimate goal was set to further enrich the methane content close to levels necessary for gas grid injection. Thus, it set the scene for the

following chapter to pursue the idea of injecting and coupling hydrogen with carbon dioxide in a grass digester.

Chapter 6: Biological methanation: Strategies for in-situ and ex-situ upgrading in anaerobic digestion

This study investigated lab-scale in-situ and ex-situ biological methanation of hydrogen and carbon dioxide to methane. The upgrading success and associated influence of increased hydrogen partial pressure on the proposed methanation strategies was discussed and contrasted. A biomethane with methane concentrations in excess of 96% should facilitate direct gas grid injection. The positive effects of hydrogen addition to the methanogenic upgrading process was used to propose novel upgrading strategies applicable to upscaling and industry. A potential for cascading systems comprising ex-situ units in series or the merging of in-situ and ex-situ units was outlined.

Chapter 2: Review of anaerobic digestion technology and systems

2.1 Optimisation potential in anaerobic digestion

Optimisation in anaerobic digestion is fore mostly driven by economic considerations and cost reduction. Those criteria ultimately define the design and choice of substrate of any anaerobic digestion system. While substrates such as wastes and residues are associated with receipt of gate fees, energy crops such as maize and grass impose additional procurement costs (Banks & Heaven, 2013). The revenue of a waste processing plant certainly benefits from high throughputs and is to be optimised for high loadings and short retention times. The extraction of the maximum amount of gas and energy is preferably, but secondary. As a result high loading and volumetric biogas production rates per reactor volume are the pivotal design criteria (Banks & Heaven, 2013). In contrast, the AD plant digesting energy crops is merely dependent on the maximum obtainable gas yield per ton of substrate input. This requires sufficient residence time or optimised process and reactor conditions. In both scenarios ideal conditions for the microbes should prevail to allow a stable digestion process. Key parameters influencing the volumetric methane production rate (VMP) and specific methane yield include for pre-treatment, reactor design, temperature, pH, organic loading rate (OLR), retention time (HRT), kinetic properties (K-values), nutrient supply and ammonium (NH_4) content of the substrate.

The relationship of increasing OLR on HRT, SMY and VMP in a continuous stirred tank reactor (CSTR) system are explained in Banks and Heaven (2013). An increase in OLR consequently elevates VMP but reduces HRT while subsequently lowering the SMY. A rise in temperature can enhance SMY and facilitates increased OLR, boosting VMP particularly when digesting at short HRT (Banks & Heaven, 2013). The temperature level is limited by ammonia concentration (Banks & Heaven, 2013; Yirong et al., 2017). The higher the temperature, pH and ammonium (NH_4) level, the more free ammonia (NH_3) will be found in solution inhibiting the methanogens.

The prevailing digester type for solids, sludges and slurries are vertically mounted cylindric CSTR digesters operating at mesophilic temperature (Banks & Heaven, 2013). As the key limiting step for solids biomass (for example maize, grass) is the hydrolysis of the substrate, any substantial optimisation to raise VMP, OLR and SMY at reduced HRT will have to comprise upstream pre-treatment.

2.2 Digestion of food waste

Commercial food waste with high degradability is amenable to low retention times and high organic loading rates (Banks & Heaven, 2013; Browne & Murphy, 2014b). Biomethane potential tests (BMP) confirmed the rapid degradability of commercial food waste; 95% of a 30 day BMP yield can be achieved in the first 10 days (Browne et al., 2014). This favours high performance anaerobic digestion systems capable of coping with intensified conditions at short retention times such as leach bed or two-stage fermentation systems (Browne & Murphy, 2014b).

Most food wastes exhibit a high level of protein fractions, contributing to high levels of total ammoniacal nitrogen (TAN) and reduced carbon to nitrogen ratios (C:N). Temperature and pH define the proportion of free ammonia nitrogen in solution with TAN levels exceeding 3-5 g L^{-1} being considered inhibitory (Yirong et al., 2017).

2.3 Two-stage digestion

The advantage of two-stage anaerobic digestion is the spatial separation of process phases, where reactor parameters such as pH can be optimised for each phase to suit the requirements of the microorganisms. The pH in the first reactor (between 4 and 6) optimises hydrolysis (Bochmann & Montgomery, 2013). In the upstream reactor hydrolysis and acidification break down macromolecules into liquid fermentation products such as volatile fatty acids (VFAs) and ethanol (Bochmann & Montgomery, 2013), precursors for the methanogens in the second reactor. The effluent from stage one (hydrolysis reactor) is the substrate for the downstream second stage methanogenic reactor. Thus, the methanogenic archaea have a homogenous feedstock in the form of VFAs and ethanol. The second stage reactor has a neutral pH and operates at longer hydraulic retention times of 10 - 20 days as compared to the hydrolytic reactor (2-5 days).

The two-stage process benefits from enhanced process stability and higher rate of substrate degradation, leading to higher biogas yields from the same amount of substrate (Browne & Murphy, 2014b; Massanet-Nicolau et al., 2015; Shen et al., 2013). Another fundamental difference and advantage of two-stage over single-stage systems is the separate gas collection for each reactor (Bochmann & Montgomery, 2013). This allows separate use of the produced gases. Biogas from the acidification

reactor consists mainly of carbon dioxide, hydrogen sulphide and hydrogen. The short retention time and low pH in the first stage is not amenable to methanogenic archaea, so methane is not produced. The production of carbon dioxide during acidification in the first reactor results in a biogas with enhanced methane content in the downstream methane reactor (Bochmann & Montgomery, 2013). The first stage reactor may be seen as both a pre-treatment and storage system for feedstock. This allows just in time storage of highly degradable substrate in the first reactor, without any associated methane production. Demand driven biogas production can be controlled by a variable feed rate of pre-acidified substrate into the second reactor. Therefore, the methane production is decoupled from the actual substrate delivery and feeding. The partial segregation of carbon dioxide in the upstream hydrolysis reactor generates a biogas rich in methane in the second reactor.

The upstream hydrolysis reactor of the two-stage digestion system potentially segregates major quantities of hydrogen sulphide (H_2S). Substrate acidification and degradation causes the hydrogen sulphide to be mainly present in its very volatile state of H_2S, rather than in its more soluble conjugate base, the bisulfide ion HS^- at more neutral pH (Waechter, 2012). As hydrogen sulphide is known to precipitate trace metals (Gustavsson et al., 2011; Karlsson et al., 2012), the upstream release of hydrogen sulphide potentially improves the bioavailability of these elements in the second stage system.

2.4 Trace element supplementation

A sufficient level of all macro- and micro-nutrients is a vital prerequisite for key enzymes and microbes associated with stable methanogenesis (Banks et al., 2012; Demirel & Scherer, 2011; Drosg, 2013; Kida et al., 2001; Yirong et al., 2014). All essential macro-nutrients, such as calcium, magnesium, nitrogen, phosphorus, potassium, sodium and sulphur, are foremost available in resources such as wastes, slurries, manures or energy crops. However, mono digestion of certain feedstock such as for example food waste or energy crops is challenging due to a lack of a sufficient level of trace elements such as cobalt, iron, nickel, molybdenum and selenium (Banks et al., 2012; Karlsson et al., 2012; Moestedt et al., 2016; Nges et al., 2012; Wall et al., 2014; Zhang & Jahng, 2012). If the substrate is deficient in

nutrients, the process performance diminishes or even fails (Drosg, 2013; Gustavsson et al., 2011; Schmidt et al., 2014; Zhang & Jahng, 2012).

In an analysis of full scale biogas plants, Lemmer et al. (2010) attributed a 10 - 50% performance reduction per unit reactor volume to digester systems with insufficient trace elements. The accessibility of trace elements is constrained by its bioavailability (Banks & Heaven, 2013; Karlsson et al., 2012; Ortner et al., 2015). In order to be available for methanogenic archaea, trace elements have to be soluble and neither be fixed in precipitated compounds (such as sulphates, sulphides, phosphates or carbonates) nor adsorbed (Banks & Heaven, 2013). Ortner et al. (2014) established that 30-70% of present trace elements were not bioavailable to the microbial community. Therefore, a general recommendation on optimal nutrient concentrations remains challenging.

The addition of trace elements to sustain stable fermentation in scientific literature ranges between 0.05-10 mg L^{-1} for Co, 5-500 mg L^{-1} for Fe, 0.0272-5 mg L^{-1} for Mo, 0.035-10 mg L^{-1} for Ni and 0.056-0.2 mg L^{-1} for Se (Banks et al., 2012; Gustavsson et al., 2011; Lemmer et al., 2010; Moestedt et al., 2016; Nordell et al., 2016; Pobeheim et al., 2011; Qiang et al., 2012; Zhang & Jahng, 2012; Zhang et al., 2012; Zhang et al., 2015). Further trace metals such as manganese, tungsten and zinc are rarely supplemented and usually not considered to be deficient for digestion. Overdosing of trace metals reduces enzyme and microbial activity (Banks & Heaven, 2013; Lemmer et al., 2010).

2.5 Challenges in grass digestion

Managing sustainable grass digestion systems, through maximum possible loading rates, whilst generating a high specific methane yield, remains a critical design challenge. Xie et al. (2011) achieved stable co-digestion of grass silage with pig manure, however mono-digestion failed. Thamsiriroj et al. (2012) investigated long-term operation of mesophilic grass mono-digestion and suggested a limit of 3 g VS L^{-1} d^{-1}. Mechanical failure was manifested when this loading rate was exceeded. This was mainly attributed to insufficient mixing caused by enhanced viscosity and a dry solids (DS) level rising above 12%. Wall et al. (2014b) assessed the optimisation of digester performance for mesophilic mono and co-digestion of grass silage at organic

loading rates up to 4 g VS L^{-1} d^{-1}. In general, the high fibre and total solids content impacts negatively on the prevailing viscosity and thus on the mixing quality in the reactor. This is the main reason why loading rates exceeding 4 g VS L^{-1} d^{-1} in grass mono-digestion have not been reported in literature. Similar to food waste, digestion of grass silage is characterised by elevated amounts of TAN; this needs to be taken into consideration in the system design.

2.6 Thermophilic digestion

An increase in temperature improves kinetic properties, increases enzyme activity, reduces viscosity, leads to higher substrate utilisation and growth rates of bacteria (Mähnert, 2007). The correlation of loading and dry solids on viscosity, based on mesophilic and thermophilic digestion of maize, rye and sugar beet silage was outlined in detail by Mähnert (2007). An increase in loading provoked a significant gain in viscosity at mesophilic temperatures. However, at similar dry solids content the thermophilic reactor displayed a lower viscosity. For 100% maize digestion the apparent viscosity at 7% DS accounted for 0.6 Pa s at mesophilic (35 °C) digestion and 0.2 Pa s for thermophilic (55 °C) digestion. The greater the loading rate and dry solids content, the more distinct this difference became. As explained in section 2.2 elevated temperature level increase free ammonia nitrogen concentrations and may impose process inhibition.

2.7 Biological methanation

2.7.1 Sabatier process

The underlying principle of biological methanation is the Sabatier process. According to the Sabatier reaction (equation 1) hydrogenotrophic methanogenic archaea are able to consume an equimolar amount of four times hydrogen (H_2) to carbon dioxide (CO_2) and generate biomethane of natural gas quality (Fukuzaki et al., 1990).

$$4H_2 + CO_2 \rightarrow CH_4 + 2H_2O \qquad \Delta G^0 = -165\ KJ\ mol^{-1} \qquad (1)$$

2.7.2 Biological methanation systems

The biological reduction of carbon dioxide to methane is referred to as biological methanation and can be performed either in-situ within a biogas digester or ex-situ in an adjacent external reactor (Angelidaki et al., 2018; Lecker et al., 2017). In an ex-situ system the initial stages of anaerobic digestion (hydrolysis and acidogenesis) are not present. The provision of carbon dioxide, hydrogen, essential nutrients and hydrogenotrophic methanogens is sufficient to establish the process (Angelidaki et al., 2018; Lecker et al., 2017).

An in-situ methanation system is based on a conventional biogas digester receiving organic substrate and hydrogen. The addition of exogenous hydrogen puts the symbiotic fermentation stages of acetogenesis and methanogenesis under stress by potentially elevating concentrations of intermediates/precursors such as volatile fatty acids, hydrogen and carbon dioxide. At standard conditions fatty acid oxidation (such as from butyrate and propionate to acetate) remains endergonic and becomes feasible at hydrogen partial pressure below 10 Pa (Fukuzaki et al., 1990). Adequate levels are sustained by interspecies hydrogen transfer between acetogenic and hydrogenotrophic methanogenic microorganisms; the addition of exogenous hydrogen drastically favours the latter. With balanced levels of hydrogen to allow fatty acid oxidation, adverse effects on acetogenesis are not to be expected and simultaneous production of biogas and upgrading to biomethane is possible. (Agneessens et al., 2017; Bassani et al., 2016; Luo & Angelidaki, 2013b; Luo et al., 2012a; Mulat et al., 2017).

2.7.3 Solubilisation of hydrogen

The solubilisation of hydrogen is the decisive step to make gaseous hydrogen available for microorganisms on a cellular level. With a solubility rate of 0.7 mmol H_2 L^{-1} bar^{-1}, hydrogen dissolves poorly in water, with solubility rates 24 times less than that of carbon dioxide at 55 °C. The hydrogen to liquid transfer is therefore the bottleneck of the process. It is influenced by system pressure, Henry constant, temperature, hydrogen partial pressure, reactor configuration, mixing speed, gas recirculation and the employed gas diffusion system.

2.7.4 Phase boundary interface

The phase boundary interface is the crucial element to provide efficient gas liquid mass transfer. Any increase for instance by smaller bubble size or enlarged contact surface, proportionally enhances the quantities of gases dissolved into liquid until maximum solubility is reached. Several gas injection methods such as hollow fibre membranes, gas diffusers and electrochemical methods have been described in the scientific literature and successfully demonstrated high gas transfer (Angelidaki et al., 2018; Bassani et al., 2016; Kraakman et al., 2011; Lecker et al., 2017). Similarly, gas recirculation systems (Alitalo et al., 2015; Bassani et al., 2016; Kougias et al., 2017; Luo et al., 2012a) or for example systems recirculating liquid in a trickle bed reactor have shown to facilitate and enhance gas liquid contact (Burkhardt et al., 2015; Rachbauer et al., 2016; Strübing et al., 2017; Ullrich et al., 2018).

2.7.5 Reactor configuration and design

The efficiency is further defined by reactor configuration and design. In the lab various systems have been investigated including: Intensely mixed reactor bottles (Agneessens et al., 2017; Guneratnam et al., 2017; Luo & Angelidaki, 2012b; Mulat et al., 2017); bubble column reactors (Kougias et al., 2017; Savvas et al., 2017); trickle bed reactors with immobilized microorganisms (Burkhardt et al., 2015; Rachbauer et al., 2016; Strübing et al., 2017; Ullrich et al., 2018); fixed bed reactors functioning as biological/anaerobic filters (Alitalo et al., 2015); hollow fibre membrane reactors (Luo & Angelidaki, 2013b); continuous stirred tank reactors (Kougias et al., 2017; Luo & Angelidaki, 2013a); and upflow anaerobic sludge blanket reactors (Bassani et al., 2016; Luo & Angelidaki, 2013b; Rittmann et al., 2015).

Novel concepts have been suggested for instance by Savvas et al. (2017) investigating ex-situ methanation in a 110 cm tall glass cylinder with 1.5 litre working volume. The gas mixture was dissolved directly by introducing it into a centrifugal pump and recirculating the liquid from bottom to top of the reactor. Kougias et al. (2017) assessed ex-situ methanation of a biogas with 60% methane content. Positive effects of gas recirculation were observed in a bubble column and two in-series connected upflow reactors. More complex ex-situ reactor

configurations such as trickle bed reactors attained high methane concentrations in the off gas at elevated methane formation rates (Strübing et al., 2017). Bassani et al. (2016) was able to upgrade biogas from 58% CH_4 content to 82% in an in-situ upflow anaerobic sludge blanket reactor. Bubbleless gas transfer in an in-situ hollow fibre membrane module with cattle manure and whey as substrate produced promising results (Luo & Angelidaki, 2013b).

Chapter 3: Assessment of increasing loading rate on two-stage digestion of food waste

Assessment of increasing loading rate on two-stage digestion of food waste

M. A. Voelklein[1, 2], A. Jacob[1, 2], R. O' Shea[1, 2], J. D Murphy [1, 2]

[1]MaREI Centre, Environmental Research Institute (ERI), University College Cork (UCC), Ireland

[2]School of Engineering, UCC, Ireland

Abstract

A two-stage food waste digestion system involved a first stage hydrolysis reactor followed by a second stage methanogenic reactor. Organic loading rates were increased from 6 to 15 g VS L^{-1} d^{-1} in the hydrolysis reactor and from 2 to 5 g VS L^{-1} d^{-1} in the methanogenic reactor. The retention time was fixed at 4 days (hydrolysis reactor) and 12 days (methane reactor). A single-stage digester was subjected to similar loading rates as the methanogenic reactor at 16 days retention. Increased OLR resulted in higher quantities of liquid fermentation products from the first stage hydrolysis reactor. Solubilisation of chemical oxygen demand peaked at 47% at the maximum loading. However, enhanced hydrolysis yields had no significant impact on the specific methane yields. The two-stage system increased methane yields up to 23% and enriched methane content by an average of 14% to levels of 71%.

Keywords: two-stage digestion; food waste; hydrolysis; biogas; high performance reactors.

3.1 Introduction

The Zero Waste Programme for Europe promotes a circular economy (European Commission, 2015) and encourages a phase out of land filling of biodegradable waste such as the organic fraction of municipal solid waste (OFMSW) by 2025. Anaerobic digestion may be considered a beneficial treatment system for OFMSW due to direct conversion to biogas whilst simultaneously retaining nutrients in the digestate (Murphy & McKeogh, 2004). Food waste (as it has a gate fee associated with its treatment) can provide the most economic source of biogas production (Murphy & Power, 2006). Biomethane potential tests highlight the rapid degradability of commercial food waste; 95% of the 30 day BMP yield was achieved in the first 10 days by Browne et al. (2014). Commercial food waste with high degradability should be amenable to low retention times and high organic loading rates.

Single-stage anaerobic digestion is a well-established technology for biogas production. The investment costs are relatively low and the process is well understood. However, hydrolytic and methanogenic microorganisms are optimised at differing pH (Bochmann & Montgomery, 2013). In a single-stage system the prevailing pH (7-8) favours the methanogenic archaea, leading to non-optimum growth conditions for acidifying hydrolytic bacteria.

The advantage of two-stage anaerobic digestion is the spatial separation of process phases, where reactor parameters such as pH can be optimised for each phase to suit requirements of the microorganisms. The pH in the first reactor (between 4 and 6) optimises hydrolysis (Bochmann & Montgomery, 2013). In the upstream reactor hydrolysis and acidification break down macromolecules into liquid fermentation products such as volatile fatty acids (VFAs) and ethanol (Bochmann & Montgomery, 2013), precursors for the methanogens in the second reactor. The effluent from stage one (hydrolysis reactor) is the substrate for the downstream second stage methanogenic reactor. Thus, the methanogenic archaea have a homogenous feedstock in the form of VFAs and ethanol. The second stage reactor has a neutral pH and operates at longer hydraulic retention times of 10 to 20 days as compared to the hydrolytic reactor (2-5 days).

The two-stage process benefits from enhanced process stability and higher rate of substrate degradation, leading to higher biogas yields from the same amount of substrate (Browne & Murphy, 2014b; Massanet-Nicolau et al., 2015; Shen et al., 2013). Another fundamental difference and advantage of two-stage over single-stage systems is the separate gas collection for each reactor (Bochmann & Montgomery, 2013). This allows separate use of the produced gases. Biogas from the acidification reactor consists mainly of carbon dioxide, hydrogen sulphide and hydrogen.

Biohydrogen systems may be optimised for hydrogen production (Guwy et al., 2011; Li et al., 2009). The short retention time and low pH in the first stage is not amenable to methanogenic archaea, so methane is not produced. The production of carbon dioxide during acidification in the first reactor results in a biogas with enhanced methane content in the downstream methane reactor (Bochmann & Montgomery, 2013). Thus, rather than optimise hydrogen production the first stage reactor may be seen as both a pre-treatment system and a partial up-grading system facilitating biogas rich in methane in the second reactor. If the energy vector for biogas is biomethane, then the upgrading facility (CO_2 removal) will be cheaper and less energy intensive for a two-stage system than a single-stage system. This is a significant benefit considering biogas upgrading can cost 30% of the capital cost of the whole biogas/biomethane system (Murphy & Power, 2009).

Previous studies on two-stage digestion have focused on novel equipment testing (Argelier et al., 1998; Browne & Murphy, 2014b; Chinellato et al., 2013; Guwy et al., 2011) and hydrogen production (Chinellato et al., 2013; Karlsson et al., 2008; Liu et al., 2013; Luo et al., 2011; Massanet-Nicolau et al., 2015). Massanet-Nicolau et al. (2015) contrasted a two-stage system digesting grass to a single-stage system and highlighted a 13.4% increase in energy yields at similar retention time. Chen et al. (2015) determined the correlation of acidogenic fermentation types with oxidation reduction potential, pH, OLR and liquid fermentation products of food waste and rice straw. The literature is very sparse in contrasting one and two-stage digestion of food waste. Gaps also exist in testing continuous two-stage processes at increasing organic loading rates.

Thus, the objectives of this paper are to assess a two-stage system through quantification of performance parameters such as hydrolysis efficiency, specific

hydrogen (SHY) and methane yields. The overall energy yield at increasing organic loading rate will be evaluated and contrasted with a similar single-stage system. The objective is not to generate maximum rates of hydrogen but to optimise the acidification process and hence maximise energy yields and organic loading rates.

3.2 Materials and Methods

3.2.1 BMP system

The biomethane potential of the substrate was tested in an automatic methane potential test system (AMPTS ll, Bioprocess Control, Sweden). The working volume of the batch BMP tests were 400ml; all tests were run in triplicate for 30 days at 37 °C. The inoculum to substrate ratio was set to 2:1. Carbon dioxide was removed by passing through a sodium hydroxide solution. The methane gas flow is recorded with gas tippers based on water displacement. This system is described in detail by Wall et al. (2013).

3.2.2 Reactor systems

Two-stage fermentation of food waste was performed at lab scale CSTR in two systems, comprised of a hydrolysis reactor and a methane reactor. The reactors had a total volume of 5 L with an internal diameter of 0.15 m and a height of 0.4 m. The working volume was 1.35 L for the hydrolysis reactor and 4.0 L for the methane reactor (figure 3.1). A third system, a single-stage reactor with the same dimensions as the methane reactor of the two-stage system was also employed (figure 3.1).

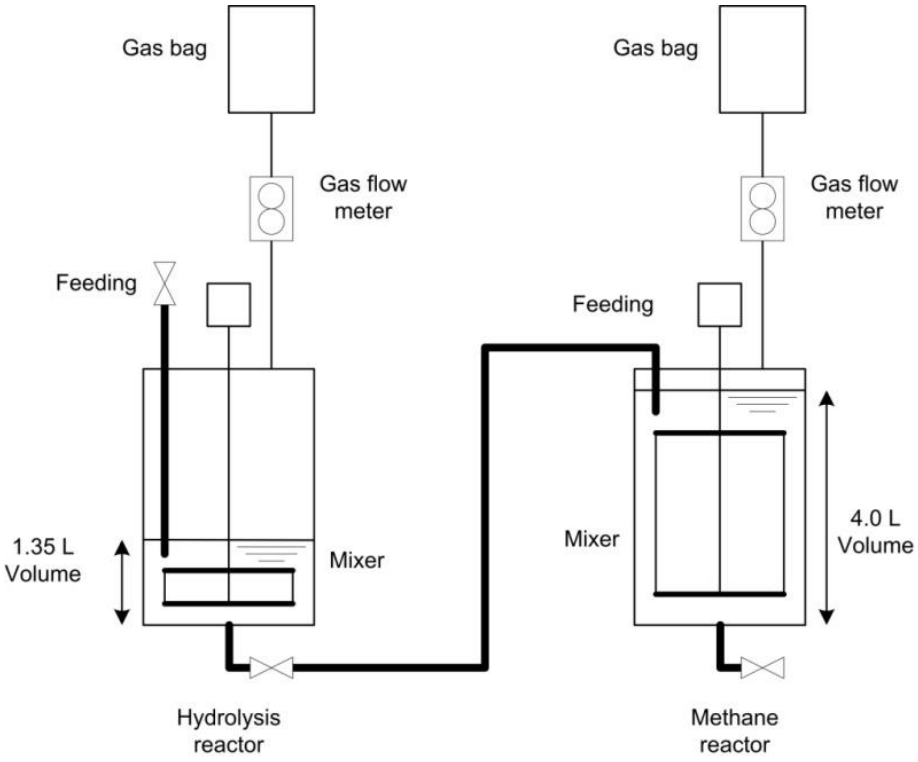

Fig. 3.1 Schematic of experiment lay out.

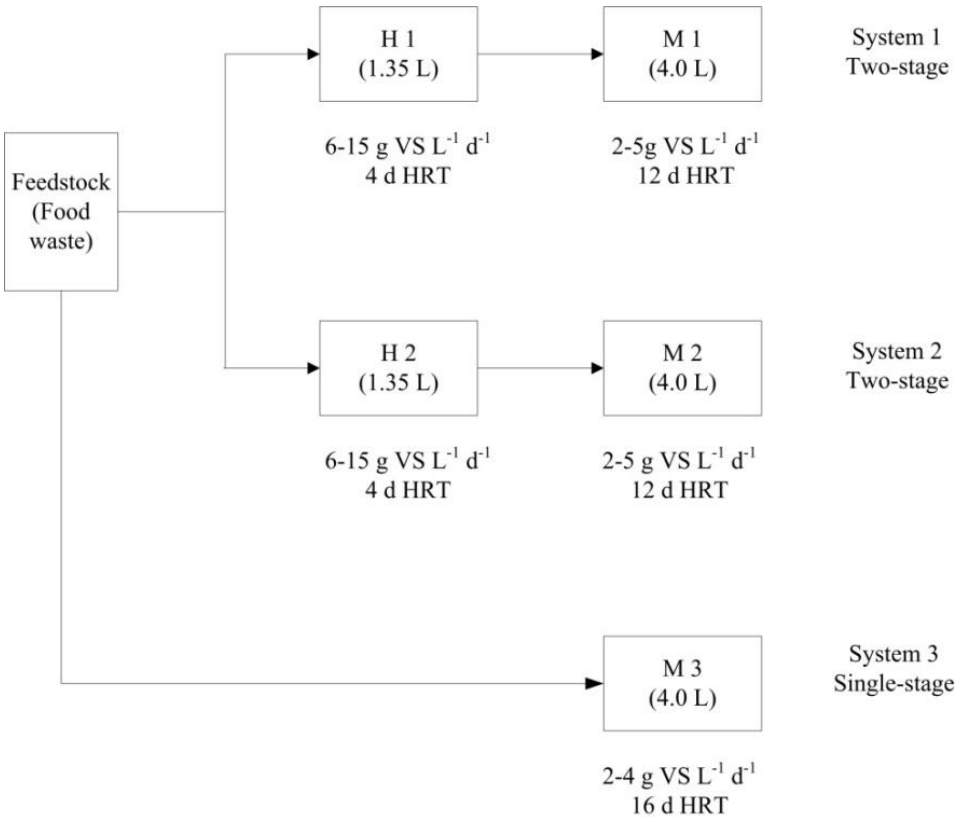

Fig. 3.2 Design of experiment.

A temperature controller unit was installed to maintain a constant temperature in the reactors at mesophilic conditions. An outer heating blanket supplied the heat. A wet gas meter recorded gas flow automatically. Collected biogas was stored in a gas bag for compositional analysis. Mixing was provided by a stirring mechanism, consisting of a vertical shaft with height adjustable paddles at the upper and lower end. A variable speed motor drove the shaft. The shaft of the stirrer was surrounded by a top mounted pipe, which sealed the top of the reactor with the rotating stirrer. The reactors were equipped with a submerged pipe on top of the reactor to prevent gas leakage and oxygen entry during the feeding process. The hydrolysis reactors were fed manually once per day. The input substrate displaced a certain amount of effluent at the lower end of the reactor through a flexible tube. In this way the same level in the reactor was always maintained and representative samples for analysis were obtained.

3.2.3 Design and operating conditions

Figure 3.2 outlines the deployed digestion systems. The reactor configurations were tested with different loading rates, while the retention time and working volume stayed the same. The two-stage system was set up in duplicate. The retention time in both two-stage systems was 4 days in the hydrolysis reactor and 12 days in the methane reactor. The single-stage reactor was set to a retention time of 16 days, to match the overall retention time of the two-stage system. This was achieved by diluting the substrate with corresponding amounts of water. The approach is partly academic, yet reflects potential for co-digestion with wastes such as slurry.

The loading rate of the hydrolysis reactors (H1 & H2) was increased gradually, starting with an initial loading rate of 6 g VS L^{-1} d^{-1} and reaching a final loading rate of 15 g VS L^{-1} d^{-1}. The subsequent loading rate in the methane reactors (M1 & M2) of the two-stage system varied from 2 to 5 g VS L^{-1} d^{-1}. The ratio of the respective volumes of the two phase reactors (3:1) was inversely proportional to the ratio of the OLR in each phase. The loading rate for the single-stage reactor (M3) ranged from 2 to 4 g VS L^{-1} d^{-1}. Results for an OLR of 5 g VS L^{-1} d^{-1} were not obtained in the single phase system due to experimental difficulties. After stabilization at each organic

loading rate the loading rate was maintained for at least 2 retention times. The pH in the hydrolysis stage was actively controlled with sodium hydroxide to maintain a pH-value at around 5.5. Without pH control, the pH of acidogenesis can readily decrease to below 4, which could significantly suppress the acid production, favouring the hydrogen producing ethanol-fermenting pathway (Chen et al., 2015; Li et al., 2009).

3.2.4 Inoculum and characterisation of food waste

The inoculum for the hydrolysis reactors was obtained from existing laboratory single-stage digester effluent based on food waste and grass. For the hydrolytic reactor a heat-shock treatment at 120 °C was conducted for 20 minutes to deactivate methanogenic archaea and allow harvest of anaerobic spore-forming acidifying bacteria. Immediately after the heat-treatment the pH was decreased to 5.5 with 1 molar hydrochloric acid to provide optimal conditions for hydrolysis bacteria. During the 20 days acclimatisation phase the reactor was fed at a low loading rate of 2.5 g VS L^{-1} d^{-1} to support bacterial growth and acclimatisation. The inoculum for the methane reactors was obtained from the same single-stage digester effluent, but without any pre-treatment.

The source segregated food waste for this experiment was obtained from a local waste management company collecting wastes form major catering premises in the city. Approximately 80 kg of food waste was first manually screened and non-biodegradable contaminants like bones and plastics were removed. The residual food waste was subsequently shredded in a mechanical meat mincer to a pasty consistence with particle size between 0.5-5 mm. Until it was processed in the anaerobic reactors, it was stored at a temperature of -20 °C.

The physical and chemical characteristics of the feedstock were determined prior to the experiment. Total solids (TS) content of 24.63 ±0.72% was identified with a share of 94.29 ±0.64% present as volatile. The residual ash content yielded in 5.71 ±0.64%. A pH in the range of 5.1 ±0.05 was determined. Elemental composition of the food waste resulted in 47.56 ±1.23% Carbon, 6.56 ±0.24% Hydrogen, 36.97 ±1.66% Oxygen and 3.20 ±0.23% Nitrogen; associated C:N ratio calculates to

14.86. A theoretical chemical oxygen demand (COD) value of 1.46 g COD g VS^{-1} (calculated in section 3.3.1) was established.

3.2.5 Analytical methods

The total solids and volatile solids were determined according to Standard Methods 2540 G. The pH value was measured using a pH meter (Jenway 3510). Soluble chemical oxygen demand (sCOD) was determined using Hach Lange cuvette tests (LCK 914) and evaluated by a DR3900 Hach Lange Spectrophotometer. Samples were centrifuged at 15,000 rpm for 10 minutes prior to testing. The concentrations of individual volatile fatty acids were analysed with gas chromatography (Hewlett Packard HP6890) using a Nukol^{TM} fused silica capillary column and a flame ionization detector (FID). Hydrogen was used as a carrier gas. Lactic acid, methanol, ethanol and propanol were determined by high performance liquid chromatography (HPLC) using an Agilent 1200 HPLC system with a refractive index detector. An Agilent Hi-Plex H 300 x 7.7 mm Column was used with 0.01N H_2SO_4 as the elution fluid, at a flow rate of 0.6 ml min^{-1}. The temperature of the column is maintained at 65 °C.

The methane content can considerably change during a 24 hour period, particularly if the digester is only fed once a day. As a result calculations based on periodic measurements would severely over or underestimate methane production, depending on when in the daily cycle methane content is measured. In order to avoid misleading measurements, biogas was stored in a gas bag and measured for its biogas composition on a weekly basis. Biogas composition was analysed for O_2, N_2, CH_4, H_2 and CO_2 using a gas chromatograph (Hewlett Packard HP6890) equipped with a Hayesep R packed column and a thermal conductivity detector (TCD). Argon was used as carrier gas. Certified gas standards are employed for the standardization of hydrogen, methane and carbon dioxide.

Biogas flow from each reactor was measured by using a water displacement mechanism. A certain amount of gas passes through a tipping mechanism, displaces the volume of water in a pre-defined chamber till it floats and releases the gas. Every release generates a digital impulse, which represents the displaced gas volume in the chamber. The measured methane volume was adjusted to the volume at standard temperature (273K) and pressure (1013mbar).

3.2.6 Calculations

The acidification yield was determined for total VFA production and for the summation of total VFA, ethanol (Et) and lactic acid (La) production, expressed as a percentage of sCOD, through use of equation 2 and 3.

$$\text{Acidification yield (VFA)} = \frac{S_{tVFA}}{S_S} \text{ x } 100 \quad (2)$$

$$\text{Acidification yield (VFA, La, Et)} = \frac{S_{t\,(VFA,LA,Et)}}{S_S} \text{ x } 100 \quad (3)$$

S_S is the sCOD measured and S_{tVFA} represents the total volatile fatty acids and $S_{t(VFA,La,Et)}$ is the total volatile fatty acids, lactic acid and ethanol expressed as g COD L^{-1}. The theoretical chemical oxygen demand (COD_{th}) equivalents for VFA, ethanol and lactic acid can be derived from stoichiometric considerations.

The hydrolysis yield defines the degree of solubilisation of organic matter. It is calculated according to equation 4.

$$\text{Hydrolysis yield} = \frac{S_S}{S_i} \text{ x } 100 \quad (4)$$

S_S is the sCOD measured and S_i represents the initial total COD (tCODi).

3.3 Results and Discussion

3.3.1 Theoretical maximum biomethane potential (BMP_{th}) and substrate chemical oxygen demand equivalent (COD_{th})

A proximate and ultimate analysis of the food waste was conducted which allowed theoretical derivation of the stoichiometric equation of the food waste and hence maximum theoretical methane yield and concentration. The calculation in table 3.1 yields a theoretical maximum biomethane potential of 548.2 L CH_4 kg VS^{-1} with a methane concentration of 56.1%.

Table 3.1. Theoretical calculation of biomethane potential and methane concentration using the Buswell Equation.

$C_{18.2}H_{30}O_{10.6}N + 5.35\ H_2O \rightarrow 10.18\ CH_4 + 7.97\ CO_2$
$417.66\ g\ mol^{-1} + 96.44\ g\ mol^{-1} \rightarrow 163.46\ g\ mol^{-1} + 350.64\ g\ mol^{-1}$
$1\ kg\ VS + 0.23 kg\ H_2O \rightarrow 0.39\ kg\ CH_4 + 0.84\ kg\ CO_2$
Density CH_4 0.714 kg m^{-3}; density CO_2 1.96 kg m^{-3}
56.1 vol.-% CH_4; 43.9 vol.-% CO_2
Theoretical biomethane potential equates to 548.2 L CH_4 kg VS^{-1} added.
It is assumed that volatile solids compounds only consist of C, H, O and N.

Initial total COD of the substrate was derived from elemental analysis. Theoretically the volatile solids of food waste could be expressed as $C_{18.2}H_{30}O_{10.6}N$. Contribution of sulphur was assumed to be negligible. Equation 5 calculates the moles of oxygen required to oxidise one mole of food waste.

$$C_{18.2}H_{30}O_{10.6}N + 19.62\ O_2 \rightarrow 18.15\ CO_2 + 13.52\ H_2O + 1\ NH_3 \quad (5)$$

Total oxidation requires 19.62 moles of oxygen (627.76 g) to oxidize 1 mol of food waste (431.11 g VS). The quotient gives the theoretical COD equivalent of 1.46 g COD g VS^{-1}.

3.3.2 Biomethane Potential Test

A 30 day bio-methane potential test was carried out in triplicate which generated a total methane yield of 492.7 ±9.3 L CH_4 kg VS^{-1} and a k-value of 0.154. The BMP results achieved 89.9% of the theoretical biomethane potential. This matches the findings of Browne et al. (2014) on highly degradable commercial food waste. Approximately 90% of total methane yield (443.3 L CH_4 kg VS^{-1}) was obtained in the first 10 days.

3.3.3 Single-stage digestion with gradually enhanced OLR

Table 3.2 shows the performance characteristics of the single-stage digester, reactor M3. Prior to the experiment an acclimatisation period of two retention times at an

OLR of 2 g VS L^{-1} d^{-1} occurred. Subsequently the OLR was increased gradually from 2 to 4 g VS L^{-1} d^{-1} at a fixed HRT of 16 days. After OLR of 2.5 g VS L^{-1} d^{-1} trace elements (Ni, Co, Se, Mb and Fe) were supplemented to ensure a stable fermentation. The initial pH dropped over time from 7 to 6.6 indicating an increase in VFA concentration and a lower buffer capacity. Consequently VFA/TIC (ratio of VFA to alkalinity) rose from 0.21 to 0.49 at the final OLR of 4 g VS L^{-1} d^{-1}. The VFA measurement confirmed the VFA/TIC relationship and revealed an accumulation of acetic and propionic acid (0.42 g L^{-1} and 0.26 g L^{-1} respectively) towards the end of the period at an OLR of 4 g VS L^{-1} d^{-1}. The biological parameters support the conclusion of a stable yet intensified fermentation. The attained methane concentration reached a level of about 54.9-55.8% and the specific methane yield varied between 316.4-326.6 L CH_4 kg VS^{-1}. The observed methane production leads to an energy yield of 11.5-11.8 MJ kg VS^{-1}, and represents an obtainable gas yield of between 64.6-66.3% of the 30 day BMP. The gas yield and composition remained at a constant level although the OLR was gradually increased at a fixed HRT.

Table 3.2. Performance characteristics of the single-stage reactor M3.

Methane reactor		M3	M3	M3	M3
OLR	g VS L^{-1} d^{-1}	2	2.5	3	4
HRT	days	16	16	16	16
pH		7 ±0.1	6.6 ±0.1	6.5 ±0.3	6.6 ±0.3
Methane concentration	vol.-%	55.3 ±1.8	55.0 ±0.8	54.9 ±1	55.8 ±1
Methane yield	L CH_4 kg VS^{-1}	324.5 ±25.5	319.3 ±9.1	326.6 ±26.2	316.4 ±17.9
Methane yield /BMP	%	65.9 ±7.9	64.8 ±2.8	66.3 ±8.0	64.2 ±5.7
Energy yield	MJ kg VS^{-1}	11.7 ±0.92	11.5 ±0.33	11.8 ±0.94	11.4 ±0.65

3.3.4 Two-stage digestion with gradually enhanced OLR

3.3.4.1 Hydrolysis reactor performance

Table 3.3 shows the performance characteristics of the first stage of the two-stage system at increasing organic loading rates. The pre-treated hydrolysis bacteria acclimatised to food waste in a 20 day commissioning phase at an initial OLR of 6 g VS L^{-1} d^{-1}. Thereafter, the hydrolysis reactor was subjected to gradually increased OLR from 6 to 15 g VS L^{-1} d^{-1} at a fixed retention time of 4 days. An average pH of

5.5 prevailed during the whole experimental period. Increased OLR required enhanced daily addition of sodium hydroxide leading to minor pH variations of ±0.5.

The gas obtained in the first stage exclusively consisted of hydrogen and carbon dioxide without any traces of methane. Hydrogen concentrations in the range of 5.6-16.2% were measured, with specific hydrogen yields of 1.7-11.8 L H_2 kg VS^{-1}. The corresponding energy yields in terms of lower heating value (10.8 MJ m^{-3}) account for 0.019-0.127 MJ kg VS^{-1}. Similar hydrogen yields of food waste and low grade biomass sources between 3-16.5 L H_2 kg VS^{-1} have also been reported by other authors assessing two-stage digestion and hydrogen production (Karlsson et al., 2008; Luo et al., 2010; Massanet-Nicolau et al., 2013). It has to be noted that a review study of hydrogen production from agricultural wastes including for food waste by Guo et al. (2010) revealed a wide range of possible yields between 3-196 L H_2 kg VS^{-1}. The purpose of this paper is not however, to generate maximum rates of hydrogen but to optimise the acidification process and hence maximise energy yields and organic loading rates.

The acidification process mainly generated ethanol, lactic acid and volatile fatty acids (C_2-C_6) in a range of 2.39-16.83 g L^{-1}, 0.60-5.44 g L^{-1} and 4.76-15.18 g L^{-1} respectively. Methanol and propanol were not detected. The VFA spectrum was dominated by acetate (2.19-5.34 g L^{-1}), butyrate (0.82-7.13 g L^{-1}), caproate (0.72-2.46 g L^{-1}), propionate (0.35-0.80 g L^{-1}) and valerate (0.14-0.73 g L^{-1}), followed by minor amounts of iso-valerate and iso-caproate and iso-butyrate. The dominance of ethanol, butyric and acetic acid among the liquid fermentation products clearly indicated a mixed type ethanol-butyric acid fermentation (Bouallagui et al., 2004; Chen et al., 2015; Li et al., 2009).

Figure 3.3 relates the generated fermentation products in terms of COD equivalent to the total COD input. It revealed a relatively constant VFA production at a level of approximately 0.15 g COD per g COD added at all loading rates. Consequently, the acidification yield varied between 34.3 and 40.8%. The acidification yield as described in equation (2) may be noted in figure 3.3 as the proportion the lowest line ($S_{t(VFA)}/COD_{added}$) is of the highest line (sCOD represented by hydrolysis yield). These values are in line with Chen et al. (2015) reporting acidification yields between 29-36% for food waste and rice straw fermentation. Orozco et al. (2013)

reported maximum acidification yields for grass silage of 35%. Comparable results for food and vegetable waste of 38.9-44.4% were found by Bouallagui et al. (2004). Higher acidification yields of 56-84% have been obtained by De La Rubia et al. (2009) at retention times of up to 10 days and lower OLR.

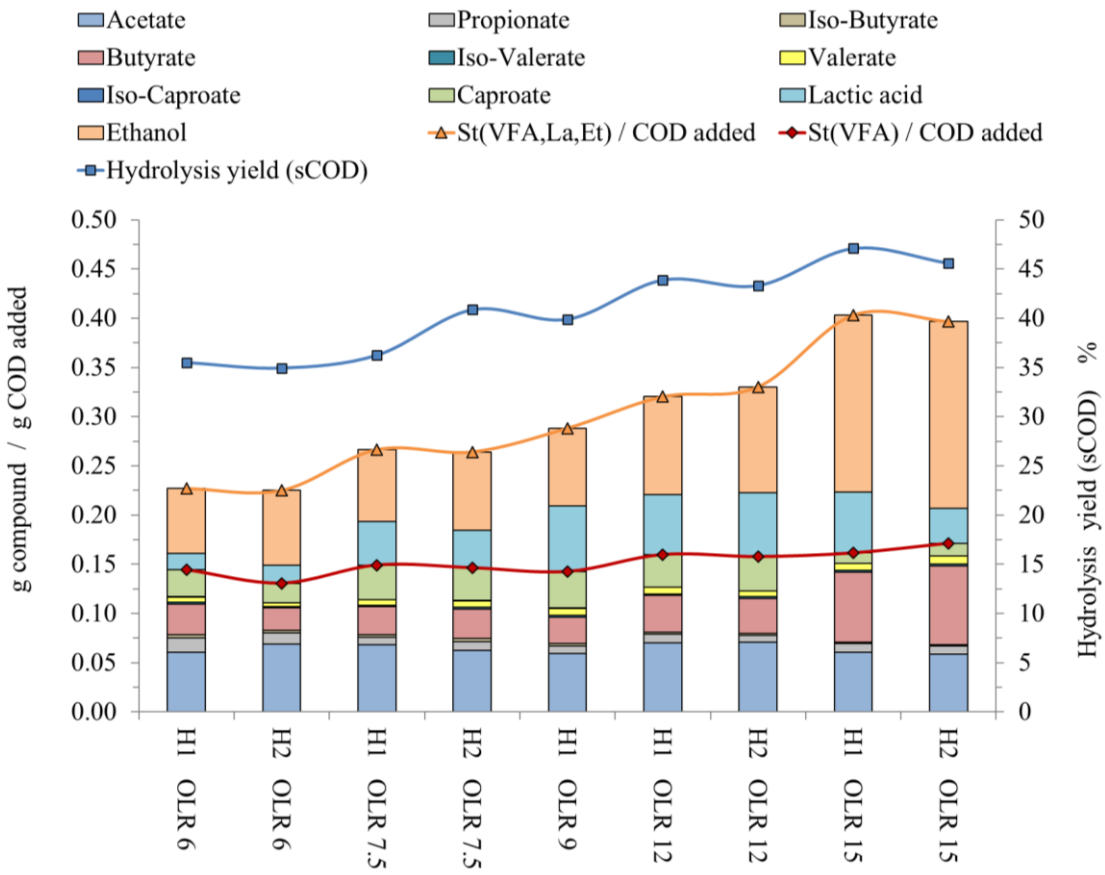

Fig. 3.3 Generated fermentation products in terms of COD added.

Increased OLR resulted in higher quantities of ethanol and lactic acid. The initial rate of 0.083 climbed to 0.242 g COD per g COD added (figure 3.3) for the highest OLR of 15 g VS L^{-1} d^{-1}. Thus, the share of VFA, ethanol and lactic acid after hydrolysis peaked at 88.5% indicating that sCOD mainly consists of these liquid fermentation products. The gap between hydrolysis yield and total amount of liquid fermentation products (referred to as $S_{t(VFA,La,Et)}$) is attributed to other intermediate volatile fermentation compounds and soluble organic matter. This gap was also observed by other authors (Argelier et al., 1998; De La Rubia et al., 2009; Orozco et al., 2013). The solubilisation of COD per unit COD added corresponded with the growth of VFA, lactic acid and ethanol concentrations at increased OLR levels. The obtained

hydrolysis yield was found to be between 34.9-47.1%. This is higher than values obtained by De La Rubia et al. (2009) and Orozco et al. (2013) who reported values of approximately 30% digesting sunflower oil cake and grass respectively. They were as high as those reported by Bouallagui et al. (2004) of 38.9-44.4% from fruit and vegetable waste. The gain in hydrolysis yield at higher OLR was also found by others (Argelier et al., 1998; De La Rubia et al., 2009; Orozco et al., 2013) and were partly attributed to the increased levels of ethanol and lactic acid in this study. This could have been triggered by the daily pH-adjustment with sodium hydroxide, causing enhanced variations of the pH at higher OLR. The increased pH levels of around 6 at the beginning of the daily acidification cycle created more favourable conditions for the butyric producing pathway. The lower pH of 5 at the end of each daily cycle facilitated lactic acid and ethanol production. This is in agreement with Chen et al. (2015) who examined the link between pH, ORP, OLR, HRT and fermentation products in food waste and rice straw fermentation trials.

Table 3.3. Performance characteristics of the first stage of the two-stage system at various organic loading rates.

Hydrolysis reactor (two-stage)		H1	H2	H1	H2	H1[a]	H1	H2	H1	H2
OLR	g VS L^{-1} d^{-1}	6.0	6.0	7.5	7.5	9.0	12.0	12.0	15.0	15.0
HRT	days	4	4	4	4	4	4	4	4	4
pH		5.5 ±0.2	5.5 ±0.2	5.5 ±0.2	5.5 ±0.2	5.5 ±0.3	5.5 ±0.4	5.5 ±0.4	5.5 ±0.5	5.5 ±0.5
Lactic acid	g L^{-1}	0.60 ±0.25	0.67 ±0.44	1.98 ±0.53	1.72 ±0.77	3.61 ±0.38	4.35 ±1.04	4.62 ±1.45	5.44 ±0.3	3.71 ±0.52
Ethanol	g L^{-1}	2.39 ±0.08	2.76 ±0.34	3.26 ±0.42	3.55 ±0.58	4.23 ±0.03	7.08 ±0.22	7.67 ±0.76	15.95 ±1	16.83 ±0.82
Acetate	g L^{-1}	2.19 ±0.2	2.50 ±0.02	3.03 ±0.56	2.80 ±0.3	3.19 ±0.42	4.98 ±0.77	5.04 ±0.61	5.34 ±0.28	5.19 ±0.47
Propionate	g L^{-1}	0.53 ±0.01	0.40 ±0.04	0.35 ±0.05	0.39 ±0.05	0.41 ±0.07	0.64 ±0.14	0.52 ±0.08	0.80 ±0.08	0.74 ±0.03
Iso-Butyrate	g L^{-1}	0.11 ±0.01	0.10 ±0.02	0.12 ±0.01	0.14 ±0.01	0.14 ±0.03	0.13 ±0.04	0.10 ±0.02	0.11 ±0.02	0.09 ±0.01
Butyrate	g L^{-1}	1.14 ±0.14	0.82 ±0.12	1.28 ±0.22	1.34 ±0.1	1.43 ±0.2	2.69 ±0.57	2.56 ±0.53	6.33 ±0.14	7.13 ±0.36
Iso-Valerate	g L^{-1}	0.06 ±0.01	0.05 ±0.01	0.04 ±0.03	0.07 ±0.02	0.10 ±0.01	0.10 ±0.02	0.11 ±0.02	0.14 ±0.01	0.16 ±0.01
Valerate	g L^{-1}	0.19 ±0.02	0.14 ±0.02	0.25 ±0.02	0.30 ±0.04	0.38 ±0.06	0.51 ±0.06	0.45 ±0.04	0.65 ±0.04	0.73 ±0.07
Iso-Caproate	g L^{-1}	0.02 ±0.01	0.01 ±0.01	0.01 ±0.01	0.02 ±0.01	0.03 ±0.01	0.01 ±0.01	0.01 ±0.01	0.01 ±0.01	0.01 ±0.01
Caproate	g L^{-1}	0.99 ±0.26	0.72 ±0.17	1.58 ±0.32	1.49 ±0.21	1.99 ±0.29	2.35 ±0.02	2.46 ±0.12	0.93 ±0.09	1.14 ±0.10
Total VFA	g L^{-1}	5.26 ±0.21	4.76 ±0.12	6.69 ±1.01	6.59 ±0.66	7.78 ±0.98	11.39 ±1.62	11.23 ±1.31	14.30 ±0.42	15.18 ±0.05
Total VFA,LA, Et	g L^{-1}	8.25 ±0.47	8.18 ±0.39	11.94 ±0.96	11.86 ±0.38	15.62 ±1.04	22.82 ±0.57	23.52 ±2.43	35.69 ±0.86	35.71 ±1.20
sCOD	g L^{-1}	12.87 ±0.60	12.67 ±0.50	17.20 ±1.13	18.27 ±0.90	21.47 ±0.99	31.27 ±0.72	30.87 ±1.82	41.70 ±1.6	40.37 ±2.12
Acidification yield (VFA)[b]	%	40.8 ±1.7	37.6 ±0.9	38.9 ±5.9	36.1 ±3.6	36.2 ±4.6	36.4 ±5.2	36.4 ±4.3	34.30 ±1.0	37.6 ±0.1
Acidification yield (VFA,Et,La)[c]	%	64.1 ±3.6	64.6 ±3.0	69.4 ±5.6	64.9 ±2.1	72.7 ±4.9	73 ±1.8	76.2 ±7.9	85.6 ±2.1	88.5 ±3
Hydrolysis yield	%	35.5 ±1.7	34.9 ±1.4	36.2 ±2.4	40.9 ±2.0	39.9 ±1.8	43.9 ±1.0	43.3 ±2.6	47.1 ±1.8	45.6 ±2.4
Hydrogen concentration	vol.-%	7.4 ±2.08	5.6 ±0.99	13.2 ±2.1	10.6 ±3.6	16.2 ±3.0	12.5 ±1.3	10.2 ±1.0	9.9 ±1.1	10.1 ±0.6
Hydrogen yield	L H_2 kg VS^{-1}	2.4 ±1.3	1.7 ±0.7	7.8 ±2.5	5.9 ±2.5	11.8 ±2.1	10.1 ±2.2	7.2 ±1.1	8.9 ±2.1	8.2 ±0.9
Energy yield	MJ kg VS^{-1}	0.026 ±0.01	0.019 ±0.01	0.084 ±0.03	0.064 ±0.03	0.127 ±0.02	0.109 ±0.02	0.078 ±0.01	0.096 ±0.02	0.088 ±0.01

[a] two-stage system 2 (reactors H2 at OLR 9 g VS L^{-1} d^{-1} & M2 at OLR of 3 g VS L^{-1} d^{-1}) was omitted due to experimental difficulties; [b] acidification yield includes for VFA; [c] acidification yield includes for VFA, lactic acid and ethanol.

3.3.4.2 Methane reactor performance

Table 3.4 shows the performance characteristics of the second stage of the two-stage system at increasing organic loading rates. The fermentation process in all methane reactors remained within stable limits as indicated by VFA/TIC values below 0.34 (data not shown). After the OLR of 2.5g VS L^{-1} d^{-1} trace elements (Ni, Co, Se, Mb and Fe) were supplemented to maintain a stable process (as for system 3 single-stage system). The pH remained between 7.5 and 7.9 with a minor increase at higher OLR, due to the increased sodium hydroxide addition in the upstream hydrolysis reactors. There was no evidence of ethanol or lactic acid in methane reactor effluent. The produced VFA in the acidification stages was almost completely destroyed (94.9-97.8%) in the downstream methane reactors. At maximum loading at an OLR of 5 g VS L^{-1} d^{-1} in methane reactor M2, an enhanced total VFA level of 1.5 g L^{-1} was recorded leading to a reduced destruction rate of 91.0%. However, a considerable reduction in SMY was not observed. The methane yield of the two-stage systems ranged between 371.1-419.0 L CH_4 kg VS^{-1} with methane concentrations between 66.7-74.3%. This is in line with Chinellato et al. (2013) and Bouallagui et al. (2004) who found enhanced methane concentrations of 65% and 69-70.6% at yields of 311-484 L CH_4 kg VS^{-1} and 363-450 L biogas per kg COD input respectively for two-stage digestion of fruit and vegetable waste. In comparison to the 30 day BMP test, this represents an obtainable gas yield of 75.3-85.0%. Even though both systems were subjected to the same reactor conditions, there were minor deviations, resulting in energy yields of 13.4-15.1 MJ kg VS^{-1}.

Table 3.4. Performance characteristics of the second stage of the two-stage system at various organic loading rates.

Methane reactor		M1	M2	M1	M2	M1	M1	M2	M1	M2
OLR	g VS L^{-1} d^{-1}	2.0	2.0	2.5	2.5	3.0	4.0	4.0	5.0	5.0
HRT	days	12	12	12	12	12	12	12	12	12
pH		7.5 ±0.1	7.5 ±0.1	7.5 ±0.1	7.5 ±0.1	7.6 ±0.1	7.7 ±0.1	7.7 ±0.1	7.9 ±0.1	7.9 ±0.1
Methane concentration	vol.-%	68.6 ±2.5	69.5 ±1.9	74.3 ±1.5	68.5 ±1.1	72.8 ±0.3	69.2 ±1.1	66.7 ±1.5	70.2 ±0.8	67.6 ±2.9
Methane yield	L CH4 kg VS^{-1}	392 ±12.6	419 ±23.2	371.1 ±5.5	391.2 ±16.7	391.4 ±7.2	373.9 ±10.9	413.9 ±22.6	381.7 ±15.5	389.2 ±31.8
Methane yield / BMP	%	79.6 ±3.2	85 ±5.5	75.3 ±1.5	79.4 ±4.3	79.5 ±1.9	75.9 ±2.9	84 ±5.5	77.5 ±4.1	79 ±8.2
Energy yield	MJ kg VS^{-1}	14.11 ±0.5	15.08 ±0.8	13.36 ±0.2	14.08 ±0.6	14.09 ±0.3	13.46 ±0.4	14.90 ±0.8	13.74 ±0.6	14.01 ±1.2
Total energy yield	MJ kg VS^{-1}	14.14 ±0.4	15.10 ±0.8	13.45 ±0.2	14.15 ±0.6	14.22 ±0.2	13.57 ±0.4	14.98 ±0.8	13.84 ±0.6	14.10 ±1.2

3.3.5 Discussion and performance comparison of single-stage versus two-stage digestion

The single-stage and the two-stage systems were subjected to the same overall reactor conditions in terms of loading rate, temperature (38 °C) and retention time (16 days). As illustrated in figure 3.4 the SMY for each reactor system was relatively constant regardless of the applied organic loading rate. This leads to the conclusion that the performance is significantly impacted by the HRT rather than just the OLR. A correlation between enhanced hydrolysis yields at increased OLR levels and SMY was not detected. The two-stage system proved to have a better energy yield (regardless the applied OLR) than the single-stage system. This suggests that easily degradable substrates such as food waste with high k-values depend less on the overall degree of hydrolysis, rather the fact that hydrolysis in a two-stage system occurred (in contrast to single-stage digestion).

The single-stage reactor only achieved 64.6-66.3% of the BMP (30 days) and 57.6-59.6% of the theoretical biomethane maximum. In contrast, the methane yield obtained from the two-stage system reached 75.3-85.0% of the BMP (30 days) and between 67.7-76.4% of the maximum biomethane potential. This reinforces the advantages of a pre-treating hydrolysis stage. The lower gas yields in the continuous trials may be attributed to the shorter retention times (16 days) and the continuous feed and removal of digestate in the larger reactor as opposed to the longer retention time (30 days) in the idealised small well mixed BMP batch system with an inoculum to substrate ratio of 2:1.

The hydrogen yields account for 1.5-3.0% of the total gas volume. After converting the hydrogen yield into energy content in terms of lower heating value, its value of 0.019-0.127 MJ kg VS^{-1} is further reduced to about 0.45-0.93% of the overall energy yield and is almost negligible (table 3.3 & 3.4). The methane energy yields obtained from the two-stage system ranged between 13.4 and 15.1 MJ kg VS^{-1} and outperformed the single-stage reactor's energy values of 11.5-11.8 MJ kg VS^{-1}. Similar results for two-stage digestion were found by Liu et al. (2013) and Luo et al. (2011) describing energy yields of 14.0 MJ kg VS^{-1} and 13.1 MJ kg VS^{-1} in food/organic waste trials.

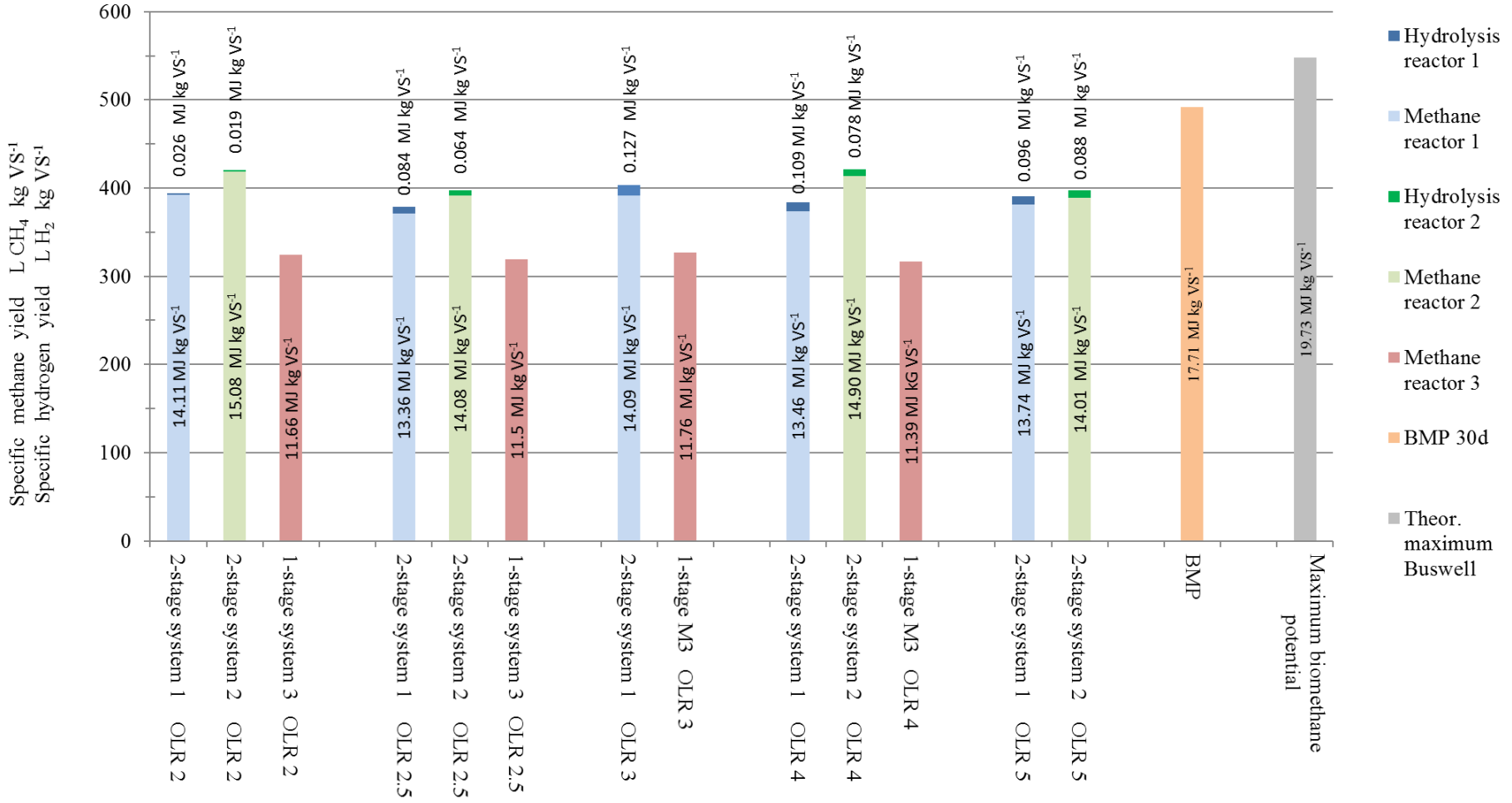

Fig. 3.4 Comparison of single-stage, two-stage, BMP and theoretical biomethane potential (two-stage system reactors H2 at OLR 9 g VS L^{-1} d^{-1} & M2 at OLR 3 g VS L^{-1} d^{-1} were omitted due to experimental difficulties).

In contrast to the single-stage reactor, the two-stage system allows separate gas capture at each stage. Thus, the hydrolysis reactor acts as a carbon dioxide stripping step, reducing the potential costs of biogas upgrading to biomethane (for use as a natural gas substitute). On average this reactor configuration allowed enrichment of the methane content by 14% as compared to the single-stage system. The two-stage system facilitated a rapid degradation of VFAs leading to enhanced SMY. The average gain in SMY was 21-23% in comparison to the single-stage system. This is in agreement with Liu et al. (2013) and Luo et al. (2011) describing enhanced gas yields from organic wastes as compared to the single-stage digestion process.
In a previous study by Browne and Murphy (2014b) the potential of a sequentially fed leach bed system based on similar food waste (to this paper) was assessed. A recirculation between the two separated stages enhanced leaching, but also provoked undesired methane formation in the upstream hydrolysis stage. Besides the advantages of retaining the methanogenic archaea in form of granular sludge, the immobilisation induced operational difficulties and blockages. The system as described in this paper requires neither recirculation nor an immobilisation system for the microbial community. No operational difficulties were faced and no methane was produced in the hydrolysis stage. Up to 76% of the theoretical maximum biomethane potential could be achieved, as compared to 64% in the leach bed UASB system (Browne & Murphy, 2014b).

The key results of this experiment are contrasted with other literature studies in table 3.5. Such a comparison remains very dependent on the experiment conditions as most studies either focus on hydrolysis or hydrogen production. In accordance with this study, short retention times (1-4 days) and moderate to high loading rates (4-20 g VS L^{-1} d^{-1}) in the first stage appeared to favour optimum conditions for hydrolysis. Thus, acidification (9.5-84%) and hydrolysis yields (15.8-44.4%) obtained by Bouallagui et al. (2004), Chen et al. (2015), De La Rubia et al. (2009) and Orozco et al. (2013) were matched with acidification (64.1-88.5%) and hydrolysis yields (34.9-47.1%) of this study. The benefits of the deployed fermentation strategy can be found in the high solubilisation of COD (hydrolysis yield of 34.9-47.1%) at low hydrogen production in the first stage and higher SMY at elevated methane content in the second stage. Thus, the SMYs of 371-419 L CH_4 kg VS^{-1} were comparable to reported results of

270-484 L CH_4 kg VS^{-1} (Chinellato et al., 2013; Luo et al., 2011; Massanet-Nicolau et al., 2015; Orozco et al., 2013). The SMY was similar to more complex reactor configurations such as anaerobic sequencing batch reactors or leach bed reactors with 209-450 L CH_4 kg VS^{-1} (Bouallagui et al., 2004; Browne & Murphy, 2014b).

Table 3.5. Results of two-stage fermentation reported in literature.

Reference	Substrate	Reactor operation mode	First stage					Second stage				
			HRT	OLR	Acidification yield	Hydrolysis yield	SHY	HRT	OLR	SMY	CH_4 - content	Single vs. two-stage
			d	g VS L^{-1} d^{-1}	%	%	L H_2 kg VS^{-1}	d	g VS L^{-1} d^{-1}	L CH_4 kg VS^{-1}	vol.-%	% increase
Bouallagui et al., 2004	Fruit and vegetable waste	Two-stage ASBR[e]	3	3.7-10.1[a]		38.9-44.4[f]		10	0.72-1.65	363-450[b]	69-71	
Browne & Murphy, 2014b	Food waste	Leach bed, UASB	18-30[c]	7.1-11.8[a]				0.56[d]	7.1-11.8	209-384	55.9-63.7	
Chen et al., 2015	Food waste rice straw	Batch BMP	8	4-12	29-36					423-535	58-63	
Chinellato et al., 2013	Food waste rice straw	Two-stage CSTR	3	15-25			0-117	12	3-6	311-484	61.2-65.6	
De La Rubia et al., 2009	Sunflower cake	Two-stage CSTR	8-15	4-9	56-84	20.5-30.1						
Luo et al., 2011	Organic wastes	Two-stage CSTR	1-3	12-18			40-48	12-14	3-4.5	320-344		4.5
Massanet-Nicolau et al., 2013	Wheat pellets	Two-stage CSTR	0.75	66.6			7	20	2.5	359	55.7-58.4	37
Massanet-Nicolau et al., 2015	Grass	Two-stage CSTR	0.75	66.6			6.7	19.3	2.6	349		12.7
Orozco et al., 2013	Grass	Batch BMP	2-10	1-6.5	9.5-35.9	15.8-30.5		20	1-6.5	270-368		30
This experiment	Food waste	Two-stage CSTR	4	6-15	64.1-88.5	34.9-47.1	1.7-11.8	12	2-5	371-419	66.7-74.3	23

[a] on a COD basis (g COD L^{-1} d^{-1}); [b] on a COD basis (L CH_4 kg COD^{-1}); [c] solid retention time; [d] recirculation of leachate; [e] anaerobic sequencing batch reactors; [f] derived from values provided.

3.4 Conclusion

Variations in loading rate impact the solubilisation of substrate in the first stage of a two-stage system; the highest solubilisation was achieved at an OLR of 15 g VS L^{-1} d^{-1}. Low hydrogen yields resulted in minimal energy in the hydrolysis gas; over 99% of energy in biogas originated from the second stage. Upstream hydrolysis facilitated much shorter retention times and higher loading rates while increasing methane concentration and yield. The SMY (75.3-85.0% of BMP) was independent of organic loading. The methane yield was more dependent on reactor configuration and retention time rather than organic loading rate.

3.5 Supplementary data

Dilution of substrate input:

The key focus of chapter 3 is to investigate in detail the acidification process at constant HRT and increasing OLR. Diluting the substrate with corresponding amounts of water and adjusting the pH with sodium hydroxide in the upstream hydrolysis reactor allowed active control of the reactor conditions while the retention time and working volume remained constant with a change in loading. The setup of the study focused on in depth analysis of sCOD composition and the quantification of reactor performance at reduced HRT. The dilution with water facilitated a comparison of single and two-stage digestion while actively reducing retention time. Without the addition of water, a reduction in retention time would not be feasible and undermine the objectives of the study. However, this setup is subjected to certain limitations. It has to be noted that this setup reflects an academic approach and is not intended to compare to upscaled reactor configurations or replicate industrial feed stock. The introduced rates of water and sodium hydroxide exceed any feasible addition to full-scale systems. They would excessively contribute to operational costs and dischargeable digestate quantities. Furthermore, most food wastes exhibit a high level of protein, contributing to high levels of NH_4 in the digestate. The addition of water reduces the NH_4 concentration within the system to a level not considered inhibitory to the subsequent methanation stage (Banks et al., 2012).

Two-stage digestion of food waste as an alternative to single-stage:

Food waste with high degradability is amenable to low retention times and high organic loading rates (Banks & Heaven, 2013; Browne & Murphy, 2014b). Both, single and two-stage systems are capable of fully exploiting the potential SMY (Browne et al., 2014; Browne & Murphy, 2014b). In commercial scale, economic considerations and cost reduction ultimately define the design and choice of any anaerobic digestion system. Thus, single-stage digestion systems have demonstrated to be the prevailing technology providing a stable and reliable process (Banks & Heaven, 2013).

However, the employed reactor configuration is dependent on a variety of process and design criteria. Any single-stage food waste processing plant operating with an

upstream food waste storage vessel, essentially reflects a two-stage system. The first stage reactor may be seen as both a pre-treatment and storage system for feedstock such as food waste. This allows just in time storage of highly degradable substrate in the first reactor, without any associated methane production or aerobic fouling. Therefore, the methane production is decoupled from the actual substrate delivery and feeding. The downstream biogas production can be controlled by a variable feed rate of pre-acidified substrate into the second reactor. This allows just in time production of biogas and the realisation of new revenue opportunities such as demand driven electricity production, without necessitating additional gas storage to the system. As an alternative, the partial segregation of carbon dioxide in the upstream hydrolysis reactor generates a biogas rich in methane in the second reactor facilitating gas grid injection.

The outlined advantages potentially can justify a more complex two-stage system as compared to single-stage. However, for low complex substrates such as food waste the SMY of a single-stage may align with a two-stage system after longer retention. In conclusion, a thorough case-to-case techno-economic assessment is needed to establish and validate the proven benefits of a two-stage system. A general recommendation of two-stage systems exceeding the overall performance of a single-stage system for commercial application can not be derived from this study.

Evaluation, accuracy and interpretation of laboratory data:

Laboratory experiments beyond small scale batch trials are associated with substantial expenditure of time and financial efforts. Rather than using a series of statistically amenable low volume reactors (135 to 400 ml), it was decided to utilize upscaled 1.35 to 4 L reactors. The elevated reactor volumes reduce interfering influences on the quality of the results, such as particle size to reactor ratio effects, sampling volumes, etc. Thus, a data basis to ensure valid statistical assessment within the continuous experiments in chapter 3 was not given. Instead, the lab scale experiments were conducted in an ongoing sequence, subsequently moving from lower to higher loading. The results of the acclimatisation period after each increase in loading rate were not taken into consideration (this period is equated to the first HRT after change in loading rate). The subsequent two retention times represent the data basis for the experimental evaluation. Results were based on averages of the

subsequent two periods of hydraulic retention time at that loading rate and replication on the fact that each day is a replication of the day before. However, a statistically significant difference between single- and two-stage digestion was not established. The results are based on numerical difference.

Hydrogen production in two-stage digestion:

A calculation estimating the theoretical maximum hydrogen production based on the obtained volatile fatty acid, lactate and ethanol spectrum in all hydrolysis reactors is given in table 3.6, 3.7 and 3.8. Theoretical maximum hydrogen production rates per input of food waste were calculated in the range 58 to 124 L H_2 kg VS^{-1}. The theoretic calculation identifies the maximum possible stochiometric yield, not necessarily reached by the microbial degradation pathway. The obtained 1.7 to 11.8 L H_2 kg VS^{-1} obtained in this study correspond to 2.6 to 15.4 % of the theoretical maximum hydrogen production. It has to be noted that a review study of hydrogen production from agricultural wastes including for food waste by Guo et al. (2010) revealed a wide range of possible yields between 3-196 L H_2 kg VS^{-1}. The actual and calculated hydrogen production both remain within this identified range. The established range could be explained by individual process parameters and pathways of fermentation. Any deviation from the predicted maximum hydrogen production range could also be influenced to some extent by potential hydrogen leakage from the reactor system.

If the upstream hydrolysis gas is segregated, the associated loss of hydrogen adversely impacts the overall energy yield. Considering the calculated maximum hydrogen yields in terms of lower heating value (average of 0.93 MJ kg VS^{-1}), between 4.2 and 8.9% of the total energy produced would originate from the first stage. It is understood that with an increase in hydrogen production the single-stage system improves its competitiveness. However, the average hydrogen energy yield of 0.93 MJ kg VS^{-1} may only reduce but not compensate the gap in total average energy yield between single (11.6 MJ kg VS^{-1}) and two-stage (14.09 MJ kg VS^{-1}) at the given 16 days retention time. As an alternative the produced hydrolysis gas may be injected into the downstream second reactor or utilised for power to gas applications.

Table 3.6. Theoretic stochiometric hydrogen production from food waste

Acetate:	$C_{18.2}H_{30}O_{10.6} + 8\ H_2O \rightarrow 5\ H_2 + 9.1\ C_2H_4O_2$
Propionate:	$C_{18.2}H_{30}O_{10.6} + 3\ H_2O \rightarrow 1\ CO_2 + 1\ H_2 + 5.7\ C_3H_6O_2$
(Iso) Butyrate:	$C_{18.2}H_{30}O_{10.6} + 1.4\ H_2O \rightarrow 2\ CO_2 + 4.1\ C_4H_8O_2$
(Iso) Valerate:	$C_{18.2}H_{30}O_{10.6} + 1\ H_2O \rightarrow 2.6\ CO_2 + 3.15\ C_5H_{10}O_2$
Lactate:	$C_{18.2}H_{30}O_{10.6} + 7.6\ H_2O \rightarrow 4.5\ H_2 + 6.1\ C_3H_6O_3$
Ethanol:	$C_{18.2}H_{30}O_{10.6} + 7.5\ H_2O \rightarrow 6\ CO_2 + 4.2\ H_2 + 6.1\ C_2H_6O$

Table 3.7. Theoretical calculation of hydrogen production in the hydrolysis reactors (example given for acetate in H1).

$C_{18.2}H_{30}O_{10.6} + 8\ H_2O \rightarrow 5\ H_2 + 9.1\ C_2H_4O_2$ (it is assumed that volatile solids compounds only consist of C, H, O).
0.55 mol H_2 / mol $C_2H_4O_2$, with 22.4 L mol^{-1} equates to 12.31 L H_2 / mol $C_2H_4O_2$.
With 60 g mol^{-1} $C_2H_4O_2$ this equates to 0.21 L H_2 / g $C_2H_4O_2$.
0.3375 L digestate exit the hydrolysis reactor H1 per day with an acetate level of 2.19 g L^{-1}.
This equates to an acetate related hydrogen production of 18.7 L H_2 / kg VS of food waste in H1.
Similar calculation pathway for propionate, (iso) butyrate, (iso) valerate, lactate and ethanol and remaining hydrolysis reactors.
With 6 kg VS L^{-1} d^{-1} entering the 1.35 L hydrolysis reactor, the theoretical maximum hydrogen production originating from volatile compounds (VFA, lactate and ethanol) in digestate of H1 results in 58 L H_2 kg VS^{-1} of food waste,

Table 3.8. Maximum theoretic hydrogen production with analysed compounds of VFA, lactate and ethanol quantities at increasing OLR.

Hydrolysis reactor		H1	H2	H1	H2	H1[a]	H1	H2	H1	H2
OLR		6	6	7.5	7.5	9	12	12	15	15
Experimental H_2 yield	L H_2 kg VS^{-1}	2.4 ±1.3	1.7 ±0.7	7.8 ±2.5	5.9 ±2.5	11.8 ±2.1	10.1 ±2.2	7.2 ±1.1	8.9 ±2.1	8.2 ±0.9
Max. theor. H_2 yield	L H_2 kg VS^{-1}	58	65	70	70	76	88	93	124	123
Max. theor. H_2 energy yield	MJ kg VS^{-1}	0.63	0.71	0.76	0.76	0.83	0.95	1.01	1.35	1.34

Chapter 4: Role of trace elements in single and two-stage digestion of food waste at high organic loading rates

Role of trace elements in single and two-stage digestion of food waste at high organic loading rates

M. A. Voelklein[1, 2], R. O' Shea[1, 2], A. Jacob[1, 2], J. D Murphy [1, 2]

[1]MaREI Centre, Environmental Research Institute (ERI), University College Cork (UCC), Ireland

[2]School of Engineering, UCC, Ireland

Abstract

This study investigated trace element deficiency and supplementation in mono-digestion of food waste. A single-stage system was contrasted to a two-stage system (hydrolysis followed by methanogenisis). Initial hydrolysis is beneficial as it releases hydrogen sulphide, while the prevailing pH prevents an associated H_2S induced precipitation of trace elements. Stable digestion took place without TE supplementation until an organic loading rate of 2.0 g VS L^{-1} d^{-1}; this was followed by severe instability at an OLR of 2.5 g VS L^{-1} d^{-1} in both systems. A major accumulation of volatile fatty acids inhibited methanogenic activity. A gradual deterioration of pH, VFA/TIC and specific methane yields provoked reactor failure. The benefit of enhanced TE availability in the two-stage system was not apparent due to the complete absence of essential TE in the feed stock. Supplementation of deficient TE Co, Fe, Mo, Ni and Se induced recovery, reflected by an immediate improvement of VFA/TIC and VFA concentrations in both systems. Specific methane yields were restored and maintained at initial levels. At a 16 day retention time, elevated loading rates as high as 5 g VS L^{-1} d^{-1} allowed stable digestion with TE supplementation.

Keywords: biogas; two-stage digestion; food waste; trace elements; high performance.

4.1 Introduction

Anaerobic digestion has become one of the dominant treatment technologies for all kinds of wet organic wastes. In particular, source segregated food waste is a very suitable substrate for AD due to its high biodegradability and volatile solids (VS) content (Browne et al., 2014). A sufficient level of all macro- and micro-nutrients is a vital prerequisite for key enzymes and microbes associated with stable methanogenesis (Demirel & Scherer, 2011; Drosg, 2013; Kida et al., 2001). All essential macro-nutrients, such as calcium (Ca), magnesium (Mg), nitrogen (N), phosphorus (P), potassium (K), sodium (Na) and sulphur (S), are available in food waste. However, mono digestion of food waste is challenging due to a lack of a sufficient level of micro-nutrients (or trace elements) such as cobalt (Co), iron (Fe), nickel (Ni), molybdenum (Mo) and selenium (Se) (Banks et al., 2012; Moestedt et al., 2016; Nges et al., 2012). Recent studies have reported a deficiency in trace elements in single-stage digestion of crop and waste based substrates (Banks et al., 2012; Karlsson et al., 2012; Wall et al., 2014; Zhang & Jahng, 2012). If the substrate is deficient in nutrients, the process performance diminishes or even fails (Drosg, 2013; Gustavsson et al., 2011; Schmidt et al., 2014; Zhang & Jahng, 2012).

In an analysis of full scale biogas plants Lemmer et al. (2010) attributed a 10-50% performance reduction per unit reactor volume to digester systems with insufficient trace elements. The accessibility of trace elements is constrained by its bioavailability (Karlsson et al., 2012; Ortner et al., 2015). In order to be available for methanogenic archaea, trace elements have to be soluble and neither be fixed in precipitated compounds (such as sulphates, sulphides, or carbonates) nor adsorbed. Ortner et al. (2014) established that 30-70% of present trace elements were not bioavailable to the microbial community.

The advantages of two-stage digestion systems potentially facilitate an increased resilience towards a deficiency of trace elements. The spatial separation with different pH in the two stages provides optimum conditions for individual anaerobic digestion phases. The substrate is initially broken down into macro-molecules and liquid fermentation products in the first reactor (Voelklein et al., 2016a). Firstly, this is associated with superior performances in terms of methane yields and process stability as compared to the single-stage system (Chen et al., 2015; Luo et al., 2011;

Voelklein et al., 2016a). Secondly, the high degree of initial substrate acidification and degradation (Voelklein et al., 2016a) releases major sulphur contents as hydrogen sulphide into the first reactor. The pKa for the first dissociation of H_2S is 6.99 (Waechter, 2012). The low pH of approx. 5 causes the hydrogen sulphide to be mainly present in its very volatile state of H_2S, rather than in its more soluble conjugate base, the bisulfide ion HS^- at more neutral pH (Waechter, 2012). As hydrogen sulphide is known to precipitate trace metals (Gustavsson et al., 2011; Karlsson et al., 2012), the upstream release potentially improves the bioavailability of these decisive elements. In addition, the actual load of sulphur entering the downstream methane reactor at neutral pH is diminished and limits the associated precipitation of trace elements. In contrast, in a single-stage reactor at neutral pH (without upstream treatment), approximately 50% of hydrogen sulphide is available as bisulfide ion HS^- (pKa 6.99) to potentially precipitate trace elements (Waechter, 2012).

A general recommendation on optimal nutrient concentrations remains challenging. The microbial community involved in the biogas process is composed of a huge variety of microorganisms with differing nutrient requirements. In addition, bioavailability and feedstock concentration of trace metals, temperature, loading and associated growth rate of microbes determine the demand of nutrient supplementation (Ortner et al., 2014; Uemura, 2010; Zhang et al., 2003). However, addition of deficient elements proved to be vital in stabilizing the digestion process and overcoming biological limitations (Demirel & Scherer, 2011; Karlsson et al., 2012; Nges et al., 2012; Pobeheim et al., 2011; Qiang et al., 2012; Ward et al., 2008). Banks et al. (2012) established a minimum trace element level for Co (0.22 mg L^{-1}) and Se (0.16 mg L^{-1}) in digestion of food waste from the UK. In their study of trace element requirements for stable food waste digestion at elevated ammonia concentrations, supplementation at levels of Co (1.0 mg L^{-1}), Fe (5.0 mg L^{-1}), Mo (0.2 mg L^{-1}), Ni (1.0 mg L^{-1}), Se (0.2 mg L^{-1}) and tungsten (W) (0.2 mg L^{-1}) were required (Banks et al., 2012). Zhang and Jahng (2012) reported addition of Co (2 mg L^{-1}), Ni (10 mg L^{-1}), Mo (5 mg L^{-1}) and Fe (100 mg L^{-1}) in digestion of food waste in Korea. A study by Zhang et al. (2015) described stable fermentation of food waste at loading rates as high as 5.0 g VS L^{-1} d^{-1} while supplementing Co (1 mg L^{-1}), Ni (1 mg L^{-1}), Se (0.2 mg L^{-1}) and Fe (5 mg L^{-1}). Gustavsson et al. (2011) suggested

supplementation of Co (0.5 mg L^{-1}), Ni (0.3 mg L^{-1}) and Fe (0.5 g L^{-1}) for digestion of wheat stillage; addition of Se and W produced no effect. Sole supplementation of Ni, Mo or Co proved to be insufficient (Moestedt et al., 2016; Zhang & Jahng, 2012).

The addition of trace elements to sustain stable fermentation ranged between 0.05-10 mg L^{-1} for Co, 5-500 mg L^{-1} for Fe, 0.0272-5 mg L^{-1} for Mo, 0.035-10 mg L^{-1} for Ni and 0.056-0.2 mg L^{-1} for Se (Banks et al., 2012; Gustavsson et al., 2011; Lemmer et al., 2010; Moestedt et al., 2016; Nordell et al., 2016; Pobeheim et al., 2011; Qiang et al., 2012; Zhang & Jahng, 2012; Zhang et al., 2012; Zhang et al., 2015). Further trace metals such as manganese (Mn), tungsten and zinc (Zn) are rarely supplemented and usually not considered to be deficient for digestion. Overdosing of trace metals reduces enzyme and microbial activity (Lemmer et al., 2010).

The key role of trace element addition and its microbiological impact in anaerobic digestion has been of major interest in recent studies. Long-term studies have assessed conditions provoking reactor failure and subsequent reactor recovery after trace element supplementation. However, research evaluating the implications of trace element deficiency in two-stage systems is not to be found. This study expands upon previous work on increasing loading rates in mono-digestion of food waste in two-stage digestion (Voelklein et al., 2016a). The objective in this work is to assess the effect of trace elements on mono-digestion of source segregated food waste in single and two-stage systems. The emphasis is not to analyse optimal concentrations of trace elements, but to determine the impact of trace element deficiency and its response after supplementation.

4.2 Materials and Methods

4.2.1 Design of experiment

The experiment investigated the impact of trace element depletion and subsequent supplementation in different reactor configurations; a duplicate two-stage system (M1 & M2) and a conventional single-stage reactor (M3). The reactors were tested with the same substrate (source segregated food waste) with stepwise increasing organic loading rates. The reactors were fed once per day. The input substrate of the first stage displaced a certain amount of effluent being introduced into the second

stage. Samples for analysis were obtained on a weekly basis from substrate, effluent stage one and stage two. Biological parameters such as pH, VFA, VFA/TIC and specific methane yield were assessed as indicators of reactor stability and performance. The single- and two stage experiments were performed at mesophilic conditions (38 °C) using 5 L CSTRs with vertically mounted stirrers. The actual working volume for the first stage hydrolysis reactors was 1.35 L. The working volume was 4 L for the subsequent methane reactors. The reactor volume of the single-stage system corresponded to the 4 L methane reactor volume of the two-stage system.

The hydraulic retention time in the two-stage system was fixed at 4 days in the upstream hydrolysis reactor and 12 days in the downstream methane reactor. This matched the 16 day retention time of the single-stage reactor M3. The retention time was achieved by diluting the substrate with specified amounts of water. The experiment was commenced with an initial acclimatisation phase of 20 days. After reaching steady state conditions (after at least 3 HRTs) the organic loading rate of M1 and M2 was increased gradually from 2 to 5 g VS L^{-1} d^{-1}. The loading rate for the single-stage reactor (M3) was increased from 2 to 4 g VS L^{-1} d^{-1}.

4.2.2 Inoculum and substrate

The inoculum was obtained from a single-stage digester fed grass silage and food waste. The source segregated food waste was obtained from a local waste management company collecting food waste from major catering premises. Approximately 80 kg of food waste was first manually screened and non-biodegradable contaminants like bones and plastics were removed. The residual food waste was subsequently shredded in a mechanical meat mincer to a pasty consistence with particle size between 0.5 to 5mm. It was stored at a temperature of -20 °C until fed to the anaerobic reactors. A total solids content of 24.63 ± 0.72% with a share of 94.29 ± 0.64% present as volatile was determined. The pH yielded in 5.1 ± 0.05 with a C:N ratio of 14.86. The physical and chemical characteristics of the substrate were analysed and are further described in Voelklein et al. (2016a).

4.2.3 Analytical methods

VFA/TIC was measured using the Nordmann-method (Nordmann, 1977). This parameter indicates the ratio of volatile fatty acids to buffering capacity. The concentrations of individual volatile fatty acids were analysed with gas chromatography (Hewlett Packard HP6890) using a Nukol^{TM} fused silica capillary column (30 m × 0.25 mm × 0.25 µm) and a flame ionization detector. Hydrogen was used as a carrier gas. All metal elements except selenium were analysed according to DIN EN ISO 11885 with inductively coupled plasma optical emission spectrometry (ICP-OES); selenium was determined according to DIN EN ISO 17294-2 (E29) with inductively coupled plasma mass spectrometry (ICP-MS). Biogas composition was analysed for CH_4, CO_2, H_2, O_2 and N_2 using a Hewlett Packard HP6890 gas chromatograph equipped with a Hayesep R packed GC column (3 m x 2 mm, mesh range of 80-100) and a thermal conductivity detector. Argon was used as carrier gas. Certified gas standards were employed for the standardization of hydrogen, methane and carbon dioxide. The utilised analytical methods are further described in Voelklein et al. (2016a).

4.2.4 Recognising reactor failure and corrective measures

The reason for reactor failure can be found mainly in organic overload, inadequate mixing, enhanced dry solids content of digestate in the reactor, temperature changes, ammonia inhibition, inhibitory substances in the feed stock or undersupply of trace elements (Drosg, 2013). Close process monitoring allows identification of changes in parameters such as pH, VFA/TIC, VFA, hydrogen concentration, biogas quality and quantity. The reactor specific interpretation and comparison of those parameters allows establishment of a characteristic baseline and immediate recognition when deviating from the norm. Strategies to counteract depend on the initial circumstances causing reactor failure. Pathways to recovery include for a reduction/cessation of feedstock, elevation of pH, dilution with water or digestate, supplementation of deficient nutrients and are always accompanied with close process monitoring.

4.3 Results

4.3.1 Nutrient supplementation

The food waste contained trace element metals Cu, Fe, Ni, Mn and Zn in the range of 0.42-31.5 mg L^{-1} (Table 4.1). Some of the key trace elements for anaerobic digestion (such as Co, Mo, Ni and Se) were undersupplied and partly below the detection limit. A similar trace element spectrum in food waste was also found in other studies (Banks et al., 2012; Qiang et al., 2012; Zhang & Jahng, 2012). The low concentrations in the substrate were further reflected by the decreased values found in the effluent of the reactors once they became critically unstable (Table 4.1).

Table 4.1. Trace element levels in food waste, in digestate at reactor failure, reported range of nutrients added in literature and nutrients added to feed stock.

Element	Unit	Food waste	M1[b]	M2[b]	M3[b]	Nutrients added in literature	Nutrients added to feed stock
Iron (Fe)	mg L^{-1} ww	31.5	21.6	25.6	19.7	5-500	160
Manganese (Mn)	mg L^{-1} ww	6.9	0.87	0.86	1.6	-	-
Zinc (Zn)	mg L^{-1} ww	7.3	0.83	0.84	1.6	-	-
Copper (Cu)	mg L^{-1} ww	1.3	0.78	1.0	1.2	-	-
Nickel (Ni)	mg L^{-1} ww	0.42	0.039	0.32	0.75	0.035-10	1
Molybdenum (Mo)	mg L^{-1} ww	< LD[a]	0.028	0.043	0.092	0.0272-5	0.2
Cobalt (Co)	mg L^{-1} ww	< LD[a]	0.019	< LD[a]	0.019	0.05-10	1
Selenium (Se)	mg L^{-1} ww	< LD[a]	< LD[a]	< LD[a]	< LD[a]	0.056-0.2	0.2
Cadmium (Cd)	mg L^{-1} ww	< LD[a]	< LD[a]	< LD[a]	< LD[a]	-	-

[a] <LD, lower than detection limit of 0.5 mg kg^{-1} dry solids; [b] at OLR 2.5 g VS L^{-1} d^{-1} after reactor failure; mg L^{-1} corresponds to mg kg^{-1} (density neglected for comparison reasons); ww: wet weight.

The experiment commenced at a low OLR of 2 g VS L^{-1} d^{-1} without any nutrient addition. Once the experiment became critically unstable, trace element supplementation commenced. The trace elements added to the feedstock of the methane reactors were designed to contain the deficient elements Co, Fe, Mo, Ni and Se according to Table 4.1. The level of trace elements in the feedstock and trace element solution consequently determines the concentration of trace elements in the digestate, with a minor increase due to conversion of solid matter into gas. The

selected concentrations for supplementation in this experiment followed levels most frequently applied and recommended in literature (Banks et al., 2012; Gustavsson et al., 2011; Zhang & Jahng, 2012; Zhang et al., 2015). Thus 1 mg L^{-1} Co, 160 mg L^{-1} Fe, 0.2 mg L^{-1} Mo, 1 mg L^{-1} Ni and 0.2 mg L^{-1} Se were added to the feedstock (Table 4.1). In the present study Co was added in the form of $CoCl_2 \cdot 6H_2O$, Fe as $FeCL_3 \cdot 6H_2O$, Mo as $H_{24}Mo_7N_6O_{24} \cdot 4H_2O$, Ni as $Cl_2Ni \cdot 6H_2O$ and Se as Na_2SeO_3. Trace elements were introduced in the single-stage reactor and the methane reactor of the two-stage system. Adequate amounts of Fe were added to precipitate emerging hydrogen sulphide to iron sulphur compounds. The bioavailability of supplemented trace elements in dissolved form was sufficient for the methanogenic archaea (Gustavsson et al., 2013; Ortner et al., 2015).

4.3.2 Single-stage reactor performance

4.3.2.1 Process performance until reactor failure

Figure 4.1 shows the performance of the single-stage reactor M3 during the 360 day operation period. After an initial commissioning period of two hydraulic retention times (equivalent to 32 days), the reactor was set at an OLR of 2 g VS L^{-1} d^{-1} and the SMY stabilised at 324.5 ±25.5 L CH_4 kg VS^{-1}. The pH and VFA/TIC values showed a minor deterioration towards the end of OLR 2 g VS L^{-1} d^{-1}. This phenomenon was explained with a decrease in measured TIC values, provoking reduced buffer capacity, raising the ratio of VFA/TIC and lowering the pH values. However, low VFA/TIC values of on average 0.21 indicated stable conditions during the overall steady state period at OLR 2 g VS L^{-1} d^{-1} (Table 4.2), as VFA/TIC ratios below 0.4 are associated with stable reactor performance (Drosg, 2013). Low VFA levels of 0.3 g L^{-1} (Table 4.2), and constant SMY, further strengthened the conclusion of stable reactor conditions. A further increase in loading rate to an OLR of 2.5 g VS L^{-1} d^{-1} was immediately accompanied by a subtle increase of VFA/TIC, enhanced VFA and declining pH. However, a decrease of the key reactor performance SMY was only gradually observed. After a continuous drop in gas production over the period of 3 HRTs, a significant deterioration of process parameters (pH, VFA/TIC, VFA) caused a distinct drop in SMY (Figure 4.1). After 3.5 HRTs at an OLR of 2.5 g VS L^{-1} d^{-1} the methane content decreased to

30.5 vol.-% and the pH dropped by 1 unit to 5.4 in only 5 days, emphasising the dynamic development in the final stage of failure. The acid consuming acetoclastic methanogens could not keep pace with the rising levels of total VFA (4.32 g L^{-1}) and were further inhibited by this accumulation. At the peak of reactor failure (day 133) SMY fell to levels as low as 82.7 L CH_4 kg VS^{-1} and a VFA/TIC value of 1.57 clearly emphasised the irreversible state, exceeding stable VFA/TIC levels of below 0.4 (Drosg, 2013). This development was attributed to major trace element depletion as confirmed by laboratory analysis in Table 4.1.

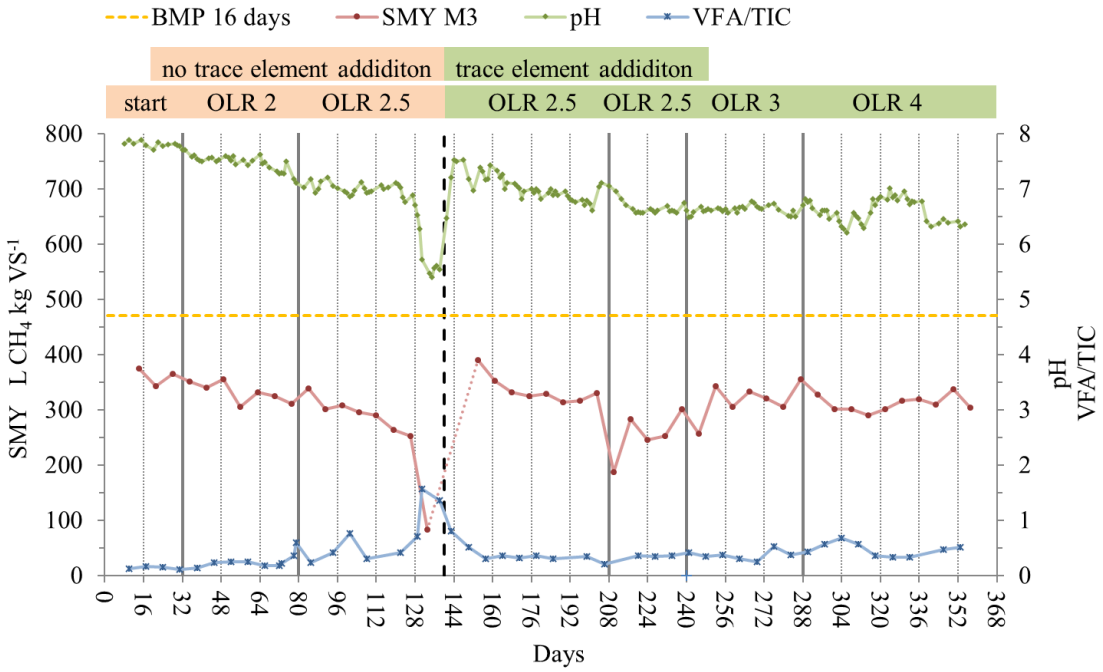

Fig. 4.1 Single-stage reactor performance before and after trace element supplementation (dotted line for SMY M3 on day 133-154 represents feeding stop for 14 days to facilitate recovery after reactor failure; calculation of SMY not applicable; stabilisation of pH with NaOH and commencement of trace element supplementation on day 140; experimental difficulties on day 208-240 with gas measuring equipment).

After severe reactor failure on day 133, it was decided to stop feeding (Figure 4.1). In order to facilitate microbiological recovery, on day 140 the pH was adjusted to neutral levels with sodium hydroxide and trace element supplementation was initiated (Table 4.1). After VFA/TIC levels dropped and a distinct improvement in gas quality and production were observed (day 147), it was decided to recommence feeding. The OLR of 2.5 g VS L^{-1} d^{-1} was further maintained for 4 HRTs. Neither an

increase in VFA/TIC, nor a significant reduction in pH was determined. The SMY reached a plateau of 319.3 ± 9.1 L CH_4 kg VS^{-1} and regained the levels achieved before reactor failure. The experiment continued with trace element addition for another 160 days with elevating OLRs. The SMY remained at 326.6 ± 26.2 and 316.4 ± 17.9 L CH_4 kg VS^{-1} at an OLR of 3 and 4 g VS L^{-1} d^{-1} respectively. The reactor performed at healthy conditions with only a minor rise in VFA and VFA/TIC. However, pH never reached the initial values of 7 again which was attributed to the gradually enhanced OLR. Table 4.2 summarises the performance characteristics of each steady state.

Table 4.2. Performance characteristics of single-stage reactor M3 at each steady state.

		M3	M3[a]	M3	M3	M3
Trace element addition		no	no	yes	yes	yes
OLR	g VS L^{-1} d^{-1}	2	2.5	2.5	3	4
HRT	days	16	16	16	16	16
pH		7 ±0.1	5.4	6.6 ±0.1	6.5 ±0.3	6.6 ±0.3
VFA/TIC		0.21 ±0.02	1.57	0.38 ±0.04	0.45 ±0.11	0.49 ±0.03
Acetate	g L^{-1}	0.16 ±0.07	1.25	0.18 ±0.02	0.31 ±0.11	0.42 ±0.04
Propionate	g L^{-1}	0.08 ±0.04	1.88	0.06 ±0.01	0.15 ±0.09	0.26 ±0.01
Iso-Butyrate	g L^{-1}	0.03 ±0.03	0.35	0.03 ±0.01	0.03 ±0.01	0.02 ±0.01
Butyrate	g L^{-1}	0.01 ±0.01	0.14	0.07 ±0.01	0.08 ±0.02	0.04 ±0.01
Iso-Valerate	g L^{-1}	0.02 ±0.04	0.33	0.02 ±0.01	0.03 ±0.01	0.02 ±0.01
Valerate	g L^{-1}	0.01 ±0.01	0.23	0.03 ±0.01	0.03 ±0.01	0.01 ±0.01
Iso-Caproate	g L^{-1}	0.01 ±0.01	0.04	0.01 ±0.01	0.01 ±0.01	0.01 ±0.01
Caproate	g L^{-1}	0.01 ±0.01	0.09	0.07 ±0.01	0.03 ±0.02	0.02 ±0.01
Total VFA	g L^{-1}	0.3 ±0.18	4.32	0.46 ±0.01	0.64 ±0.23	0.78 ±0.05
Methane concentration	vol.-%	55.3 ±1.8	30.5	55 ±0.8	54.9 ±1	55.8 ±1
Methane yield	L CH_4 kg VS^{-1}	324.5 ±25.5	82.7	319.3 ±9.1	326.6 ±26.2	316.4 ±17.9

[a] no standard deviation applied as values only represent the final state of reactor failure.

4.3.3 Two-stage reactor performance

4.3.3.1 Process performance until reactor failure

Figure 4.2 & 4.3 show the reactor performances of methane reactors (M1 & M2) deployed in a two-stage system. The experiments commenced with a 3 HRT starting

period to acclimatise the microorganisms to food waste digestion. Thereafter, the OLR was brought to 2 g VS L^{-1} d^{-1} until a steady state was reached after 3 HRTs. The SMY for M1 and M2 settled at 392 ±12.6 and 419 ±23.2 L CH_4 kg VS^{-1} respectively. Low levels of VFA/TIC and pH indicated stable biological conditions. As the OLR was increased in M1 and M2 to 2.5 g VS L^{-1} d^{-1}, the SMY dropped acclimatising to the higher load. This was to be expected and from day 84 onwards the reactors temporarily appeared to recover, indicated by lower VFA/TIC and pH improvements after the initial deterioration. However, the advance of the experiment revealed a massive VFA/TIC increase and pH drop. A SMY reduction to levels as low as one third (M1) and a half (M2) of SMY as compared to that at an OLR of 2 g VS L^{-1} d^{-1} was identified. The magnitude and the dynamic change of process parameters exceeded previous observations significantly. As a consequence, the initial performance of M1 could not be re-obtained. M2 remained at unsteady levels (VFA/TIC, pH) for longer whilst showing a temporary gain in SMY, before ultimately being unable to cope with the loading.

The higher level of Ni and Mo in the digestate of M2 as compared to M1 (Table 4.1) might have initially mitigated and delayed the final break down. In the final stage of reactor failure M1 (day 96-108) and M2 (day 132-144) pH values dropped as far as 6.69 (M1) and 6.92 (M2) whilst VFA/TIC analysis ultimately peaked at 1.42 and 1.34 respectively. A major accumulation of VFA in the range of 4.98 (M1) and 3.44 g L^{-1} (M2), dominated by acetic and propionic acid, reinforced the theory of an inhibition of the acetoclastic pathway in methanogenesis. Subsequent reactor failure was attributed to major trace element depletion as confirmed by laboratory analysis in Table 4.1.

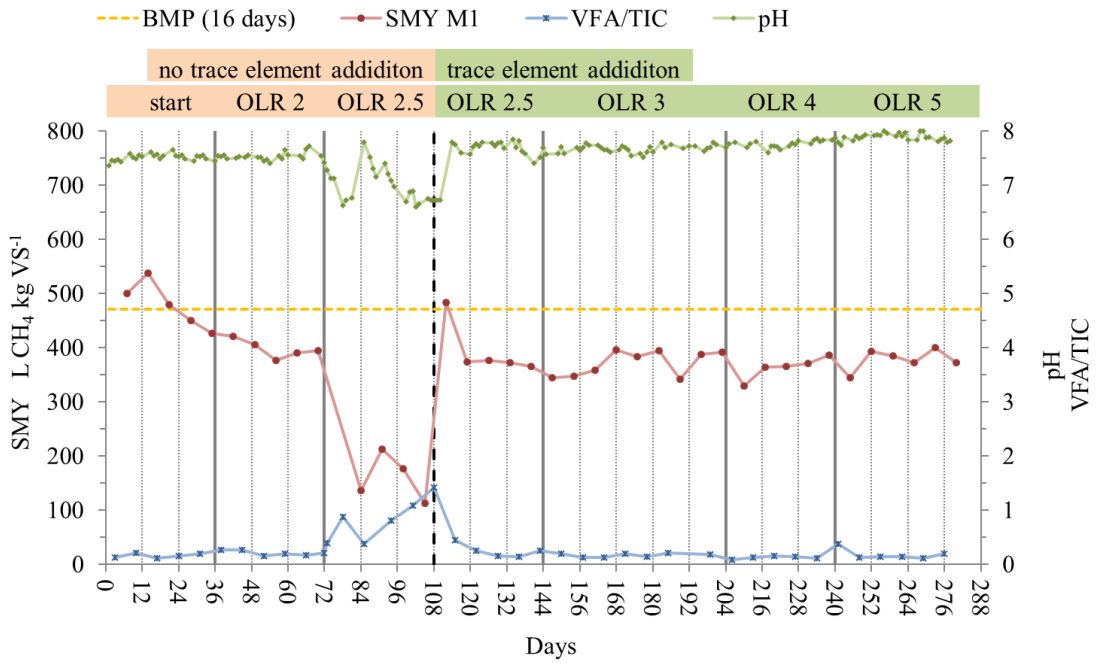

Fig. 4.2 Two-stage reactor performance (M1) before and after trace element supplementation.

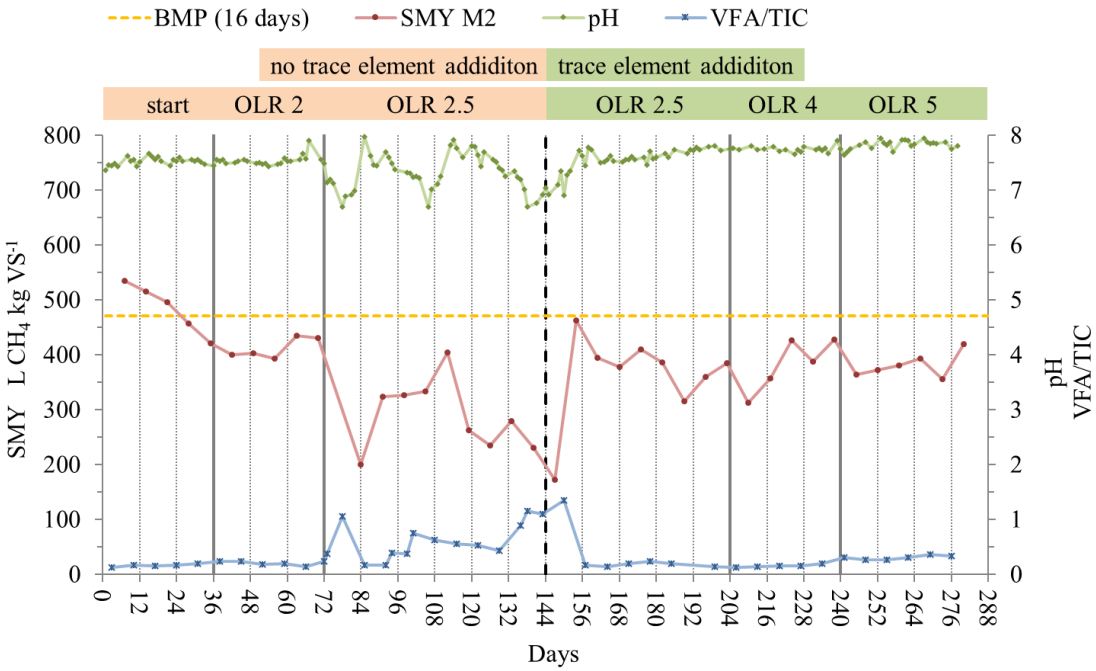

Fig. 4.3 Two-stage reactor performance (M2) before and after trace element supplementation.

After the reactors failed, trace element supplementation as recorded in Table 4.1 was started for M1 and M2 on day 108 and 144 respectively. As the reactor failure of M1 was more severe than M2, feeding was suspended for 3 days and pH was raised with sodium hydroxide to levels before failure. After 6 days (0.5 HRT) pH and VFA/TIC in M1 indicated stable fermentation and matched the results at OLR 2 g VS L^{-1} d^{-1} again. The SMY quickly reached 371.1 ±5.5 L CH_4 kg VS^{-1} and corresponded with results before supplementation of trace elements. M2 neither received an alkaline solution for pH stabilisation nor a feeding stop. Therefore, the pH only gradually increased over time and VFA/TIC recovery to levels below 0.5 experienced a minor delay of 12 days. The OLR of M1 and M2 was further increased until an OLR of 5 g VS L^{-1} d^{-1} was reached whilst maintaining an HRT over the two stages of 16 days. Constant low VFA/TIC and VFA levels were observed with a gradual increase corresponding to rising OLR. The SMY ranged between 373.9 ±10.9 and 413.9 ±22.6 L CH_4 kg VS^{-1} corresponding with values achieved before trace element addition. Stable fermentation conditions were restored and maintained after trace element supplementation, confirming the failure was induced by a deficiency of essential trace elements. Table 4.3 summarises the performance characteristics of each steady state.

Table 4.3. Performance characteristics of second stage of two-stage reactors, M2 & M3 at each steady state.

		M1	M2	M1[a]	M2[a]	M1	M2	M1	M1	M2	M1	M2
Trace element addition		no	no	no	no	yes	yes	yes	yes	yes	yes	yes
OLR	g VS L^{-1} d^{-1}	2.0	2.0	2.5	2.5	2.5	2.5	3.0	4.0	4.0	5.0	5.0
HRT	days	12	12	12	12	12	12	12	12	12	12	12
pH		7.5 ±0.1	7.5 ±0.1	6.7	6.9	7.5 ±0.1	7.5 ±0.1	7.6 ±0.1	7.7 ±0.1	7.7 ±0.1	7.9 ±0.1	7.9 ±0.1
VFA/TIC		0.17 ±0.03	0.16 ±0.01	1.42	1.34	0.15 ±0.01	0.22 ±0.04	0.17 ±0.04	0.13 ±0.03	0.17 ±0.03	0.15 ±0.06	0.34 ±0.02
Acetate	g L^{-1}	0.45 ±0.1	0.11 ±0.09	5.70	2.86	0.12 ±0.03	0.08 ±0.02	0.09 ±0.01	0.15 ±0.09	0.38 ±0.33	0.33 ±0.1	1.33 ±0.2
Propionate	g L^{-1}	0.09 ±0.01	0.01 ±0.02	0.78	0.36	0.04 ±0.01	0.01 ±0.01	0.04 ±0.01	0.01 ±0.01	0.04 ±0.01	0.05 ±0.01	0.05 ±0.02
Iso-Butyrate	g L^{-1}	0.04 ±0.01	0.01 ±0.01	0.21	0.13	0.01 ±0.01	0.01 ±0.01	0.01 ±0.01	0.01 ±0.01	0.01 ±0.01	0.01 ±0.01	0.01 ±0.01
Butyrate	g L^{-1}	0.02 ±0.01	0.01 ±0.01	0.56	0.09	0.04 ±0.01	0.03 ±0.01	0.03 ±0.01	0.03 ±0.01	0.04 ±0.01	0.4 ±0.09	0.09 ±0.07
Iso-Valerate	g L^{-1}	0.01 ±0.01	0.01 ±0.01	0.24	0.13	0.01 ±0.01	0.01 ±0.01	0.01 ±0.01	0.01 ±0.01	0.01 ±0.01	0.01 ±0.01	0.01 ±0.02
Valerate	g L^{-1}	0.01 ±0.01	0.01 ±0.01	0.13	0.04	0.02 ±0.02	0.01 ±0.01	0.02 ±0.02	0.01 ±0.01	0.03 ±0.01	0.03 ±0.01	0.01 ±0.02
Iso-Caproate	g L^{-1}	0.01 ±0.01	0.01 ±0.01	0.02	0.03	0.01 ±0.01	0.01 ±0.01	0.02 ±0.01	0.01 ±0.01	0.01 ±0.01	0.01 ±0.01	0.01 ±0.01
Caproate	g L^{-1}	0.01 ±0.01	0.02 ±0.01	0.32	0.06	0.06 ±0.05	0.05 ±0.01	0.06 ±0.03	0.06 ±0.01	0.07 ±0.01	0.05 ±0.02	0.02 ±0.03
Total VFA	g L^{-1}	0.6 ±0.1	0.16 ±0.14	7.9	3.7	0.3 ±0.17	0.16 ±0.03	0.29 ±0.11	0.25 ±0.1	0.55 ±0.36	0.87 ±0.23	1.52 ±0.29
Methane concentration	vol.-%	68.6 ±2.5	69.5 ±1.9	55.4	61.2	74.3 ±1.5	68.5 ±1.1	72.8 ±0.3	69.2 ±1.1	66.7 ±1.5	70.2 ±0.8	67.6 ±2.9
Methane yield	L CH_4 kg VS^{-1}	392 ±12.6	419 ±23.2	112.6	172.4	371.1 ±5.5	391.2 ±16.7	391.4 ±7.2	373.9 ±10.9	413.9 ±22.6	381.7 ±15.5	389.2 ±31.8

[a] no standard deviation applied as values only represent the final state of reactor failure.

4.3.4 Impact and comparison of trace element supplementation on single and two-stage digestion

All reactors were subjected to the same overall conditions in terms of loading rate, retention time and temperature. Figure 4.4 illustrates and compares the steady state key performance parameters VFA, VFA/TIC and SMY of the second stage of the two-stage systems (M1 & M2) with the one-stage reactor (M3). Without any addition of trace elements an elevated SMY of 392 ±12.6 and 419 ±23.2 L CH_4 kg VS^{-1} was obtained at an initial OLR of 2 g VS L^{-1} d^{-1} in the two-stage reactors M1 & M2 respectively, as opposed to 324 ±25.5 L CH_4 kg VS^{-1} for M3. The superior gas yields in the two-stage digestion is a result of the upstream hydrolysis and is further described in Voelklein et al. (2016a).

After increasing the OLR to 2.5 g VS L^{-1} d^{-1} the VFA/TIC level in all reactors (M1, M2 & M3) severely deteriorated by up to one order of magnitude to levels of 1.34-1.57. The reactors failed and significantly exceeded levels of fermentation considered stable (Drosg, 2013). Similar observations of unstable reactor behaviour at low OLR have been reported by Climenhaga and Banks (2008), Gustavsson et al. (2011), Nordell et al. (2016) and Zhang et al. (2015). The VFA spectrum of M1 and M2 was dominated by acetic (3.59 g L^{-1} and 2.67 g L^{-1} respectively) and propionic acid (0.52 g L^{-1} and 0.31 g L^{-1} respectively) with minor shares of longer chained fatty acids (C_4-C_6). In contrast the share of 1.88 g L^{-1} of propionic acid exceeded the share of 1.25 g L^{-1} of acetic acid in the single-stage reactor M3. The accumulation of VFA is an associated consequence of trace element deficiency (Banks et al., 2012; Nordell et al., 2016; Pobeheim et al., 2011).

The severe drop in SMY caused by reactor failure ultimately affected all reactors to the same extend regardless of the reactor configuration. The initial acidification and break down of substrate in the upstream reactor of the two-stage system resulted in a prevailing pH of approx. 5 (Voelklein et al., 2016a). This allowed part of the hydrogen sulphide to be released and present as H_2S (gas), not resulting in precipitation and potential deficiency of trace elements. A more robust and beneficial behaviour of the two-stage process in respect of its upstream hydrolytic pre-treatment was not observed, due to the complete lack of some trace elements in the feedstock (Table 4.1). Therefore, the two-stage system did not show any better resilience to

nutrient deficiency in general, neither towards the potential advantage of reduced precipitation nor to enhanced availability of trace elements.

However, the hypothesis of increased bioavailability in a two-stage system remains, as an absence of trace element Co, Mb and Se can not be compensated by increased bioavailability. The trace element supplementation after failure stimulated methanogenic activity in all reactors, triggering a reduction in VFA and subsequently sustained low VFA/TIC values. This is in line with observations made in studies assessing the long term effects of trace element supplementation (Karlsson et al., 2012; Nges et al., 2012; Pobeheim et al., 2011). The dynamic response in both reactor configurations restored and enabled SMY levels comparable to the experimental period before failure. Immediate beneficial effects after addition of deficient nutrients were also obtained by Moestedt et al. (2016), Nordell et al. (2016), Qiang et al. (2012) and Zhang et al. (2015).

The gap in SMY between the one and two-stage remained after stabilizing the reactors with trace elements. The 16 day BMP performance of 471.94 L CH_4 kg VS^{-1} was never reached regardless of the elimination of nutrient deficiency. This is a result of fully mixed continuous stirred tank reactors causing fresh matter to leave the reactor prior to complete digestion. The shorter the retention time the more significant this effect becomes. The gas yields further confirmed the observed conclusion that trace element addition had negligible impact on SMY (at a fixed HRT of 16 days), yet is essential for a stable fermentation with low VFA levels after exceeding a threshold OLR of 2.0 g VS L^{-1} d^{-1}. The positive effects of trace element addition are in line with studies conducted by Banks et al. (2012), Gustavsson et al. (2011), Qiang et al. (2012), Zhang and Jahng (2012) and Zhang et al. (2015).

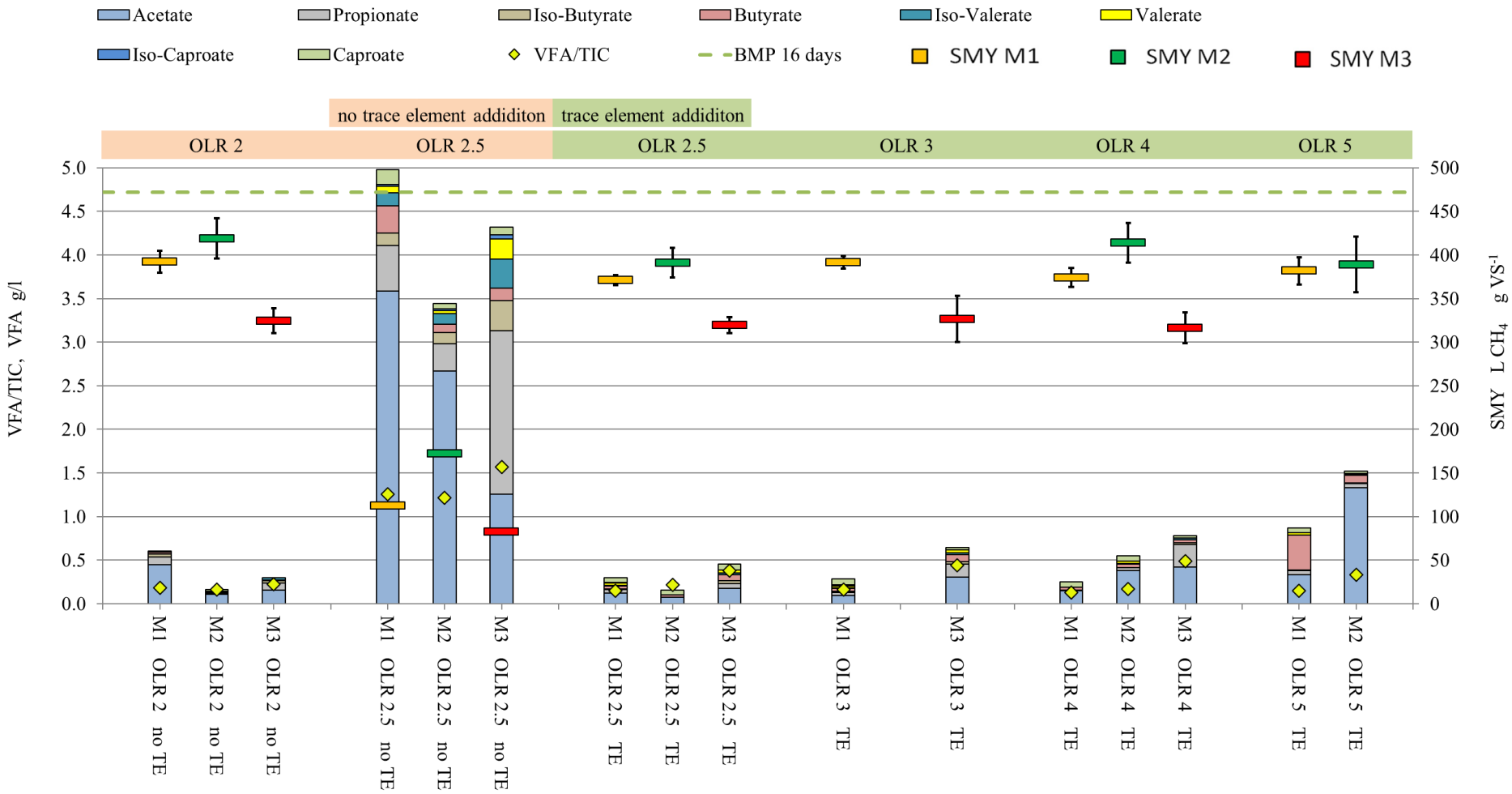

Fig. 4.4 Performance comparison of single and two-stage digestion at steady state with and without trace element supplementation (gas yields at OLR 2.5 no TE without error bars as values only represent the final state of reactor failure).

4.4 Conclusion

Food waste lacked essential nutrients causing instable single and two-stage reactor performance after exceeding a threshold OLR of 2.0 g VS L^{-1} d^{-1}. The break down was characterised by pH, VFA/TIC, VFA and CH_4 concentrations far beyond stable limits and a reduction in SMY. TE addition of Co, Fe, Mo, Ni and Se restored a stable process and allowed increased loading rates. TE addition did not increase SMY beyond levels at initial stable digestion. The two-stage system incorporating hydrolytic pre-treatment showed improved SMY than the single-stage system but did not show any better resilience to nutrient deficiency.

4.5 Supplementary data

Relation of two-stage digestion and H_2S induced precipitation of trace elements:
The acidification of substrate in the upstream reactor of the two-stage system allowed part of the hydrogen sulphide to be present and released as H_2S (gas), not resulting in precipitation and potential deficiency of trace elements. However, hydrogen sulphide concentrations were not obtained during the experiment to substantiate a more beneficial behaviour of the two-stage process in respect of its upstream hydrolytic pre-treatment and trace element availability. The brief remarks in chapter 4 concerning hydrogen sulphide and trace element availably may be seen as an explanation and a rational to further expand on the idea of two-stage digestion, rather than a definitive finding of the study. A general recommendation of two-stage systems facilitating elevated trace metal availability can not be derived from this study.

Addition of trace elements and associated improvement in the two-stage food waste:

A sufficient level of all macro- and micro-nutrients is a vital prerequisite for key enzymes and microbes associated with stable VFA degradation and methanogenesis (Banks et al., 2012; Demirel & Scherer, 2011; Drosg, 2013; Kida et al., 2001; Yirong et al., 2014). The substrate in chapter 4 was lacking a sufficient level of trace elements such as cobalt, iron, nickel, molybdenum and selenium (Banks et al., 2012; Karlsson et al., 2012; Moestedt et al., 2016; Nges et al., 2012; Wall et al., 2014; Zhang & Jahng, 2012). The associated demand for specific trace elements at different methanogenic pathways can impact reactor stability. For instance, selenium is understood to be an essential element to facilitate hydrogenotrophic methanogenesis (Banks et al., 2012; Deppenmeier, 2002; Thauer et al., 2008). Previous studies have identified syntrophic acetate oxidation and hydrogenotrophic methanogenesis as the principle methanogenic route at elevated ammoniacal nitrogen level (Jiang et al., 2018; Karakashev et al., 2005). Thus, a deficiency in selenium could mark a potential limitation in this study. However, elevated ammoniacal nitrogen levels were not present in this study due to the dilution of food waste with

water. Thus, the possible impact of a selenium deprived substrate may not have hampered hydrogenotrophic methanogenesis performance. The increase in VFA at low TAN concentrations is more likely associated with an interference in acetoclastic anaerobic degradation pathways (Diekert et al., 1980; Fermoso et al., 2009; Myszograj et al., 2018; Zhang et al., 2003). For example, nickel and cobalt are essential co-factors of enzymes in acetoclastic methane formation (Diekert et al., 1980; Fermoso et al., 2009; Myszograj et al., 2018; Zhang et al., 2003). Methyl-coenzyme M (Co-factor F_{430}) and the acetate converting enzyme carbon monoxide dehydrogenase both contain nickel (Diekert et al., 1980; Fermoso et al., 2009; Myszograj et al., 2018; Zhang et al., 2003). Coenzyme M methyl transferase contains cobalt (Diekert et al., 1980; Fermoso et al., 2009; Myszograj et al., 2018; Zhang et al., 2003). A deficiency of these elements may have influenced subsequent fermentation pathways causing diminishing process performance, VFA accumulation and reactor failure.

A lack of performance in full scale mono-digestion of food waste is often observed after 1-2 years of operation, after the initial nutrients are washed out and a new equilibrium is established. Besides the lack of trace metals in the food waste (table 4.1), the short HRT and addition of water further facilitated a reduction of trace element concentration in the digestate. The addition of water allowed enhanced wash out of nutrients and reflects a long term depletion of trace elements within a shorter time frame. Despite some trace elements still being present in the digestate in chapter 4, the accessibility may have been constrained by its bioavailability (Banks & Heaven, 2013; Karlsson et al., 2012; Ortner et al., 2015). Ortner et al. (2014) established that 30-70% of present trace elements were not bioavailable to the microbial community. In order to be available for methanogenic archaea, trace elements had to be soluble and neither be fixed in precipitated compounds (such as sulphates, sulphides, phosphates or carbonates) nor adsorbed.

Chapter 5: Increased loading rates and specific methane yields facilitated by digesting grass silage at thermophilic temperatures rather than mesophilic

Increased loading rates and specific methane yields facilitated by digesting grass silage at thermophilic temperatures rather than mesophilic

M. A. Voelklein[1, 2], D. Rusmanis[1, 2], J. D Murphy[1, 2]

[1]MaREI Centre, Environmental Research Institute (ERI), University College Cork (UCC), Ireland

[2]School of Engineering, UCC, Ireland

Abstract

This study was conducted to advance the understanding of thermophilic grass digestion. Late harvested grass silage was fermented at thermophilic conditions at increasing organic loading rates. Stable digestion took place at an OLR between 3 and 4 g VS L^{-1} d^{-1}. This enabled specific methane yields as high as 405 L CH_4 kg VS^{-1}. An accumulation of volatile fatty acids, accompanied by a gradual deterioration of pH, VFA/TIC arose at an OLR between 5 and 7 g VS L^{-1} d^{-1}, yet inhibition did not occur. SMY decreased with reduced retention time ranging between 336 and 358 L CH_4 kg VS^{-1} at OLR 7 and 5 g VS L^{-1} d^{-1} respectively. The biomethane efficiencies remained high (92-103%) at corresponding retention times. Comparative results indicated a superior performance with respect to higher loading and SMY as compared with mesophilic conditions.

Keywords: biogas; thermophilic digestion; grass; high organic loading rate; anaerobic digestion.

5.1 Introduction

Ireland's temperate climate provides ideal conditions for grass production and grazing based livestock systems. Grass silage surplus to livestock requirements has been identified as a potential source for biomethane production in Ireland (McEniry et al., 2013; Murphy & Power, 2009; Wall et al., 2013). In respect of Ireland's EU 2020 targets, 1.1% of grassland co-digested with the majority of slurry from dairy cows could satisfy 10% of renewable energy supply in transport (Wall et al., 2013). Furthermore, grass as a renewable gaseous transport fuel gives at least a 50% better net energy yield per hectare than the next best indigenous European liquid biofuel system (Smyth et al., 2009).

Grassland not suitable for grazing or forage, such as roadside plantings, green wastes, nature conservation biomass or fallow land are a valuable source of substrate for anaerobic digestion. Those resources are typically only harvested once or twice a year at an advanced growth stage and exhibit a lignocellulosic composition. The more complex form of this biomass includes for enhanced fractions of lignin and hemi-cellulose, locking accessibility to easily degradable carbohydrate fractions. This results in more incomplete fermentation and reduced rates of degradation at standard conditions. Possible technologies to break up the lignocellulosic structure and facilitate accessibility to easy degradable fractions include for substrate specific mechanical, chemical, biological, sonic or thermal treatment methods. Current research proposed increasing yields via chemical treatment with acids, biologically with enzymes, hydrolysis pre-treatment, and change in pH or temperature (Amnuaycheewa et al., 2016; Kumar et al., 2015; Wall et al., 2016).

The potential for grass digestion systems has been extensively examined at mesophilic temperatures in Ireland (Allen et al., 2016; Nizami & Murphy, 2010; Nizami et al., 2012; Singh et al., 2011; Thamsiriroj et al., 2012; Wall et al., 2014a; Wall et al., 2014b). Yields from 349 to 451 L CH_4 kg VS^{-1} have been obtained depending on harvest date and maturity. Other studies suggest methane yields of 253-394 L CH_4 kg VS^{-1} for mesophilic mono and co-digestion of various grass species (Koch et al., 2009; Mähnert et al., 2005; Seppälä et al., 2009; Xie et al., 2011).

Managing sustainable grass digestion systems, through maximum possible loading rates, whilst generating a high specific methane yield, remains a critical design challenge. Xie et al. (2011) achieved stable co-digestion of grass silage with pig manure, however mono-digestion failed. Thamsiriroj et al. (2012) investigated long-term operation of mesophilic grass mono-digestion and suggested a limit of 3 g VS L^{-1} d^{-1}. Mechanical failure was manifested when this loading rate was exceeded. This was mainly attributed to insufficient mixing caused by enhanced viscosity and a dry solids (DS) level rising above 12%. Wall et al. (2014b) assessed the optimisation of digester performance with increasing organic loading rates for mesophilic mono and co-digestion of grass silage. Recirculation of liquid effluent was incorporated to maintain a dry solids content below 12% in the reactor. Optimum conditions were assessed for grass mono-digestion at an organic loading rate of 3.5 to 4 g VS L^{-1} d^{-1}. Despite the benefits of grass digestion, it remains a challenging substrate for anaerobic digestion, in particular if no dilution, co-digestion or recirculation of liquor occurs. The high fibre and total solids content impacts negatively on the prevailing viscosity in the reactor. This is the main reason why loading rates exceeding 4 g VS L^{-1} d^{-1} in grass mono-digestion have not been reported in literature.

However, an increase in temperature mitigates those limiting effects due to improved kinetic properties, increased enzyme activity, reduced viscosity, higher substrate utilisation and growth rates of bacteria (Mähnert, 2007). The correlation of loading and dry solids on viscosity, based on mesophilic and thermophilic digestion of maize, rye and sugar beet silage was outlined in detail by Mähnert (2007). An increase in loading provoked a significant gain in viscosity at mesophilic temperatures. However, at similar dry solids content in the reactor the thermophilic reactor displayed a lower viscosity. For 100% maize digestion the apparent viscosity at 7% DS accounted for 0.6 Pa s at mesophilic (35 °C) digestion and 0.2 Pa s for thermophilic (55 °C) digestion. The greater the loading rate and dry solids content, the more distinct this difference became.

The relevant gap in the state of the art is that though the advantages of thermophilic systems have been widely described, there is no literature on assessing thermophilic

digestion of late cut grass silage at increasing organic loading rates and comparing to mesophilic digestion.

The innovation in this paper is that it:

- Assesses the biomethane potential of late cut grass silage at a range of retention times at thermophilic temperatures.
- Contrasts BMP values at thermophilic and mesophilic temperatures.
- Assesses the specific methane yield of late cut grass silage in continuous thermophilic digestion at increasing loading rates.
- Assesses the ratio of the SMY to the BMP at thermophilic temperature ranges at the same retention times.

5.2 Materials and Methods

5.2.1 Inoculum and substrate

The inoculum was obtained from a full scale thermophilic digester based on manure and crops operating at an OLR of 7 g VS L^{-1} d^{-1}. The feedstock was a first-cut perennial ryegrass (Lolium perenne), harvested on the 24th June (a late growth stage for Ireland) to address the utilisation of a more mature and lignocellulosic substrate. The wilted grass was ensiled for 5 weeks in 1.2 m diameter cylindrical bales wrapped in polyethylene foil and subsequently repacked into stretch-film wrapped 25 kg bales. The particle size of the grass silage was further reduced with a heavy duty mincer to a size between 5-10 mm. It was stored at a temperature of -20 °C until fed to the anaerobic reactors. The characteristics of the substrate grass silage (harvest 24th June) are indicated in table 5.1. The delayed time of harvest influenced the digestibility of the silage, reflected by increased neutral detergent fibre (NDF) and acid detergent fibre (ADF). As a result, dry solids digestibility (DSD) remained at lower levels than normal for Irish first cut grass silage.

Table 5.1. Characteristics of the substrate grass silage (harvest 24th June).

Parameters		Grass silage
pH		4.6
Dry solids (DS)	g kg^{-1}	199
Volatile solids (VS)	g kg^{-1}	181
VS/DS	g kg^{-1}	910
Neutral detergent fibre (NDF)	g kg^{-1} DS	716
Acid detergent fibre (ADF)	g kg^{-1} DS	400
Dry solids digestibility (DSD)	g kg^{-1} DS	555
Crude protein	g kg^{-1} DS	148
Water soluble carbohydrate	g kg^{-1} DS	71
C:N ratio		26.5
Cadmium	mg kg^{-1}	<0.19
Cobalt	mg kg^{-1}	<0.29
Copper	mg kg^{-1}	1.95
Iron	mg kg^{-1}	106.5
Manganese	mg kg^{-1}	11.1
Molybdenum	mg kg^{-1}	1.16
Nickel	mg kg^{-1}	0.70
Selenium	mg kg^{-1}	<0.19
Zinc	mg kg^{-1}	6.50

5.2.2 Nutrient supplementation

The grass silage contained trace element metals such as cobalt, copper, iron, nickel, manganese, molybdenum, nickel, selenium and zinc in the range of 0.19-11.2 mg L^{-1} (Table 5.1). Some of the key trace elements for anaerobic digestion (such as Co, Mo, Ni and Se) were undersupplied and partly below the detection limit as suggested by others (Banks et al., 2012; Lemmer et al., 2010; Pobeheim et al., 2011; Thamsiriroj et al., 2012; Voelklein et al., 2017; Wall et al., 2014a). Thamsiriroj et al. (2012) and Wall et al. (2014a) found positive effects in supplementing deficient elements such as cobalt, iron and nickel to grass digestion trials. The selected concentrations for supplementation of trace elements in this experiment followed the supplementation levels in operation at the full scale digester (where the inoculum was sourced) and coincided with concentrations most frequently applied and recommended values from literature (Banks et al., 2012; Lemmer et al., 2010; Pobeheim et al., 2011; Thamsiriroj et al., 2012; Voelklein et al., 2017; Wall et al., 2014a). Levels of

0.5 mg L^{-1} Co, 500 mg L^{-1} Fe, 5 mg L^{-1} Mo, 5 mg L^{-1} Ni and 0.5 mg L^{-1} Se were added to the feedstock. In the present study Co was added in the form of $CoCl_2 \cdot 6H_2O$, Fe as $FeCL_3 \cdot 6H_2O$, Mo as $H_{24}Mo_7N_6O_{24} \cdot 4H_2O$, Ni as $Cl_2Ni \cdot 6H_2O$ and Se as Na_2SeO_3. Adequate amounts of iron were added to precipitate emerging hydrogen sulphate to iron sulphur compounds and maintain increased bioavailability of the trace elements in the reactor.

5.2.3 Biomethane potential

5.2.3.1 Biomethane potential test

The BMP of the substrate was tested in an automatic methane potential test system (AMPTS ll, Bioprocess Control, Sweden) at thermophilic conditions (55 °C). The working volume of the batch BMP tests was 400 ml. All tests were run in triplicate for 63 days at thermophilic conditions (55 °C). The inoculum to substrate ratio was chosen as 2:1. Carbon dioxide was removed by passing the biogas through a sodium hydroxide solution. The methane gas flow was recorded with gas tippers based on water displacement. This system is described in detail by Wall et al. (2013).

5.2.3.2 Biomethane potential test calculations

Kinetic analyses were conducted with software package Matlab R2009a (TheMathWorks Inc., Natick, MA, USA). A first order differential equation (equation 6) and a modified Gompertz equation (equation 7) were fitted to the cumulative methane production curves (Allen et al., 2016; Herrmann et al., 2015). Equation 6 was used to calculate the decay constant value k.

$$Y(t) = Y_m \cdot \left(1 - exp^{(-kt)}\right) \quad (6)$$

where, Y(t) is the cumulative methane yield (L CH_4 kg VS^{-1}) at time t (days). Y_m represents the maximum methane potential (L CH_4 kg VS^{-1}) of the added substrate. K is the decay constant ($days^{-1}$). The lag-phase and half-life (T_{50}) in days were determined from the modified Gompertz equation (equation 7). The lag-phase expresses the time (days) until methane production sets in. Half-life (days) represents the time to reach 50% of the maximum specific methane yield.

$$M(t) = P \cdot exp\left\{-exp\left[\frac{R_{max} \cdot e}{P}(\Delta - t)\right] + 1\right\} \quad (7)$$

where, M(t) represents the cumulative methane yield (L CH_4 kg VS^{-1}) at time t (days), P the maximum methane production potential established in the BMP (L CH_4 kg VS^{-1}), R_{max} the maximum methane production rate (L CH_4 kg VS^{-1} d^{-1}) and Δ the lag phase and t the time (days).

5.2.4 Design and operation conditions of semi continuous trials

The digestion of grass silage was performed at thermophilic conditions (55 °C). The experiment was split into 3 individual reactors and tested at different loading rates for 3 consecutive retention times. Figure 5.1 outlines the specific digestion systems. Reactor 1 (R1) operated at 3 g VS L^{-1} d^{-1} with a hydraulic retention time of 63 days. Reactor 2 (R2) was maintained at 4 g VS L^{-1} d^{-1} and 46 days HRT. Reactor 3 (R3) started with an initial OLR of 5 g VS L^{-1} d^{-1} and was further subjected to higher loading of 6 and 7 g VS L^{-1} d^{-1} resulting in retention times of 36, 30 and 25 days respectively. Due to the five-day feeding regime (Monday to Friday), the theoretical OLR was adjusted by the factor 5/7 and represents a loading comparable to daily feeding. The corresponding HRT was changed by 7/5 to consider the 2 days without feeding on Saturday and Sunday. This reflected the actual loading and retention time corresponding to a daily feeding regime. It has to be noted that some studies relate their performance characteristics without these correction factors, which would enhance the maximum loading to 10 g VS L^{-1} d^{-1} in this study. The system was not subjected to any dilution or recirculation of liquids, hence the retention time was solely determined by the actual feeding volume of grass silage.

The thermophilic semi-continuous trials were performed at three individual lab scale reactors. The reactors had a total volume of 5 L with an internal diameter of 0.15 m and a height of 0.4 m. The working volume was 4.0 L. A temperature controller unit was installed to maintain a constant temperature in the reactors at thermophilic conditions (55 °C). An outer heating blanket supplied the heat. A wet gas meter recorded gas flow automatically. Collected biogas was stored in a gas bag for compositional analysis. Mixing was provided by a stirring mechanism, consisting of

a vertical shaft with in total 4 small paddles attached. A variable speed motor drove the shaft. The shaft of the stirrer was surrounded by a top mounted pipe, which sealed the top of the reactor with the rotating stirrer.

The biomethane efficiency is defined as the SMY from continuous digestion divided by the SMY obtained from the BMP test of the same substrate at the same retention time. Thus, the retention time dependent yields of the continuous trials refer to similar retention time in the BMP system.

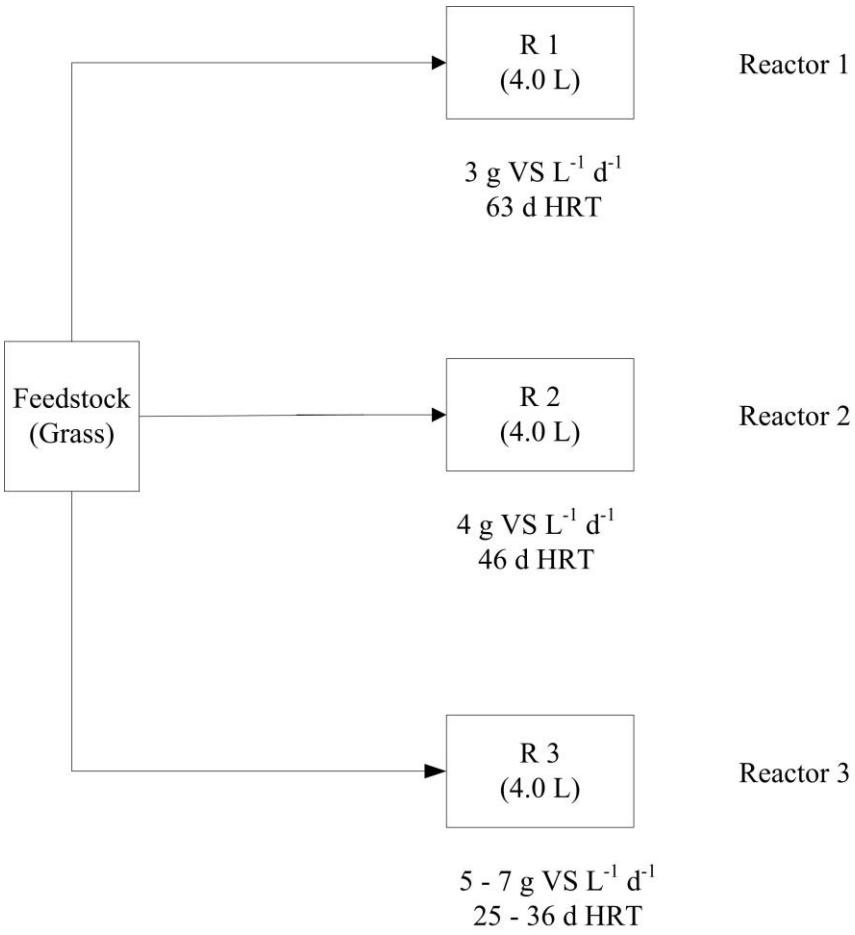

Fig. 5.1 Design of experiment.

5.2.5 Analytical methods

Total solids and volatile solids (VS) were analysed according to Standard Methods 2540 G. The pH value was determined using a pH meter (Jenway 3510). VFA/TIC was measured using the Nordmann-method (Nordmann, 1977). This parameter describes the ratio of volatile fatty acids to alkalinity (buffering capacity). A VFA/TIC value below 0.4 indicates stable reactor conditions (Drosg, 2013). The

concentrations of individual volatile fatty acids were analysed by gas chromatography (Hewlett Packard HP6890) using a Nukol^{TM} fused silica capillary column (30 m × 0.25 mm × 0.25 μm) and a flame ionization detector. Hydrogen was used as a carrier gas. All metal elements except selenium were determined according to DIN EN ISO 11885 with inductively coupled plasma optical emission spectrometry (ICP-OES); selenium was analysed according to DIN EN ISO 17294-2 (E29) with inductively coupled plasma mass spectrometry (ICP-MS).

Biogas flow from each reactor was measured by using a water displacement mechanism. A certain amount of gas passes through a tipping mechanism, displaces the volume of water in a pre-defined chamber till it floats and releases the gas. Every release generates a digital impulse, which represents the displaced gas volume in the chamber. The measured methane volume was adjusted to the volume at standard temperature (273 K) and pressure (1013 mbar). The produced biogas was stored in a gas bag and measured for its biogas composition on a weekly basis. Biogas composition was analysed for methane (CH_4), carbon dioxide (CO_2), hydrogen (H_2), oxygen (O_2) and nitrogen (N_2) using a Hewlett Packard HP6890 gas chromatograph equipped with a Hayesep R packed GC column (3 m x 2 mm, mesh range of 80-100) and a thermal conductivity detector (TCD). Argon was used as carrier gas.

5.3 Results and discussion

5.3.1 Biomethane potential

5.3.1.1 Theoretical maximum biomethane potential (BMPth)

A proximate and ultimate analysis of the grass silage was conducted which allowed theoretical derivation of the stoichiometric equation and hence maximum theoretical methane yield and concentration. The calculation in table 5.2 yields a theoretical maximum biomethane potential of 445 L CH_4 kg VS^{-1} with a methane concentration of 52%.

Table 5.2. Theoretical calculation of biomethane potential and methane concentration using the Buswell Equation for grass silage.

$C_{30.97}H_{53.03}O_{24.15} + 5.64\ H_2O \rightarrow 16.07\ CH_4 + 14.89\ CO_2$

811.85 g mol^{-1} + 101.56 g mol^{-1} → 258.00 g mol^{-1} + 655.42 g mol^{-1} + 17.01 g mol^{-1}

1 kg VS + 0.13 kg H_2O → 0.32 kg CH_4 + 0.81 kg CO_2

Density CH_4 0.714 kg m^{-3}; Density CO_2 1.96 kg m^{-3}

51.94 vol.-% CH_4; 48.06 vol.-% CO_2

Theoretical biogas potential equates to 856.9 L kg VS^{-1} added. 51.94 vol.-% CH_4; 48.06 vol.-% CO_2. Theoretical biomethane potential equates to 445.08 L CH_4 kg VS^{-1} added. It is assumed that volatile solids compounds only consist of C, H, O. N is neglected.

5.3.1.2 Biomethane potential test

A biomethane potential test was carried out in triplicate. After 20 days the gain in daily gas production was less than 1% of the total gas production produced to that day. According to the VDI 4630 guideline 'Fermentation of organic materials, characterisation of the substrate, sampling, collection of material data, fermentation tests' published by Association of German Engineers (VDI) (VDI, 2006), this is a possible criteria to determine the experimental duration. After 30 days (standardised duration for BMP) a total methane yield of 374 ±1.8 L CH_4 kg VS^{-1} and a k-value of 0.173 was obtained. The BMP achieved 84.0% of the theoretical maximum biomethane potential. An extended retention time of in total 63 days increased the specific methane yield further by 4.6% to 392 ±4.4 L CH_4 kg VS^{-1}, corresponding to 88.0% of the theoretical maximum biomethane potential. This matched the findings of Allen et al. (2016) determining a range of 316-393 L CH_4 kg VS^{-1} for mesophilic late cut grass silage in a 30 day BMP trial.

5.3.2 Single-stage reactor performance at increasing loading rates

Table 5.3 illustrates the process characteristics of the continuous thermophilic digestion trials. Biological parameters such as pH, VFA, VFA/TIC and SMY were assessed as indicators of reactor stability and performance. The results shown for each OLR display the data at steady state conditions. Thus, it represents average values obtained in the last HRT of the total of 3 hydraulic retention times at each loading rate. The significance of differences between means was tested by analysis of variance (ANOVA) and multiple comparisons applying the Tukey-Kramer test procedure with a significance level of 0.05.

5.3.2.1 Organic loading rate: 3-4 g VS L^{-1} d^{-1}

The experiment commenced at a moderate loading rate of 3 g VS L^{-1} d^{-1} (R1) and 4 g VS L^{-1} d^{-1} (R2). The initial pH at OLR 3 g VS L^{-1} d^{-1} was as high as 8.15 ±0.16; it was marginally lower (8.05 ±0.1) at an OLR 4 g VS L^{-1} d^{-1}. An elevated pH at thermophilic digestion is commonly observed (Franke-Whittle et al., 2014). Total VFA reached a maximum of 0.92 and 1.18 g L^{-1} at an OLR of 3 g VS L^{-1} d^{-1} and 4 g VS L^{-1} d^{-1} respectively, with acetic and propionic acid being the only detectable compounds. The VFA/TIC values did not exceed levels of 0.25, indicating a stable fermentation process. Sufficient retention times of 63 days (OLR 3 g VS L^{-1} d^{-1}) and 46 days (OLR 4 g VS L^{-1} d^{-1}) allowed for generation of high SMYs of 405 ±26.4 L CH_4 kg VS^{-1} (R1) and 381 ±12.6 L CH_4 kg VS^{-1} (R2) respectively (figure 5.2). The SMY obtained for OLR 3 and 4 g VS L^{-1} d^{-1} numerically differed, yet did not show statistically significant difference ($P>0.05$), see table 5.3. A statistically significant higher SMY of OLR 3 g VS L^{-1} d^{-1} compared to OLR 5, 6 and 7 g VS L^{-1} d^{-1} was evident ($P<0.05$). While numerically exceeding the SMY of OLR 5, 6 and 7 g VS L^{-1} d^{-1}, the SMY of OLR 4 g VS L^{-1} d^{-1} only statistically significantly differed from the maximum OLR of 7 g VS L^{-1} d^{-1} ($P<0.05$). The gained yields resulted in a biomethane efficiency of 1.03 (HRT 63 days) and 0.98 (HRT 46 days), based on similar retention time of BMP assay and continuous trials. Thus 88.8% and 85.5% of the maximum biomethane potential (as assessed using the Buswell equation) was reached at an OLR of 3 and 4 g VS L^{-1} d^{-1} respectively. The increased degradation at longer HRT is further reflected by lower TS and VS contents in the digestate effluent (table 5.3). The TS and VS at the longest HRT of 63 days reached levels as low as 10.7% and 76.5% respectively, in contrast to 12.2% TS and 81.8% VS at the shortest retention time of 25 days. The methane content of 52.3% (OLR 3) and 51.5% (OLR 4) were similar to the theoretical calculation (51.9%) derived from the Buswell Equation.

The ammonia (NH_3) level in a digester is mainly dependent on its ammonium (NH_4) level, pH and prevailing temperature. Thus, in these trials the equilibrium of NH_4/NH_3 shifted towards NH_3 with levels of 991 mg L^{-1} at an OLR of 3 g VS L^{-1} d^{-1} and 878 mg L^{-1} at an OLR of 4 g VS L^{-1} d^{-1}. About 1/3rd of the total NH_4-N was

present in its more toxic NH_3 form, which diffuses more easily through cell membranes than the ammonium ion. In contrast, at a mesophilic temperature of 38°C and a more neutral pH of 7.5, the equivalent NH_3 share would be calculated at only 5%. Similar results were obtained by Franke-Whittle et al. (2014) contrasting mesophilic and thermophilic digestion of feedstock cow manure and food wastes in Austria in examining the effect of temperature and different ammonia loads. The NH_3 levels found at the OLR 3-4 g VS L^{-1} d^{-1} were within the non-inhibiting range of 700 mg L^{-1} NH_3 (Angelidaki & Ahring, 1994) and 1200 mg L^{-1} NH_3 (Franke-Whittle et al., 2014) previously reported in literature. As the inoculum was well adapted due to long term full scale operation of similar substrate and NH_3 levels, and no performance reduction was monitored, it was understood that no ammonia inhibition was present.

Table 5.3. Performance parameters of thermophilic (55 °C) grass mono-digestion at increasing loading rate.

Retention time (days)		25	30	36	46	63
Batch-system						
BMP[a]	L CH_4 kg VS^{-1}	364 ±0.5	374 ±1.8	381 ±1.7	388 ±3.2	392 ±4.4
CSTR-system						
OLR	g VS L^{-1} d^{-1}	7	6	5	4	3
SMY	L CH_4 kg VS^{-1}	336[d] ±6.6	351[d,e] ±6.6	358[d,e] ±9.7	381[e,f] ±12.6	405[f] ±26.4
CH_4	%	52.2 ± 0.25	52.9 ±0.17	51.7 ±0.28	51.5 ±0.59	52.3 ±0.23
TS	%	12.2 ±0.04	12.3 ±0.03	12.1 ±0.08	11.4 ±0.20	10.7 ±0.38
VS/TS	% TS	81.8 ±0.40	81.5 ±0.55	80.9 ±0.56	78.9 ±0.60	76.5 ±0.84
pH		7.65 ±0.29	7.93 ±0.08	7.99 ±0.07	8.05 ±0.1	8.15 ±0.16
VFA/TIC		0.55 ±0.1	0.58 ±0.03	0.67 ±0.04	0.23 ±0.1	0.25 ±0.02
TAN [b]	mg L^{-1}	3077 ±219	3060 ±145	2913 ±229	3027 ±87	2917 ±159
Free NH_3-N [c]	mg L^{-1}	431 ±31	724 ±34	765 ±60	878 ±25	991 ±54
VFA						
Acetate	g L^{-1}	3.12 ± 0.75	2.19 ± 0.24	1.76 ± 0.24	0.85 ± 0.09	0.67 ± 0.23
Propionate	g L^{-1}	3.45 ± 0.07	4.58 ± 0.22	8.21 ± 0.22	0.32 ± 0.05	0.24 ± 0.09
Iso-butyrate	g L^{-1}	0.25 ± 0.05	0.27 ± 0.05	0.51 ± 0.05	0	0
Butyrate	g L^{-1}	0.11 ± 0.05	0.15 ± 0.05	0.17 ± 0.05	0	0
Iso-valerate	g L^{-1}	0.40 ± 0.05	0.46 ± 0.05	0.75 ± 0.05	0	0
Valerate	g L^{-1}	0.07 ± 0.05	0.10 ± 0.05	0.15 ± 0.05	0	0
Iso-caproate	g L^{-1}	0	0	0	0	0
Caproate	g L^{-1}	0	0	0	0	0
Sum of VFAs	g L^{-1}	7.40 ± 0.64	7.77 ± 0.12	11.6 ± 0.20	1.18 ± 0.12	0.924 ± 0.33

[a] Biomethane Potential Test with 4.27 g VS grass silage in 0.4 L effective volume; [b] total ammonium nitrogen; [c] free NH_3-N of TAN

[d-f] Means within line with no lowercase superscript letter in common differ significantly ($\alpha = 0.05$).

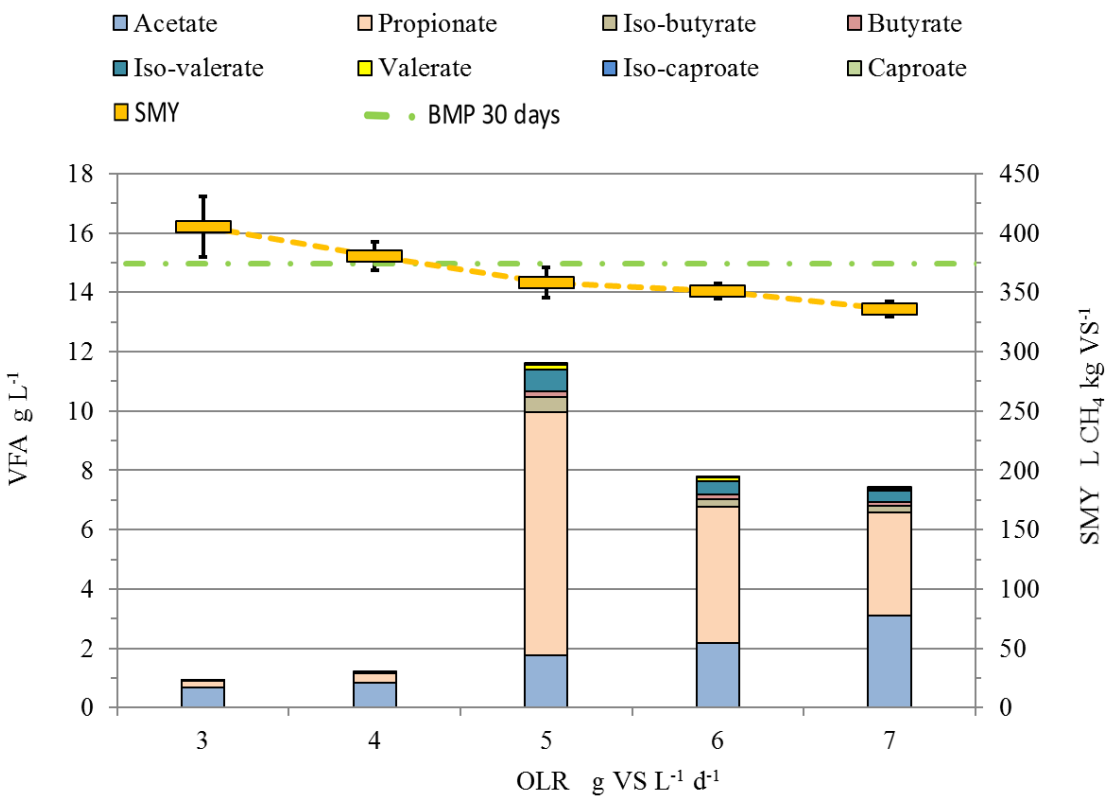

Fig. 5.2 Steady state specific methane yield and volatile fatty acids spectrum at increasing loading rate.

The increase of OLR in R3 had a significant impact on the process as illustrated in figure 5.2 and table 5.3. With enhanced substrate input a distinct rise in VFA level was observed. The pH fell to levels of 7.99, 7.93 and 7.65 at OLR of 5, 6 and 7 g VS L^{-1} d^{-1} respectively. Subsequently the free ammonia (NH_3) diminished to concentrations as low as 431 mg L^{-1} while TAN remained unchanged. The accumulation of VFA was the result of an imbalance between acid producing bacteria and acid consuming methanogenic archaea. At an OLR of 5 g VS L^{-1} d^{-1} a major accumulation of VFA (11.62 g L^{-1}) occurred, dominated by acidic and propionic acid (1.76 and 8.21 g L^{-1} respectively), followed by minor quantities of longer chain fatty acids. A further increase of OLR in R3 to 6 and 7 g VS L^{-1} d^{-1} induced lower overall VFA levels of 7.77 and 7.40 g L^{-1} respectively. The propionic acid concentration approximately halved, yet the acidic level was slightly elevated as compared to that at an OLR of 5 g VS L^{-1} d^{-1}. This indicates a recovery and adaption of the acetoclastic methanogens. Ahring (1995) observed acetate and propionate concentrations of up to 6000 mg L^{-1} and 3000 mg L^{-1} respectively, in the absence of

performance reductions. However, the elevated propionic levels and occurrence of longer chain fatty acids indicated stress and possible inhibition on the acetoclastic methanogens.

The deterioration of biological parameters in this trial had less impact on the SMY than previous studies had implied (Voelklein et al., 2017; Wall et al., 2014). Angelidaki et al. (1993) outlined the importance of individual digester characteristics emphasizing the necessity to consider reactor specific rather than general levels in assessing stability. Ahring (1995) and Franke-Whittle et al. (2014) showed that full-scale digesters can sustain higher levels of VFA while still maintaining stable performance. However, an elevated VFA level at lower pH possesses potential to harm the microbial community (Zhou et al., 2013). This equilibrium of acids shifts to its more undissociated (protonated) state causing damage through increased permeability to the cell membrane. The elevated leakage of VFA due to the shift in concentration gradient into the cell supresses overall activity and eventually reduces survival rates. In this trial increased levels of pH restricted the VFA to its more dissociated (unprotonated) state. Therefore, even the higher VFA concentration was less harmful to the cell membrane of the methanogenic archaea, as compared to a reactor close to failure at low pH.

The VFA/TIC trend matched the gain in VFA concentration and increased to 0.67 ±0.04 at an OLR of 5 g VS L^{-1} d^{-1}. At higher substrate input during OLR 6 and 7 g VS L^{-1} d^{-1}, the reduction in VFA also led to decreased VFA/TIC values of 0.58 and 0.55 respectively. Although the VFA concentrations exceeded the general recommended level of 2 g L^{-1}, the VFA/TIC only marginally overshot the stable fermentation threshold of 0.5 (Drosg, 2013). This was attributed to the increased pH and buffer capacity of the system (Franke-Whittle et al., 2014).

The SMY corresponded to the stepwise reduction in retention time (from 36 to 30 to 25 days) of the substrate in the system. A gradual drop in methane yield from 358 ±9.7 to 351 ±6.6 to 336 ±6.6 L CH_4 kg VS^{-1} respectively was observed (table 5.3). Although a numerical reduction in SMY was identified while increasing OLR from 5 to 6 to 7 g VS L^{-1} d^{-1}, a statistically significant difference was not found ($P>0.05$), see table 5.3. A statistically significant lower SMY at OLR 7 g VS L^{-1} d^{-1} compared to OLR 3 and 4 g VS L^{-1} d^{-1} was determined ($P<0.05$). The SMY at OLR

4 g VS L^{-1} d^{-1} did not statistically significant exceed the SMY of OLR 5 and 6 g VS L^{-1} d^{-1} ($P>0.05$).

The methane content ranged between 51.7% and 52.9% corresponding to the theoretical expected value of 51.9% established from the Buswell Equation. The gas yield of the reactor with the longest HRT (63 days) was 28 L CH_4 kg VS^{-1} higher compared to a retention time of only 25 days. This resulted in a 7.7% increased methane yield for a retention time increase of 2.5. The biomethane efficiency was calculated as 94% (HRT 36 days), 94% (HRT 30 days) and 92% (HRT 25 days) as compared to the corresponding HRT of the batch BMP assays. Between 75.4 to 80.4% of the maximum biomethane potential was reached at an OLR between 5 and 7 g VS L^{-1} d^{-1}. The reduced degradation at shorter HRT is further reflected by higher TS and VS contents in the digestate effluent (table 5.3). The TS and VS at the shortest HRT of 25 days remained at a higher level of 12.2% TS and 81.8% VS, as compared to the longest HRT (63 days: 10.7% TS; 76.5% VS) in these trials.

The systems resilience towards the high loading was mainly attributed to the beneficial characteristics of increased temperature (enhanced microbial activity & viscosity reduction of digestate), trace element addition and improved mixing system. Loading rates in excess of 7 g VS L^{-1} d^{-1} (retention time below 25 days) caused mechanical failure of the agitation system and a total solid contents of above 13% at an OLR of 8 g VS L^{-1} d^{-1} (data not shown in table 5.3). A maximum total solids content of 12% was also recommended by other studies (Koch et al., 2009; Thamsiriroj et al., 2012; Wall et al., 2014b). The achieved OLR of 7 g VS L^{-1} d^{-1} in this study exceeded maximum loadings of mesophilic and thermophilic grass silage mono-digestion of 3-4 g VS L^{-1} d^{-1} previously described in literature (Linke & Mähnert, 2005; Thamsiriroj et al., 2012; Wall et al., 2014b).

5.3.3 Contrasting batch and continuous digestion

The obtained yields of the continuous stirred tank reactor (CSTR) are compared to the batch digestion trials in figure 5.3 and table 5.3. It became apparent that at an HRT of 46 days the methane yields of the batch and continuous trials matched. At shorter HRT the methane yield of the CSTR were 6-8% lower than corresponding BMP results. This is explained by the fact that no fresh matter leaves the batch

system undigested. In contrast, a retention time dependent share of substrate leaves the continuous fed reactor not entirely digested. The longer the retention time the less this effect impacts on the SMY. At the longest HRT of 63 days the SMY of the CSTR aligned (within the measurement accuracy) with the batch system as the statistical effect of undigested substrate leaving the reactor becomes less significant. In addition, the floating effects of the grass due to the lower digestate dry solids content, as compared to that at the higher OLR and dry solids content in R3, may prolong the solid retention time as compared to the hydraulic retention time (Thamsiriroj et al., 2012). This suggests that thermophilic grass digestion in a continuous system is complete after 63 days.

However, the elevated VFA level at shorter HRT (<36 days) may impose an inhibition on the methanogens impacting on the possible SMY. The results suggested that within 30 days, 95% (BMP) and 87% (CSTR) of the final methane yield were obtained. The system's optimum behaviour was identified at an OLR of 4 and HRT of 46 days resulting in 94% of the final methane yield. This enabled a very stable digestion process and sufficient gas yields, while remaining within economically sustainable boundaries.

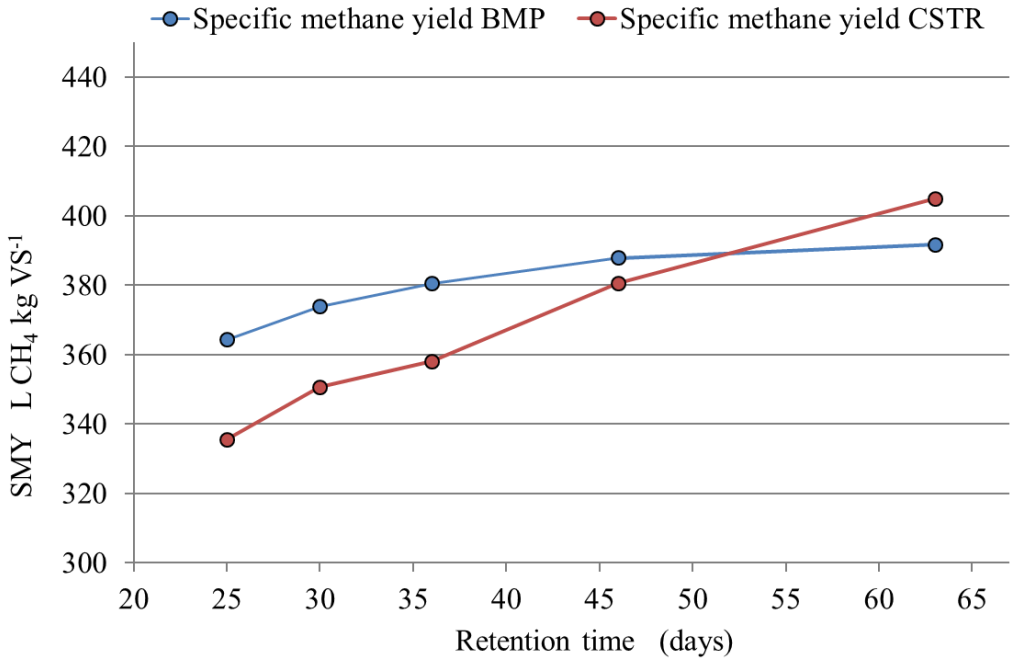

Fig. 5.3 Comparison of specific methane yield between batch (BMP) and continuous (CSTR) trials at increasing retention time.

5.3.4 Performance comparison of mesophilic versus thermophilic digestion

Biochemical and biological reactions may be distinguished by temperature. Thermodynamics dictate the speed of degradation where an increase in temperature is associated with an enhanced growth and reaction rate. This behaviour is theoretically described by the ARRHENIUS-equation. However, the kinetics are further influenced by substrate concentration as described by the MONOD-equation.

The methane yields were in the range of typical grass digestion trials 310-493 L CH_4 kg VS^{-1} as shown in table 5.4 (Allen et al., 2016; Mähnert et al., 2005; Nizami & Murphy, 2010; Nizami et al., 2012; Thamsiriroj et al., 2012; Wall et al., 2014a; Wall et al., 2014b). A comparison of the results of this study to other literature data is difficult as methane yields and kinetics mainly depend on the characteristics of the employed substrate. The results obtained in this study were therefore contrasted to mesophilic digestion of the same late cut grass silage of continuous (O'Shea et al., 2016) and batch (Wall et al., 2016) digestion trials. Figure 5.4 compares a 30 day 38 °C mesophilic (Wall et al., 2016) and 55 °C thermophilic batch biomethane potential test (this study) of grass silage. The final SMY resulted in 343 ±6.3 L CH_4 kg VS^{-1} for the mesophilic trial with a k-value of 0.134 (Wall et al., 2016). In contrast, the thermophilic BMP yielded 374 ±1.8 L CH_4 kg VS^{-1} with a k-value of 0.173. This indicates that the thermophilic process reached 84% of the theoretical maximum biomethane potential after 30 days, whereas the mesophilic trial yielded 77%. The corresponding gas yields at 30 days coincide with findings of Linke and Mähnert (2005) correlating k-values to maximum biomethane potential and retention time. The lag phase of the thermophilic and mesophilic BMP was 1.1 and 2.9 days respectively, confirming the rapid initial start and adaption of the thermophilic trials. The lag phase values match the data for grass digestion obtained by Allen et al. (2016).

The enhanced k-values of the thermophilic process reflected the dynamic capability of a process at elevated temperature level. Figure 5.4 confirms the rapid initial production of methane. This corresponds to 6.5 days for the mesophilic and 3.5 days for the thermophilic BMP to reach 50% (T_{50}) of the final 30-day gas production. However, the mesophilic methane yield almost aligns with the thermophilic yields after 10 days. The last 10 days of the trials are characterised by an additional gain in

methane yield of the thermophilic BMP. After 30 days retention the thermophilic BMP exceeded the mesophilic by 31 L CH_4 kg VS^{-1}, which represents a gain in SMY of 9%. The mesophilic (0.123) and thermophilic (0.198) k-values for cellulose control run approximately matched the corresponding k-values obtained from grass silage.

The methane yields of the continuous thermophilic digestion were compared to continuous mesophilic trials run on an identical feedstock, which yielded a SMY of 326 L CH_4 kg VS^{-1} at an OLR of 2 g VS L^{-1} d^{-1} at 36 days retention. At the same retention time, the thermophilic digestion of this study established an SMY of 358 L CH_4 kg VS^{-1}, yet at an OLR of 5 g VS L^{-1} d^{-1}. This indicates an increased methane yield of 10% of the thermophilic system and confirms the findings of the mesophilic vs. thermophilic BMP comparison. Even though the retention time of the thermophilic system was further reduced to 25 days (OLR 7 g VS L^{-1} d^{-1}), it still exceeded the methane yield of the 36 day mesophilic system by 10 L CH_4 kg VS^{-1}. However, at significantly longer retention times the mesophilic process may have an increased SMY and align with yields obtained under thermophilic conditions (Mähnert, 2007).

The superior gas yields at elevated loading and reduced retention time demonstrated the more resilient characteristics of the thermophilic process. The viscosity difference was identified as a key factor for improved grass digestion. In comparison to mesophilic temperature at the same retention time, the viscosity at thermophilic levels is firstly reduced due to enhanced degradation and lower dry solids content. Secondly, the natural behaviour of lower viscosity at increasing temperature is of major importance. This correlation and enhanced performances of the thermophilic process was also obtained and examined by Mähnert (2007).

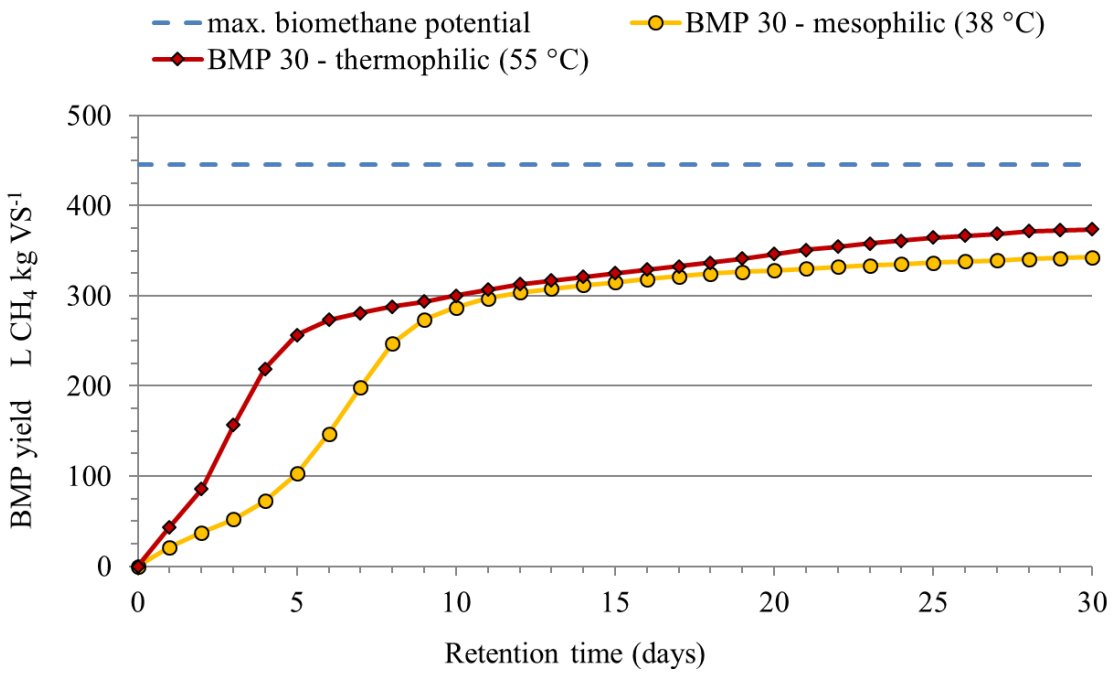

Fig. 5.4. Comparison of mesophilic and thermophilic BMP assay at 30 days.

Table 5.4. Results of grass digestion reported in literature.

Reactor operation mode	Reference	Temperature	HRT	OLR	SMY
		°C	d	g VS L^{-1} d^{-1}	L CH_4 kg VS^{-1}
Batch-BMP	Allen et al., 2016	38	30		315.6
Batch-BMP	Maehnert et al., 2005	38	28		310-360
Batch-BMP	Nizami & Murphy, 2010	38	22-35		350-493
Batch-BMP	Wall et al., 2016	38	30		343[a]
Batch-BMP	This experiment	55	30		374[a]
Batch-BMP	This experiment	55	25-63		364-392[a]
Continuous-CSTR	O'Shea et al., 2016	38	36	2	326[a]
Continuous-CSTR	Thamsiriroj et al., 2012	37	60	0.5-2.5	363-455
Continuous-CSTR	Wall et al., 2014a	37	19[b]	4	404[b]
Continuous-CSTR	Wall et al., 2014b	37	21-37[b]	2-3.5	398-414[b]
Continuous-CSTR	This experiment	55	36	5	358[a]
Continuous-CSTR	This experiment	55	25-63	3-7	336-405[a]

[a] on the same substrate basis; [b] recirculation of liquor.

5.4 Conclusion

Thermophilic grass digestion enabled higher loading and superior methane yields as compared to mesophilic digestion. The resilience at thermophilic temperature at high loading rates was attributed to the beneficial viscosity characteristics of increased temperature, trace element addition and improved mixing. Decreased retention time at enhanced loading rates reduced the gas yield, yet retention times of 25 days and loading rates of 7 g VS L^{-1} d^{-1} were feasible. The optimum system was identified at a 46 day retention time at a loading rate of 4 g VS L^{-1} d^{-1} yielding 86% of the maximum theoretical methane yield.

5.5 Supplementary data

All standard conditions mentioned in chapter 5 refer to standard temperature at 273K and standard pressure at 1013mbar.

Evaluation and interpretation of laboratory data:

The grass digestion trials were conducted in an ongoing sequence, subsequently moving from high to lower retention time. The data base does not include the results of the first retention time (acclimatisation period) after each increase in loading. The subsequent two retention times represent the data basis for the experimental evaluation. The experiments focused on thermophilic digestion of grass silage and evaluated statistically significant differences between an increase in retention time, loading rate and SMY. A data base of mesophilic digestion to ensure a valid statistical comparison and assessment within the continuous experiments in chapter 5 was not given. Therefore, a statistically significant difference between mesophilic and thermophilic digestion was not established. The comparison between mesophilic and thermophilic are based on numerical differences on the same substrate basis and similar retention time.

Comparison of mesophilic and thermophilic grass digestion:

The inoculum for the mesophilic and thermophilic BMP assays were both sourced from previous grass digestion reactors. The fibres in the digestate were removed to ensure a rapid depletion in gas production. After a 10-day waiting period and full gas depletion the remaining digestate represented an inoculum rich in methanogens and dissolved nutrients. The lag phase of the thermophilic and mesophilic BMP was 1.1 and 2.9 days respectively, confirming the rapid initial start and adaption of the thermophilic trials. The mesophilic BMP kinetics match the data for grass digestion obtained by Allen et al. (2016) with differently sourced mesophilic inoculum. To further strengthen the difference of mesophilic and thermophilic digestion in BMP assays more trails with differently sourced inoculum and determination of statistical differences are required, to further substantiate the observed conclusion.

The thermophilic temperature level was postulated to stimulate microbial activity, facilitate rapid degradation and reduce viscosity properties of the digestate (Mähnert, 2007). Therefore, the resilience of the thermophilic systems towards the high loading was mainly attributed to the beneficial characteristics of increased temperature (enhanced microbial activity & viscosity reduction of digestate) and subsequent improved mixing system. The viscosity properties of mesophilic and thermophilic digestate were not obtained during the course of the experiment. A detailed evaluation and comparison to substantiate the impact of viscosity on the digestion process can therefore not be given. In comparison to mesophilic temperature at the same retention time, the viscosity at thermophilic levels is firstly reduced due to enhanced degradation and lower dry solids content. Secondly, the natural behaviour of lower viscosity at increasing temperature is of major importance. The remarks in the result and conclusion section in chapter 5 may be seen as a theoretic explanation for the observed high rate in loading, rather than a finding of the study.

The outlined benefits of thermophilic as compared to mesophilic digestion only apply at similar retention times or loading and are associated with a higher energy input to maintain the elevated temperature level. If heat is an abundant source at a biogas plant and not used otherwise (such as the excess heat from a combined heat and power facility, from pasteurisation or from an exothermic biomethanation process), it may also be utilised to benefit from the outlined advantages in this study. However, it has to be stated that at prolonged retention, the difference in SMY of mesophilic and thermophilic may disappear. A general recommendation extrapolated for thermophilic systems exceeding the overall performance in a single-stage system can not be derived from this study. In conclusion, a case to case cost-benefit assessment may facilitate the choice of reactor temperature level.

Specific methane yields including gas potential from VFA in the digestate:
An elevated VFA level leaving the digester at shorter HRT (<36 days) may impact on possible SMYs achieved. The potential gas production originating from these VFAs is outlined in table 5.5, 5.6 and 5.7. In table 5.7 the VFA corrected SMY yields of the CSTR are compared to the SMY of the continuous and batch digestion trials. Retention times below 36 days revealed a VFA related SMY of 16.6 to 28.3 L CH_4 kg VS^{-1}. This corresponds to an increase in methane yield of 4.9 to 7.9%

sourced from undigested VFA in the digestate. Therefore, the numerical difference between the CSTR and BMP system (as outlined figure 5.3) at defined retention times is further reduced.

If a digestion system is not followed by a secondary digester or covered storage vessels, the potential SMY from VFA is lost and may adversely affect GHG savings of the system reducing its sustainability. However, additional sequential vessels or covered storage vessels may compensate for the otherwise lost gas potential in a full scale systems.

Table 5.5. Theoretic stochiometric methane production from VFA (C_2 – C_4) according to Buswell equation.

Acetate:	$C_2H_4O_2 \rightarrow 1\ CH_4 + 1\ CO_2$	(374 L CH_4 kg^{-1})
Propionate:	$C_3H_6O_2 + 0.5\ H_2O \rightarrow 1.75\ CH_4 + 1.25\ CO_2$	(530 L CH_4 kg^{-1})
(Iso) Butyrate:	$C_4H_8O_2 + 1\ H_2O \rightarrow 2.5\ CH_4 + 1.5\ CO_2$	(637 L CH_4 kg^{-1})
(Iso) Valerate:	$C_5H_{10}O_2 + 1.5\ H_2O \rightarrow 3.25\ CH_4 + 1.75\ CO_2$	(715 L CH_4 kg^{-1})

It is assumed that volatile solids compounds only consist of C, H, O, N.

Table 5.6. Theoretical calculation of potential methane production from VFA in the digestate.

Exemplary calculation pathway for acetate at HRT 25 days:

3.12 g L^{-1} (acetate concentration digestate)[a] x 374 L CH_4 kg VS^{-1} (SMY from acetate as in table 5.5) x 0.0327 L (digestate leaving reactor per day) / 7 g VS L^{-1} d^{-1} equates to a gas potential of 5.5 L CH_4 kg VS^{-1} for acetate in the digestate exiting reactor per day.

Similar calculation pathway for propionate, (iso) butyrate, (iso) valerate add up to a total SMY potential (summarised in table 5.7) sourced from VFA in the digestate leaving the reactor after an HRT of 30, 36, 46, 63 days.

[a] values retrieved from table 5.3 in section 5.3.2.

Table 5.7. Performance parameters of thermophilic (55 °C) grass mono-digestion at increasing loading rate and corrected SMY including gas potential from VFA in digestate.

Retention time	d	25	30	36	46	63
Batch-system:						
BMP	L CH_4 kg VS^{-1}	364	374	381	388	392
CSTR-system:						
SMY	L CH_4 kg VS^{-1}	336	351	358	381	405
SMY $_{VFA\ digestate}$[a]	L CH_4 kg VS^{-1}	16.6	18.3	28.3	2.3	1.8
SMY $_{VFA\ corrected}$[b]	L CH_4 kg VS^{-1}	352	369	386	383	407
Increase in gas yield	%	4.9	5.2	7.9	0.6	0.4

[a] SMY potential originating from VFA in digestate; [b] SMY includes gas potential from VFA.

Chapter 6: Biological methanation: Strategies for in-situ and ex-situ upgrading in anaerobic digestion

Biological methanation: Strategies for in-situ and ex-situ upgrading in anaerobic digestion

M. A. Voelklein[1, 2], Davis Rusmanis[1, 2], J. D Murphy[1, 2]

[1]MaREI Centre, Environmental Research Institute (ERI), University College Cork (UCC), Ireland

[2]School of Engineering, UCC, Ireland

Abstract

This study investigated in-situ and ex-situ biological methanation strategies for biogas upgrading potential. The addition and circulation of hydrogen with a ceramic gas diffuser unit revealed positive effects on the methanogenic process. A short-term maximum methane productivity of 2.5 L CH_4 per L reactor volume per day (L_{VR}^{-1} d^{-1}) was obtained in-situ. Adverse effects of elevated dissolved hydrogen concentrations on acetogenesis became evident. Ex-situ methanation in a reactor subjected to gas recirculation for recurrent 24 hour periods achieved methane formation rates of 3.7 L CH_4 L_{VR}^{-1} d^{-1}. A biomethane with methane concentrations in excess of 96% successfully demonstrated the potential for gas grid injection. A theoretic model supplying gases continuously into a sequential ex-situ reactor system and steadily displacing the upgraded biogas confirmed similar methane formation performance and was advanced to a full-scale concept. Gas conversion efficiency of 95% producing biomethane at 85% methane content was attained. A hybrid model, where an in-situ grass digester is followed by an ex-situ reactor, is proposed as a novel upgrading strategy.

Keywords: biogas; in-situ; ex-situ; biological methanation; upgrading strategies; power to gas.

6.1 Introduction

6.1.1 Introduction and background

Anaerobic digestion of organic wastes and energy crops has become a key sustainable technology to provide green gas to natural gas grids in Europe (Wall et al., 2017). The physiochemical removal of excess carbon dioxide in biogas elevates the calorific value to match requirements for gas grid injection (Angelidaki et al., 2018). A further utilisation of this segregated carbon dioxide by biological reduction to methane emerged as a potential pathway in recent years (Angelidaki et al., 2018; Burkhardt & Busch, 2013; Lecker et al., 2017; O'Shea et al., 2017). According to the Sabatier reaction (equation 8) hydrogenotrophic methanogenic archaea are able to consume an equimolar amount of four times hydrogen (H_2) to carbon dioxide (CO_2) and generate biomethane of natural gas quality (Fukuzaki et al., 1990).

$$4H_2 + CO_2 \rightarrow CH_4 + 2H_2O \qquad \Delta G^0 = -165\ KJ\ mol^{-1} \qquad (8)$$

6.1.2 Biological methanation

The exergonic reaction in equation 8 is catalysed by hydrogenotrophic methanogenic archaea and referred to as biological methanation. It can be performed either in-situ within a biogas digester or ex-situ in an adjacent external reactor (Angelidaki et al., 2018; Lecker et al., 2017). In an in-situ methanation system organic substrate and additional hydrogen (such as from electrolysis of preferably surplus green electricity) is added to the digester where the biogas is produced. As per conventional anaerobic digestion, the substrate degradation steps (hydrolysis and acidogenesis) provide intermediates such as volatile fatty acids (VFA) and precursors like carbon dioxide for the methanation process. On the contrary, in an ex-situ system carbon dioxide (such as from a fermentation process), hydrogen, essential nutrients and hydrogenotrophic methanogens are required (Angelidaki et al., 2018; Lecker et al., 2017). The initial stages of anaerobic digestion (hydrolysis and acidogenesis) are not present in an ex-situ system. Thus, reactor stability and performance only depend on sufficient provision of those four ingredients.

6.1.3 Constraints of in-situ biological methanation

The associated increase in dissolved hydrogen influences microorganisms utilising hydrogen in their metabolic pathway. This includes for hydrogen producing acidogenic and acetogenic bacteria, as well as hydrogen consuming homoacetogenic microorganisms and hydrogenotrophic methanogenic archaea (Angelidaki et al., 2018; Fukuzaki et al., 1990). Thus, the symbiotic fermentation stages of methanogenesis (equation 8) and acetogenesis (equation 10) are exposed to altered conditions and as such a system in equilibrium is put under stress. The reason can be found in thermodynamics which dictate the feasibility of fatty acid oxidation such as from butyrate (equation 9) and propionate (equation 10) to acetate via acetogenesis (Fukuzaki et al., 1990).

$$CH_3CH_2COOH + 2H_2O \rightarrow CH_3COOH + CO_2 + 3H_2 \quad \Delta G^0 = +76.1\ kJ\ mol^{-1} \quad (9)$$

$$CH_3CH_2CH_2COOH + 2H_2O \rightarrow 2CH_3COOH + 2H_2 \quad \Delta G^0 = +48.3\ kJ\ mol^{-1} \quad (10)$$

At standard conditions these reactions remain endergonic and become feasible only when hydrogen partial pressure is kept below 10 Pa (Fukuzaki et al., 1990). Adequate levels are sustained by interspecies hydrogen transfer between acetogenic and hydrogenotrophic methanogenic microorganisms (equation 8). This balance of immediate production and consumption of hydrogen, with the associated transfer of electrons, is stressed by the addition of exogeneous hydrogen to the process. Elevated hydrogen partial pressure (>10 Pa) drastically favours methanogenic activity (equation 8), however adversely affects acetogenesis (equation 10) and ultimately inhibits the oxidation of longer chained volatile fatty acids to acetate (Fukuzaki et al., 1990).

Secondly, when exogenous hydrogen is introduced to an anaerobic digestion process, the elevated hydrogen partial pressure stimulates homoacetogenesis (equation 11). In an conventional anaerobic digester only 2 - 5% of hydrogen is consumed by homoacetogenesis (Mackie & Bryant, 1981). In contrast, when exogenous hydrogen is added, up to 40% of hydrogen maybe consumed by the Wood-Ljungdahl pathway

(homoacetogenesis), significantly contributing to acetate production and subsequently acetoclastic methane formation, as shown in equation 12 (Angelidaki et al., 2018; Liu et al., 2016).

$$4H_2 + 2CO_2 \rightarrow CH_3COOH + 2H_2O \quad \Delta G^0 = -104.5\ kJ\ mol^{-1} \quad (11)$$

$$CH_3COOH \rightarrow CH_4 + CO_2 \quad \Delta G^0 = -31.0\ kJ\ mol^{-1} \quad (12)$$

In a balanced in-situ system, with adequate levels of hydrogen in solution to allow fatty acid oxidation, simultaneous production of biogas and upgrading to biomethane is possible (Agneessens et al., 2017; Bassani et al., 2016; Luo & Angelidaki, 2013b; Luo et al., 2012a; Mulat et al., 2017).

6.1.4 Solubilisation of hydrogen

Regardless of the methanation system, the solubilisation of hydrogen is the decisive step to make gaseous hydrogen available for microorganisms on a cellular level. With a solubility rate of 0.7 mmol H_2 L^{-1} bar^{-1}, hydrogen dissolves poorly in water, with solubility rates 24 times less than that of carbon dioxide at 55 °C. The hydrogen to liquid transfer is therefore the bottleneck of the process and can be described by equation 13.

$$R_{H_2} = (k_L a)_{H_2} \cdot \left(c_{H_{2,G}} - c_{H_{2,L}}\right) \quad (13)$$

Where R_{H_2} is the volumetric hydrogen mass transfer rate in mol L^{-1} h^{-1}. The volumetric mass transfer coefficient is described by k_La in L h^{-1} and foremost characterised by reactor configuration, mixing speed, gas recirculation and the employed gas diffusion system (Kraakman et al., 2011; Orgill et al., 2013). The gradient between the gaseous hydrogen concentration $c_{H_2,G}$ and the dissolved hydrogen concentration $c_{H_2,L}$ in mol L^{-1} defines the driving force for hydrogen gas to liquid transfer. Further the system pressure, solubility (Henry constant), temperature and hydrogen partial pressure determine the final amounts of hydrogen going into solution (Angelidaki et al., 2018; Ullrich et al., 2018).

The hydrogen partial pressure is further influenced by the volume reduction in the headspace during upgrading. The amounts of gases dissolving in liquid in comparison to the concentration in the headspace can be seen in figure 6.1 and figure 6.2 (ideal gas to liquid transfer at 50°C and 1013 mbar assumed). Although 80% of the initial gas mix in the head space comprises hydrogen (figure 6.1), only a minor fraction of hydrogen is dissolved in liquid (figure 6.2). At increasing gas conversions, the total volume in the headspace reduces (to 20% at complete conversion as compared to the start) as a result of the hydrogen coupling with carbon dioxide to produce methane. This causes a non-linear change in partial pressures. Therefore, the amount of hydrogen dissolved remains at elevated levels during gas conversion. At 90% conversion 35% of the initial 0.52 mmol L^{-1} of hydrogen are still dissolved in water. However dissolved hydrogen concentrations drastically decrease in excess of 90% conversion, significantly impacting the possible upgrading performance. With the potential methane content at 90% conversion being 64.3% and with hydrogen in solution drastically reducing, the final 10% gas conversion to reach 100% methane content in the off gas appears challenging. In addition, figure 6.1 and 6.2 allow the validation of gas concentrations in the off gas at certain gas conversions. They further provide an estimation of dissolved gases in solution at ideal conditions at 50°C at 1013 mbar.

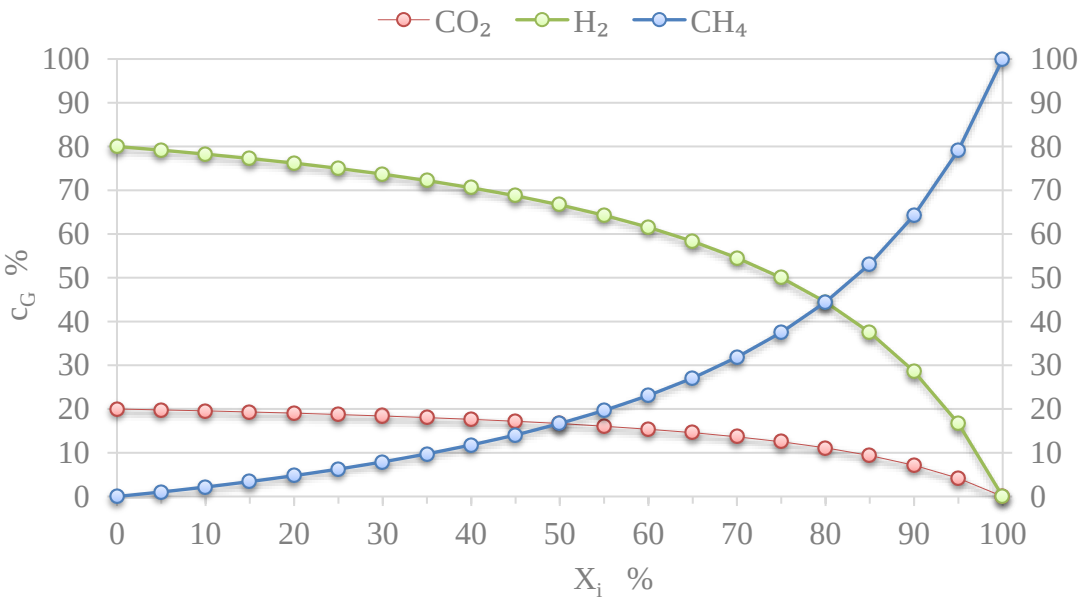

Fig. 6.1. Theoretic model of gas concentrations (c_G) in the headspace of the reactor at increasing gas conversions (X_i) at 50°C at 1013 mbar.

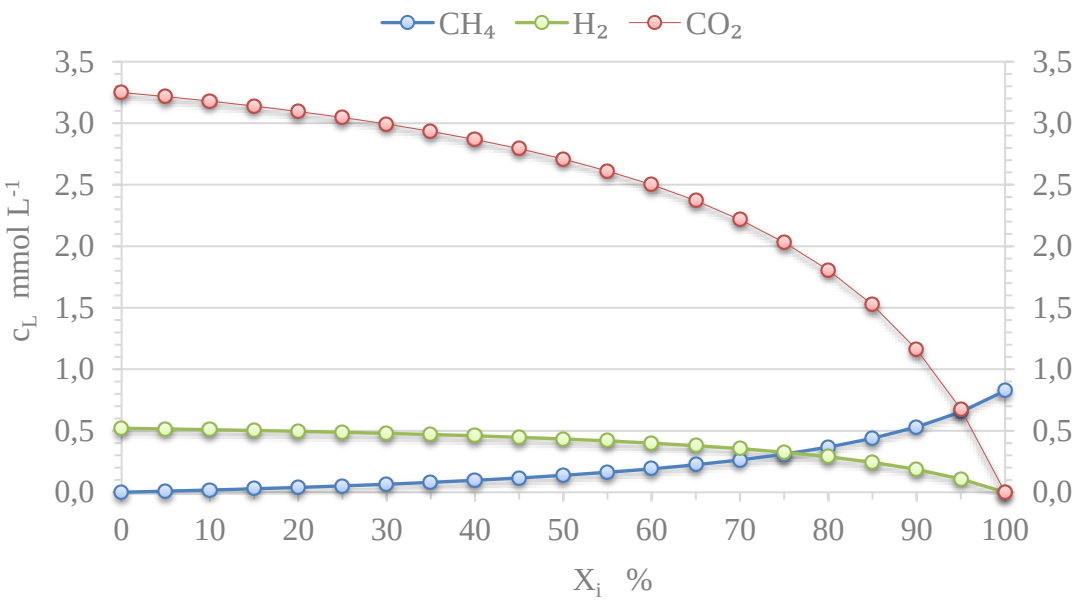

Fig. 6.2. Theoretic model of dissolved gas concentrations in liquid (c_L) at increasing gas conversions (X_i) at 50°C at 1013 mbar.

6.1.5 State of the art biological upgrading concepts in laboratory scale

In the lab various systems have been investigated including: intensely mixed reactor bottles (Agneessens et al., 2017; Guneratnam et al., 2017; Luo & Angelidaki, 2012b; Mulat et al., 2017); bubble column reactors (Kougias et al., 2017; Savvas et al., 2017); trickle bed reactors with immobilized microorganisms (Burkhardt et al., 2015; Rachbauer et al., 2016; Strübing et al., 2017; Ullrich et al., 2018); fixed bed reactors functioning as biological/anaerobic filters (Alitalo et al., 2015); hollow fibre membrane reactors (Luo & Angelidaki, 2013b); continuous stirred tank reactors (Kougias et al., 2017; Luo & Angelidaki, 2013a); and upflow anaerobic sludge blanket reactors (Bassani et al., 2016; Luo & Angelidaki, 2013b; Rittmann et al., 2015).

Novel concepts have been suggested for instance by Savvas et al. (2017) investigating ex-situ methanation in a 110 cm tall glass cylinder with 1.5 litre working volume. The gas mixture was dissolved directly by introducing it into a centrifugal pump and recirculating the liquid from bottom to top at a rate of 6 L min^{-1}. A methane formation rate (MFR) per litre reactor volume (VR) of 12 L CH_4 L_{VR}^{-1}

d^{-1} was achieved when total upgrading to methane was accomplished. Kougias et al. (2017) assessed ex-situ methanation of a biogas with 60% methane content. Positive effects of gas recirculation were observed in a bubble column and two in-series connected upflow reactors. At gas recirculation rates of 12 L h^{-1} an MFR of 1.2 and 0.5 L CH_4 L_{VR}^{-1} d^{-1} at 98% methane content was attained. More complex ex-situ reactor configurations such as trickle bed reactors attained 98% methane concentrations at 15.4 L CH_4 L_{VR}^{-1} d^{-1} (Strübing et al., 2017). Bassani et al. (2016) was able to upgrade biogas from 58% CH_4 content to 82% at an MFR of 1.3 L CH_4 L_{VR}^{-1} d^{-1} in an in-situ upflow anaerobic sludge blanket reactor; this led to a VFA increase by a factor of 1.5 to 5.1 g L^{-1}.

Guneratnam et al. (2017) identified a more efficient process at 65 °C compared to 55 °C. An increase in system pressure from 1.5 bar to 9 bar in a trickle bed reactor revealed an elevation of methane content from 64% to 86% at an MFR of up to 4.3 L CH_4 L_{VR}^{-1} d^{-1} (Ullrich et al., 2018). An increase in mixing intensity proved to have positive effects on MFRs (Luo et al., 2012a; Rachbauer et al., 2016; Seifert et al., 2014). In conclusion, the upgrading success could be improved by elevated pressure, gas retention time, phase boundary interface and temperature.

6.1.6 Novelty and objectives

Novel concepts and various upgrading strategies have been proposed in the scientific literature, with the main focus on ex-situ systems; data on in-situ methanation systems is limited (Agneessens et al., 2017; Bassani et al., 2016; Luo & Angelidaki, 2013b; Luo et al., 2012a; Mulat et al., 2017). This is most likely a result of the described biological constraints. A gap in the state of the art is the examination of in-situ methanation utilising complex substrates such as grass silage and making a direct comparison with ex-situ reactors on the basis of hydrogen injection rates and MFR. As continuous stirred tank reactors (CSTR) dominate current biogas facilities, a modified CSTR-system with gas recirculation and improved gas distribution appears as a promising in-situ concept to investigate.

The objectives of this paper include the assessment of lab-scale in-situ biological methanation in grass silage fed digesters, contrasted with ex-situ biological methanation. The upgrading success and associated influence of increased hydrogen

partial pressure on the proposed methanation strategies is discussed and contrasted as part of this study. The research results are used to propose novel upgrading models and concepts. The innovation in this paper is the connection of ex-situ units in series and merging in-situ and ex-situ units to a hybrid model estimating detailed set ups of full-scale applications based on lab scale experimental data.

6.2 Materials and Methods

6.2.1 Reactor systems

This study investigated in-situ and ex-situ upgrading strategies for biogas and carbon dioxide to biomethane. Figure 6.3 shows the three employed reactor systems: Batch in-situ (BIS), batch ex-situ (BES) and continuous ex-situ (CES). The employed stainless-steel reactor had a total volume of 9.5 litres with an internal diameter of 0.15 m and a height of 0.6 m. Externally injected gases such as hydrogen, carbon dioxide or methane were measured with Ritter drum type gas meter TG5/5 (for BIS and BES) and digital mass flow meters Voegtlin compact regulator GCR (for CES). A 100 litre gas bag provided gas storage, before recirculation through a gas diffuser to the bacterial bed. The success of the upgrading process was ultimately quantified with a Ritter drum type gas meter TG5/5 and a Hewlett Packard (HP6890) gas chromatograph. The deployed system was subsequently used for all applied upgrading strategies. However, stirring was only necessary in the batch in-situ experiment.

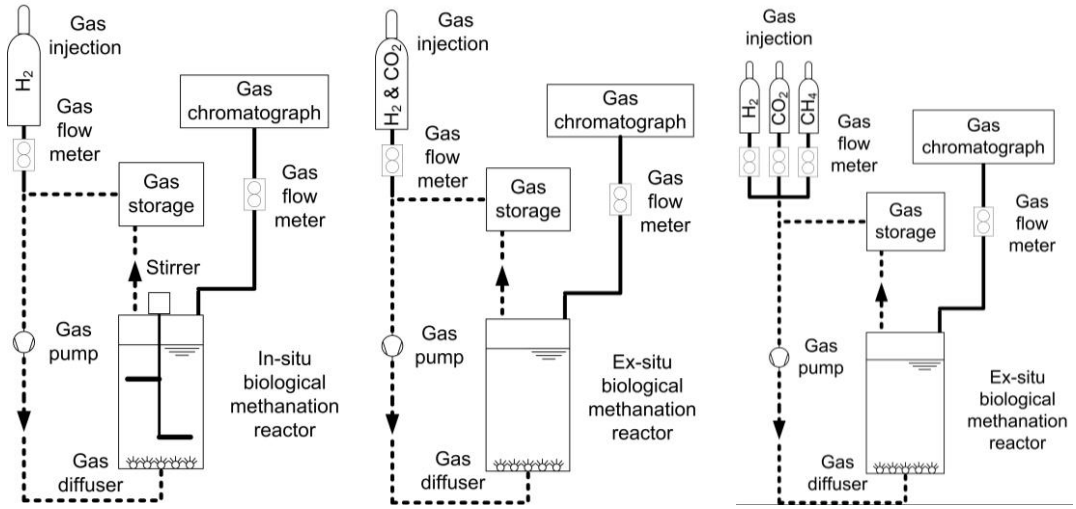

Fig. 6.3. Schematic of experiment lay out: a) Batch in-situ (BIS 1 - BIS 6), b) Batch ex-situ (BES 1 - BES 2), c) Continuous ex-situ (CES 1 - CES 6).

6.2.2 Design and operation conditions in-situ methanation

The in-situ upgrading of grass silage was performed at thermophilic conditions (55 °C) and ambient pressure. Prior to the experiment, the reactor was filled with inoculum from a thermophilic lab scale reactor operating at the same conditions, feedstock and nutrient supply (Voelklein et al., 2016). The feedstock was previously ensiled first-cut perennial rye grass with a dry solids content of 20%, 91% of which were volatile. Undersupplied trace elements were supplemented according to Voelklein et al. (2016) during the whole course of the in-situ experiment.

A loading rate of 4 g VS L^{-1} d^{-1} was applied resulting in 46 days substrate retention time. In a series of thermophilic grass digestion trials, Voelklein et al. (2016) showed stable thermophilic grass digestion at increasing organic loading rates (OLR) rising from 3 - 8 g VS L^{-1} d^{-1} with supplementation of deficient trace elements. An organic loading rate of 4 g VS L^{-1} d^{-1} was chosen here so as not to overload the microorganisms and still enable a viscous digestate medium to be established. The viscous conditions in the digestate were thought to enhance gas residence time and to capture ultra-fine bubbles, facilitating gas to liquid mass transfer. Table 6.1 shows the design and sequence of the in-situ methanation trials. The batch in-situ process

received grass silage as feedstock on a daily basis and an equimolar amount of four times hydrogen to the expected carbon dioxide production in the biogas. In order to enhance contact between the introduced hydrogen, the produced biogas and the microbial community, a gas pump continuously recirculated the gases through the bacterial bed for a 24 hour batch period at a rate of 4 L min^{-1}. As a consequence, carbon dioxide is converted to methane.

The experiment was conducted in an ongoing sequence, subsequently moving from BIS 1 to BIS 6 over time (results of the acclimatisation period BIS 2 not reported because of measuring equipment failure). Prior to each in-situ upgrading period (BIS 3, BIS 5, BIS 6) with external hydrogen, the specific methane yield with the sole substrate grass silage was assessed (BIS 1 and BIS 4) to match results of previous trials at similar conditions (Voelklein et al., 2016). The batch in-situ trials were further split into operation stages with low (BIS 3) and high performance (BIS 5 and BIS 6) gas diffusing systems. The low performance gas diffusing system comprised a low-pressure gas pump (0.2 bar) diffusing the gases with a fish stone. The fish stone diffuser was chosen due to its limited diffusing capacity. This should prevent elevated hydrogen partial pressure in the digestate causing overloading and inhibition. On the contrary, the high-performance ceramic gas diffusing system (Ceramic Dome Fine Bubble Diffuser, 304 SS Base) was selected to evaluate the impact of increased hydrogen concentrations both on the microbial community and performance. The ceramic diffuser covered the entire bottom area of the reactor to maximise the gas to liquid contact phase. It required a necessary gas compression in excess of 2 bar (increased pressure only between pump and diffuser). The elevated pressure allowed diffusion of the gases with smaller bubble size maximising hydrogen gas to liquid transfer.

6.2.3 Design and operation conditions ex-situ methanation

Table 6.2 shows the design and sequence of the ex-situ methanation trials. The ex-situ methanation was run at ambient pressure and thermophilic conditions (55 °C). It was divided into three major stages: Batch ex-situ with hydrogen and carbon dioxide injection (BES 1 and BES 2), continuous ex-situ with hydrogen and carbon dioxide injection (CES 1 to CES 3) and continuous ex-situ with hydrogen, carbon dioxide

and methane injection (CES 4 to CES 6). The continuous ex-situ methanation (CES 1 to CES 6) investigated the impact of a steady gas injection and release, in contrast to the total amount being supplied once a day for a 24-hour upgrading period in BES 1 and BES 2. As a result, the hydrogen partial pressure remained at a steadier level, rather being the initial sole constituent and gradually declining over the course of a 24-hour period. In addition, the gas retention time decreased from 24 hours to less than 2 hours (table 6.2).

Gases were introduced and recirculated through a ceramic gas diffuser after compression to 2 bar. The batch ex-situ systems BES 1 and BES 2 operated with a gas residence time of 24 hours, at low (BES 1) and medium (BES 2) hydrogen/carbon dioxide loading. In contrast, the continuous ex-situ systems CES 1 to CES 6 experienced a steady displacement of gases at varying hydrogen/carbon dioxide loading. CES 1 to CES 3 were subjected to an injection of hydrogen and carbon dioxide. CES 4 to CES 6 received additional methane quantities to represent a synthetic biogas injection (carbon dioxide and methane mixture). In order to compensate for reactor dilution with water during the methanation process (formation of water according to equation 8 and 11), a nutrient solution retrieved from the liquid phase of a grass digester (free of fibre and VFA) was added to the process periodically (Voelklein et al., 2016). The nutrient solution was subjected to a filtration and incubation process to ensure fibre and complete volatile fatty acids removal (cessation of gas production).

6.2.4 Analytical methods

The total solids and volatile solids (VS) were determined according to Standard Methods 2540 G. The pH value was analysed using a pH meter (Jenway 3510). The concentrations of individual volatile fatty acids were analysed by a gas chromatograph (Hewlett Packard HP6890) using a Nukol TM fused silica capillary column and a flame ionisation detector (FID). Hydrogen was used as a carrier gas. A Hewlett Packard HP6890 gas chromatograph, equipped with a Hayesep R packed GC column (3 m x 2 mm, mesh range of 80 - 100) and a thermal conductivity detector (TCD) analysed the gas composition for methane, carbon dioxide, hydrogen, oxygen and nitrogen. Argon was used as the carrier gas. Certified gas standards were

employed for the standardization of hydrogen, methane and carbon dioxide. Gas flows were measured by using a Ritter drum type gas meter TG5/5 and digital mass flow meters Voegtlin compact regulator GCR. The measured gas volume was adjusted to the volume at standard temperature (273 K) and pressure (1013 mbar).

6.2.5 Calculations

The most important parameters to characterise the performance and efficiency of a methanation system are methane formation rate (MFR), gas retention time (RT) and gas conversion (X_i). The MFR (equation 14) is a function of the volumetric methane flow rate entering ($F_{CH_4\ in}$) and leaving ($F_{CH_4\ out}$) the digester based on the reactor volume V_R.

$$MFR = \frac{F_{CH_4,out} - F_{CH_4,in}}{V_R} \quad (14)$$

The retention time (RT) of the gases in the reactor is based on equation 15. The volume change of reactant gases is reflected by an average residence time of the flow in ($F_{gas\ in}$) and out ($F_{gas\ out}$) in relation to the reactor Volume (V_R).

$$RT = \frac{V_R}{(F_{gas\ in} + F_{gas\ out})/2} \quad (15)$$

The success of hydrogen and carbon dioxide forming methane is defined by the conversion rate (X_i). The gas conversion rate of the educt gases is calculated according to equation 16, where $F_{CH_4\ out}$ is the outgoing and $F_{CH_4\ in}$ the incoming volumetric methane flow.

$$X_i = \frac{F_{CH_4\ out} - F_{CH_4\ in}}{F_{CH_4\ out}} \quad (16)$$

The gas conversion in the in-situ process was allocated to a share of methane formation derived from carbon dioxide and hydrogen denoted as $X_{CO_2+H_2 \rightarrow CH_4}$ (equation 17) and methane formation from grass labelled $X_{Grass \rightarrow CH_4}$ (equation 18), where $F_{CH_4\ out}$ is the outgoing volumetric methane flow, $F_{H_2\ in}$ and $F_{H_2\ out}$ the volumetric hydrogen flow entering and leaving the reactor. The daily mass based on

volatile solids added to the reactor is represented by m_{VS}. The specific methane yield is indicated by SMY.

$$X_{CO_2 + H_2 \rightarrow CH_4} = \frac{F_{H_2\ in} - F_{H_2\ out}}{F_{H_2\ in}} \quad (17)$$

$$X_{Grass \rightarrow CH_4} = \frac{F_{CH_4\ out} - (F_{H_2\ in} - F_{H_2\ out})/4}{m_{VS} * SMY} \quad (18)$$

6.3 Results and discussion

6.3.1 In-situ methanation of grass silage

6.3.1.1 In-situ methanation - low performance gas diffuser

Table 6.1 outlines the experimental stages and performance characteristics of the in-situ trials. The experiment commenced (BIS 1) with a loading rate at a level of 4 g VS L^{-1} d^{-1}, resulting in a retention time of 46 days (table 6.1). No hydrogen was added at this stage. Stable digestion was monitored and confirmed by low volatile fatty acid values of around 472 mg L^{-1} as suggested by Drosg (2013). Fos/Tac (free organic acids/total inorganic carbon) and pH remained within stable limits of 0.37 and 7.81 respectively. A specific methane yield of 388 L CH_4 kg VS^{-1} and a methane concentration of 54.8% was measured. This corresponds to an MFR of 1.5 L CH_4 L_{VR}^{-1} d^{-1} and matches findings previously established by Voelklein et al. (2016) on the exact same substrate.

Period BIS 2 and BIS 3 followed the grass mono digestion period of BIS 1 (results of the acclimatisation period BIS 2 not reported because of measuring equipment failure). The reactor operation mode was changed to batch in-situ methanation. Thus, hydrogen was introduced together with the feedstock on an everyday basis. During BIS 3 external hydrogen was injected through a fish stone diffuser at a rate of 5.05 L H_2 L_{VR}^{-1} d^{-1} and recirculated together with the produced biogas for a 24-hour batch period. The hydrogen added equated to four times the expected carbon dioxide production (equimolar ratio), based on the specific methane yield found in BIS 1.

In theory, complete upgrading almost doubles the methane output (as CO_2 is converted to an equal volume of CH_4) elevating the specific methane yield from 388

L CH_4 kg VS^{-1} (at a CH_4 concentration in the biogas of 54.8%) to 708 L CH_4 kg VS^{-1}. However, the specific methane yield raised only to 460 L CH_4 kg VS^{-1} equating to 65% of the predicted final methane yield. A detailed evaluation of the upgrading process and off gas revealed the gas conversion and individual contributions to the gained methane yields. 92% of the possible methane yield from grass was reached. In contrast, only 33% of the potential methane from hydrogen was attained. This was attributed to the characteristics of the lower performance gas diffuser limiting the gas to liquid mass transfer.

In total, the MFR of 1.82 L CH_4 L_{VR}^{-1} d^{-1} lead to an increase by 19% compared to grass mono digestion. The incomplete upgrading let to a dilution of methane concentration to 32.1% compared to 54.8% in BIS 1. Compared to BIS 1 the volatile fatty acids concentration quadrupled. The main contributors towards the total amount of 1897 mg L^{-1} were acetic and propionic acid. This is still considered uncritical using anaerobic digestion guidelines developed by Drosg (2013) and is further confirmed by low Fos/Tac values of 0.4 (Drosg, 2013).The absence of significant accumulation of volatile fatty acids indicates fast consumption of exogeneous hydrogen by hydrogenotrophic or homoacetogenic microbes.

Table 6.1. Performance characteristics of grass in-situ methanation.

		BIS 1	BIS 3	BIS 4	BIS 5	BIS 6
Operation mode Diffuser		CSTR	CSTR & batch Fish stone	CSTR	CSTR & batch Ceramic diffuser	CSTR & batch Ceramic diffuser
Injected substrates		Grass	Grass	Grass	Grass	Grass
Injected gases		None	H_2	None	H_2	H_2
Hydrogen loading		-	Equimolar	-	Equimolar	Equimolar
OLR	g VS/L/d	4	4	4	4	4
HRT_{Grass}	d	46	46	46	46	46
Gas retention time	h	-	24	-	24	24
H_2 (hydrogen loading)	L H_2 L_{VR}^{-1} d^{-1}	-	5.05	-	5.29	5.29
Gas composition out:						
H_2	%	-	56.5 ±4.9	-	34.6 ±7.7	93.9 ±1.9
CO_2	%	45.2 ±0.8	11.4 ±1.7	46.8 ±0.8	5.1 ±2.1	0.0
CH_4	%	54.8 ±0.8	32.1 ±4.9	53.2 ±0.8	60.3 ±7.4	6.1 ±1.9
Methane formation rate	L CH_4 L_{VR}^{-1} d^{-1}	1.53 ±0.27	1.82 ±0.20	1.51 ±0.30	2.52 ±0.07	0.33 ±0.11
SMY theory.	L CH_4 kg VS^{-1}	381	708	381	719	719
SMY experiment	L CH_4 kg VS^{-1}	388 ±10	461 ±37	382 ±11	640 ±19	47 ±12
Gas conversion:						
$X_{CO_2 + H_2 \rightarrow CH_4}$ [1]	%		33		72	4
$X_{Grass \rightarrow CH_4}$ [2]	%		92		104	18
X_{Total} [3]	%		65		89	12
VFA	mg L^{-1}	472 ±95	1,897 ±823	621 ±228	7,807 ±335	11,827 ±278
pH		7.81 ±0.07	7.88 ±0.01	7.89 ±0.04	8.34 ±0.06	8.05 ±0.47
VFA/TIC		0.37 ±0.07	0.40 ±0.03	0.22 ±0.03	0.76 ±0.10	0.90 ±0.03

Results of acclimatisation period BIS 2 not shown; [1] $X_{CO_2 + H_2 \rightarrow CH_4}$: Conversion carbon dioxide to methane; [2] $X_{Grass \rightarrow CH_4}$: Conversion grass to methane; [3] X_{Total}: Total conversion to methane.

6.3.1.2 In-situ methanation - high performance gas diffuser

The results with a higher performance ceramic gas diffuser during BIS 4 to BIS 6 represent the second part of the in-situ trials and are illustrated in figure 6.4 and table 6.1. During the initial stage (BIS 4) the reactor was subjected to mono digestion of grass for 46 days (1 HRT) at a loading rate of 4 g VS L^{-1} d^{-1}. No hydrogen was added at this stage. Stable digestion was confirmed by volatile fatty acid values of approximately 621 mg L^{-1}, Fos/Tac of 0.22 and pH of 7.89 (Drosg, 2013). A specific methane yield of 382 L CH_4 kg VS^{-1} and a methane concentration of 53.2% was measured. This equals to a MFR of 1.5 L CH_4 L_{VR}^{-1} d^{-1} and matches the findings given in BIS 1 and previously described by Voelklein et al. (2016) on the same substrate.

At the start of BIS 5 on day 291 (figure 6.4) 5.29 L H_2 L_{VR}^{-1} d^{-1} was introduced daily in addition to the feedstock grass silage. A gradual yet volatile increase in methane yield was observed during the first 9 days. Beginning with day 300 a specific methane yield of 640 L CH_4 kg VS^{-1} was determined for 4 days, corresponding to 89% of the potential total methane yield. The conversion of grass to methane was complete (104%). The added hydrogen successfully combined with excess carbon dioxide from the fermentation process to an extent of 72%. A methane production of 2.5 L CH_4 L_{VR}^{-1} d^{-1} was obtained. However, this performance lasted only for a period of four days and was characterised by a major escalation of volatile fatty acid concentration. The amount of 7807 mg L^{-1} was mainly dominated by acetic (4015 mg L^{-1}) and propionic acid (2451 mg L^{-1}). The deterioration was further accompanied by a rise in Fos/Tac to 0.76. However, the pH only experienced a minor increase to 8.37.

The drastic deterioration of microbial performance became evident during the period of BIS 6. The specific methane yield and methane concentration gradually dropped to values as low as 47 L CH_4 kg VS^{-1} and 6.1% respectively. This decline was accompanied by a distinct drop in carbon dioxide production till its ultimate depletion on day 308. This phenomenon was explained with volatile fatty acids accumulation of 11,827 mg L^{-1} inhibiting the subsequent break down of grass silage into acids and its ultimate release as carbon dioxide along the degradation pathway (Fukuzaki et al., 1990; Mackie & Bryant, 1981). In addition, the thermodynamic

requirement of low hydrogen partial pressure for further oxidation of longer chained fatty acids (e.g. propionate, butyrate) effectively limited acetogenesis (Fukuzaki et al., 1990). Consequently, the high concentration of volatile fatty acids impaired the acetoclastic methanogenic archaea reinforcing a self-perpetuating cycle of acid accumulation. Without the release of carbon dioxide during acidification the carbon source for hydrogenotrophic methanogens depleted, further contributing to rising hydrogen partial pressures and adversely affecting acetogenesis. Thus, methanogenesis reached only 12% of its total potential in this in-situ period (Bis 6), emphasising ultimate reactor failure. The assumption of system failure was further supported by consistently elevated Fos/Tac values as high as 0.9 and reduced pH of 7.93 with a final drop to 7.61.

In conclusion, the main cause for reactor failure was attributed to the high gas diffusing capability of the ceramic gas diffuser inducing significant biological and performance constraints. Since the necessary hydrogen quantity for complete upgrading was introduced together with the feedstock only once a day, the initial peak hydrogen partial pressure may have adversely influenced the symbiotic process of acetogenesis and methanogenesis. Continuous or pulse injection of hydrogen and intermittent gas recirculation could potentially remedy the impact of aggravated hydrogen partial pressure. Thus, the supply of dissolved hydrogen may be maintained at a lower more continuous rate to prevent adverse effects of elevated dissolved hydrogen concentrations on acetogenesis. Considering the lower MFR of an in-situ process as compared to ex-situ reactor configurations, an adequate hydrogen supply for acetogenesis dominates the importance of increased hydrogen to liquid transfer.

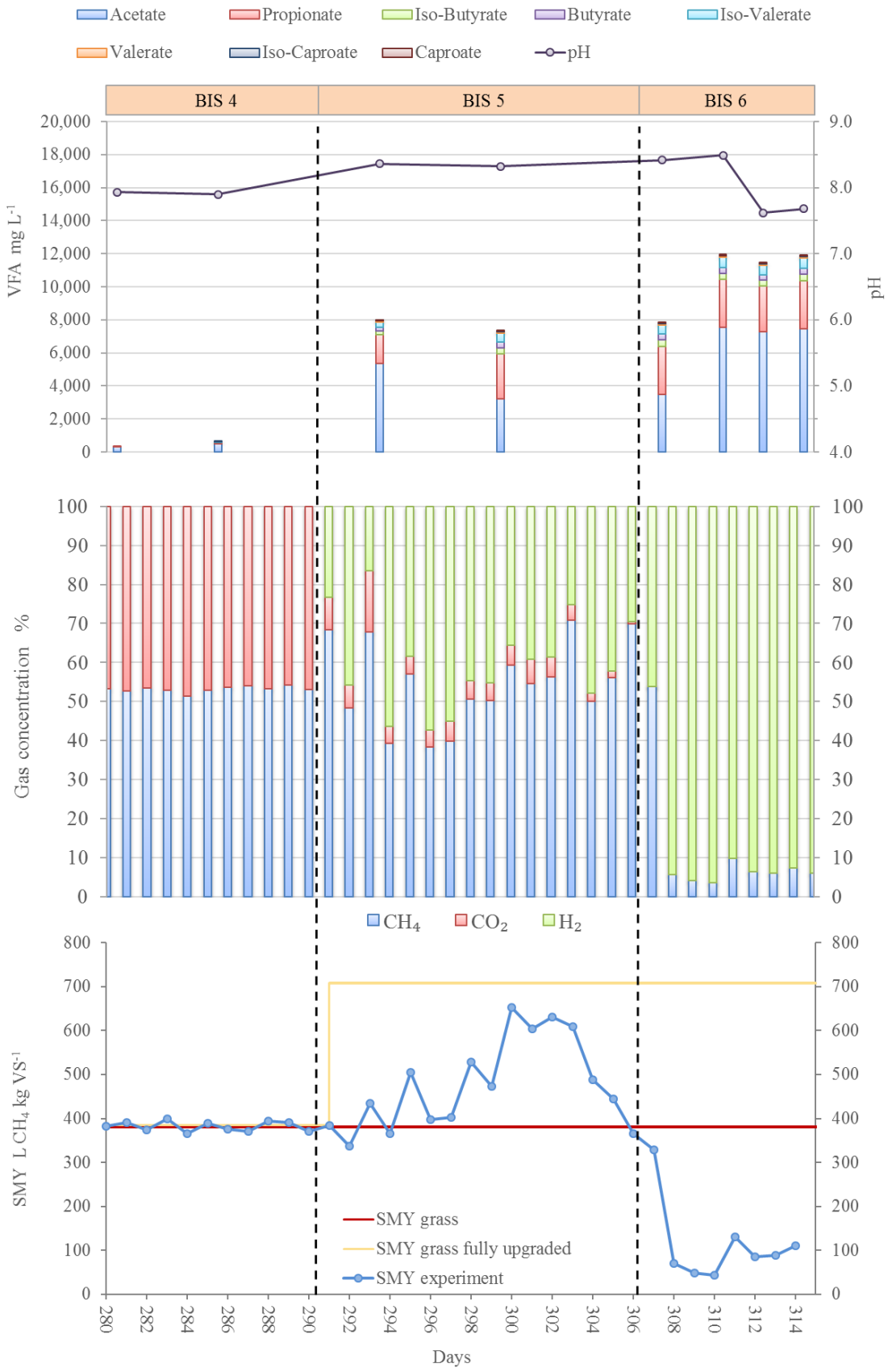

Fig. 6.4. Performance of in-situ upgrading in a grass fed anaerobic reactor.

The results compare to Bassani et al. (2016) who also performed in-situ methanation. They recorded an increase in methane content from 58% to 82% at a MFR of 0.12 L CH_4 L_{VR}^{-1} d^{-1}. Mulat et al. (2017) obtained an MFR of 0.13 L CH_4 L_{VR}^{-1} d^{-1} by elevating the methane concentration from 65% to 89%. An in-situ trial on cattle manure and whey by Luo and Angelidaki (2013b) revealed a biogas production rate maximised at 0.9 L CH_4 L_{VR}^{-1} d^{-1} at 96% methane content. Those experiments were conducted under a low organic loading rate resulting in an MFR of between 0.12 to 0.9 L CH_4 L_{VR}^{-1} d^{-1} with a hydrogen flow of 0.5 to 2.1 L H_2 L_{VR}^{-1} d^{-1}. In contrast, this study was performed at a hydrogen loading of 5.1 to 5.3 L H_2 L_{VR}^{-1} d^{-1} yielding a stable MFR of 1.8 L CH_4 L_{VR}^{-1} d^{-1} and a short term MFR of 2.5 L CH_4 L_{VR}^{-1} d^{-1}.

Further observations during the experimental process were noted as follows. A total solids content in the digestate of between 10 - 11%, of which approximately 80% were volatile, was determined during the whole in-situ experiment. Sedimentations of sand and fibre formed during the period of BIS 3 around the fish stone diffuser. It was assumed that the rising gas bubbles lowered the density of the reactor digestate. The ceramic gas diffuser covered the total bottom area of the reactor and effectively eliminated sedimentation. The injection of hydrogen in all in-situ upgrading trials led to immediate foaming events within 5 minutes. After a period of 30 minutes the foam completely receded.

6.3.2 Ex-situ methanation

6.3.2.1 Batch gas injection in ex-situ methanation

After completion of the in-situ trials the fibres in the digestate were removed to ensure a rapid depletion in methane production from sources other than externally injected gases. The remaining digestate represents a medium rich in methanogens and dissolved nutrients. The reactor was then run in various operation modes starting with batch ex-situ (BES) followed by continuous ex-situ methanation (CES). The carbon source for methane production shifted from grass silage to externally injected carbon dioxide. Introduced gases were constantly recirculated through the microbial bed to facilitate gas to liquid mass transfer at a rate of 4 L min^{-1}. A change of process variables between each stage in the ex-situ series resulted in a rapid response. Steady

performance values were attained within the first 24 hours. Each experimental stage was maintained for 4 weeks with results of the last 2 weeks depicted in table 6.2.

The hydrogen loading in BES 1 represents the base scenario for all following ex-situ methanation trials (BES 2 to CES 6). BES 1 was exposed to a daily injection of 7.3 L H_2 L_{VR}^{-1} d^{-1} for a 24-hour period. In BES 1 hydrogen was completely consumed resulting in an MFR of 1.7 L CH_4 L_{VR}^{-1} d^{-1} with methane concentrations as high as 92%. Total gas conversion was not achieved; the maximum conversion was 93%. This was a result of premature depletion of hydrogen in the pre-configurated gas mixture. As a consequence of the successful upgrading in BES 1, the hydrogen loading was doubled to 15.4 L H_2 L_{VR}^{-1} d^{-1} in BES 2. The MFR increased to 3.7 L CH_4 L_{VR}^{-1} d^{-1} with methane concentrations of 96%. Similar to BIS 1 gas conversion reached a maximum of 96%. The results in this study partially compare to the more complex trickle bed systems obtaining high methane concentrations in the off gas in excess of 98% (Burkhardt & Busch, 2013; Savvas et al., 2017; Strübing et al., 2017). It has to be noted that some of these trickle bed systems attained elevated methane formation performances in the range 1.17 - 15.4 L CH_4 L_{VR}^{-1} d^{-1}.

Table 6.2. Performance characteristics of ex-situ upgrading systems.

		BES 1	BES 2	CES 1	CES 2	CES 3	CES 4	CES 5	CES 6
Operation mode		Batch ex-situ		Continuous ex-situ			Continuous ex-situ		
Diffuser		Ceramic diffuser		Ceramic diffuser			Ceramic diffuser		
Injected gases		H_2, CO_2		H_2, CO_2			H_2, CO_2, CH_4		
Hydrogen loading		Low	Medium	Medium	High	Highest	High	Medium	Low
Gas retention time	h	24	24	1.99	0.57	0.33	0.41	1.14	1.63
Gas injection:									
H_2	%	80	80	80	80	80	73	54	30
CO_2	%	20	20	20	20	20	18	14	8
CH_4	%	-	-	-	-	-	8	32	61
H_2 (Hydrogen loading)	L L_{VR}^{-1} d^{-1}	7.3	15.4	14.7	47.1	73.3	50.5	13.7	5.4
CO_2	L L_{VR}^{-1} d^{-1}	1.8	3.9	3.7	11.8	18.3	12.6	3.5	1.6
CH_4	L L_{VR}^{-1} d^{-1}	-	-	-	-	-	5.7	8.2	9.9
Gas out:									
H_2	%	0	0	41 ± 3.4	54 ± 2.8	68 ± 1.2	61 ± 1.2	30 ± 2.3	12 ± 2.4
CO_2	%	8 ± 1.7	4 ± 0.5	10 ± 1.3	14 ± 1.2	17 ± 1.2	17 ± 1.1	8 ± 2.1	4 ± 1.2
CH_4	%	92 ± 1.7	96 ± 0.6	49 ± 3.9	32 ± 3.0	15 ± 1.0	23 ± 1.8	61 ± 3.9	84 ± 2.1
H_2	L L_{VR}^{-1} d^{-1}	0	0	2.4 ± 0.3	13.7 ± 0.7	37.3 ± 3.3	29.2 ± 0.6	5.4 ± 0.1	1.3 ± 0.1
CO_2	L L_{VR}^{-1} d^{-1}	0.1 ± 0.03	0.2 ± 0.02	0.6 ± 0.1	3.5 ± 0.4	9.2 ± 1.0	7.9 ± 0.9	1.6 ± 0.3	0.4 ± 0.1
CH_4	L L_{VR}^{-1} d^{-1}	1.7 ± 0.1	3.7 ± 0.2	2.9 ± 0.2	8.2 ± 0.8	9.1 ± 1.0	10.8 ± 0.6	9.9 ± 0.4	11 ± 0.2
Methane production rate	L L_{VR}^{-1} d^{-1}	1.7 ± 0.1	3.7 ± 0.2	2.9 ± 0.2	8.2 ± 0.8	9.1 ± 1.0	5.1 ± 0.6	1.7 ± 0.4	0.85 ± 0.2
Gas conversion	%	93	96	78	70	49	40	49	53
pH		8.5 ± 0.2	8.5 ± 0.1	8.1 ± 0.04	7.1 ± 0.2	7.4 ± 0.3	8.2 ± 0.2	8.1 ± 0.2	8.2 ± 0.2
VFA		456 ± 81	328 ± 13	290 ± 16	1317 ± 515	765 ± 718	1420 ± 411	1673 ± 441	1370 ± 849

A detailed insight into the 24-hour upgrading period of BES 2 is revealed in figure 6.5. Hourly measurements of the gas content (in triplicate) allowed establishment of a dynamic upgrading profile. The first 12 hours were characterised by a rapid initial start until 93% carbon dioxide conversion to methane was reached. In this 12 hour period, the methane content reached 80%. In the following 12 hours the methane conversion rose to 97%. Methane concentration after 24 hours peaked at 95.5%, with 2.9% and 1.6% carbon dioxide and hydrogen remaining in the gas mixture respectively.

The initial linear gas conversion and associated decrease in hydrogen partial pressure indicates that sufficient dissolved hydrogen levels were present until CO_2 levels fell below 9%. It is understood that in the first 11 hours gas to liquid mass transfer was not a limiting factor, mainly due to the sufficient hydrogen concentration in the gas and positive performance characteristics of the ceramic gas diffuser. At carbon dioxide levels below 9% the conversion rate drastically declined. This is in line with the findings of Agneessens et al. (2017), Luo et al. (2012a) and Mulat et al. (2017) who observed rapidly decreasing hydrogen uptake rates below 12 - 15%. The explanation can be found in the low concentrations of dissolved hydrogen in water at conversion rates in excess of 90% (figure 6.1 and figure 6.2). The dynamic initial conversion in figure 6.5 suggests additional potential of the batch ex-situ process. Any further increase in loading was restricted by the size of the gas bag in this reactor configuration. Therefore, the operation mode was changed from daily batch injections to a continuous gas injection.

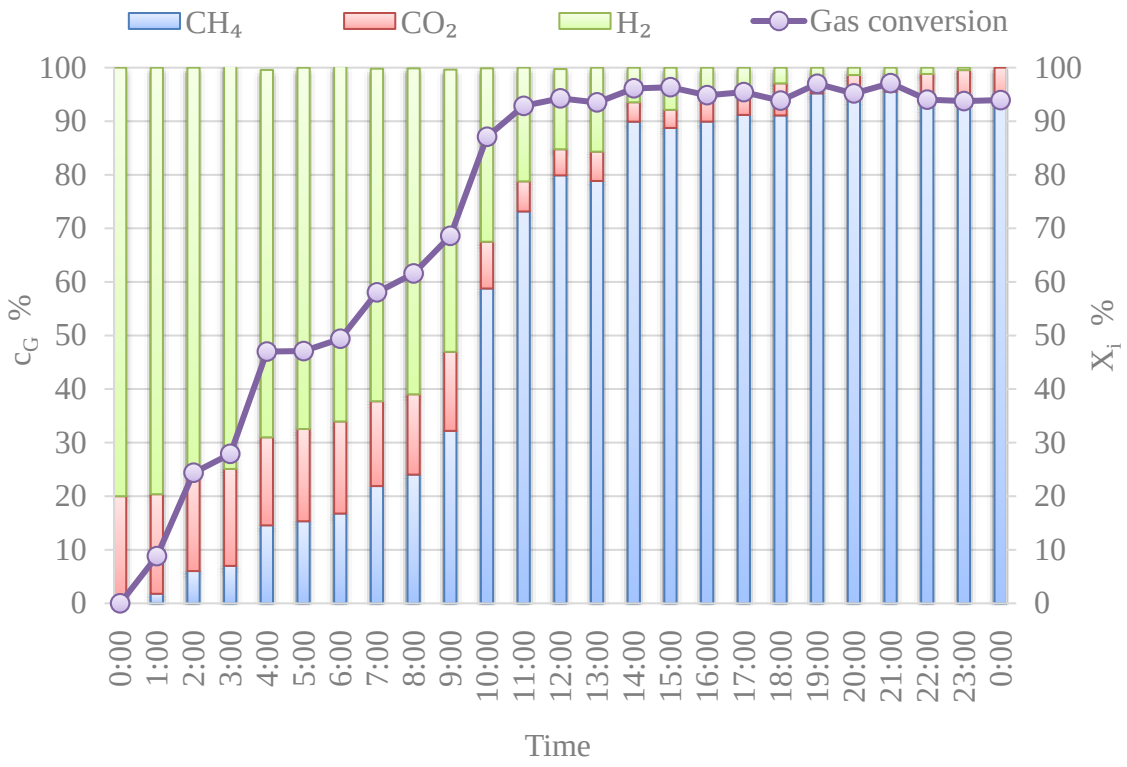

Fig. 6.5. Hourly performance of ex-situ methanation in BES 2 (c_G: gas concentration in headspace; X_i: gas conversion).

6.3.2.2 Continuous gas injection in ex-situ methanation

The hydrogen loading of CES 1 was set to approximately match the hydrogen loading of BES 2 receiving 14.7 L H_2 L_{VR}^{-1} d^{-1} (table 6.2). However, the gas conversion to methane of CES 1 could not keep pace with the batch process in BES 2 and dropped from 96% to 78% at an MFR of 2.9 L CH_4 L_{VR}^{-1} d^{-1}. Inevitably the methane content experienced dilution and suffered a decline to 49%. In CES 2 the hydrogen loading was approximately tripled to 47.1 L H_2 L_{VR}^{-1} d^{-1} compared to CES 1 (table 6.2). The gas conversion rate only experienced a drop by 8% to a level of 70%. The corresponding methane concentration decreased to 32%. A final 5-fold increase in hydrogen loading to 73.3 L H_2 L_{VR}^{-1} d^{-1} let to a 29% reduction of gas conversion to 49% in comparison to CES 1 (table 6.2). Methane concentration declined to a level of 15%. In conclusion, higher volumetric loading of hydrogen and carbon dioxide is typically linked to lower final methane concentrations in the off gas in ex-situ methanation.

Incomplete upgrading at higher loadings have been observed by Ullrich et al. (2018) reporting a methane formation rate of up to 4.28 L CH_4 L_{VR}^{-1} d^{-1} at 86.5% methane content. Using continuous cultures (M. *marburgensis*) the methane content as recorded by Seifert et al. (2014) dropped from 85% to 60% when the MFR increased from 6.1 to 22.8 L CH_4 L_{VR}^{-1} d^{-1}. A fair comparison of literature data and upgrading systems remains difficult. Special caution is required as intensely mixed reactors easily outperform other configurations. The internal power consumption of a system or the additional effort of maintaining a pure culture and associated nutrient supply has to be considered.

The final series of the ex-situ methanation (CES 4 to CES 6) assessed the implication of reduced hydrogen partial pressure by adding methane to the injected gas mixture. CES 4 was set to a similar hydrogen loading (50.5 L H_2 L_{VR}^{-1} d^{-1}) mixture as CES 2. The introduced biogas mixture without considering hydrogen would represent a biogas with a methane content of 31%. Consequently, the methane component in the feed gas lowers the quantity of dissolved hydrogen in the liquid phase. Thus, gas conversion dropped from 70% (CES 2) to 40% (CES 4). In CES 5 the hydrogen loading was further reduced to match CES 1. The applied biogas mixture without considering hydrogen included for a methane concentration of 70% and caused the conversion of carbon dioxide to methane to drop from 78% (CES 1) to 49% (CES 5).

The attained conversion corresponds to levels found in CES 3, which was exposed to 5 times elevated hydrogen loading. In conclusion, the addition of methane markedly reduced gas conversion rates compared to trials at similar hydrogen loading without methane. This was mainly attributed to the decreased hydrogen partial pressure and associated gas to liquid transfer (Lecker et al., 2017). Furthermore, it adversely affected the potential residence time for gases to be converted. With increasing quantities of methane at similar hydrogen loadings, the residence time diminished by 28% and 43% comparing CES 1 with CES 5 and CES 2 with CES 4 respectively.

Within all ex-situ trials (BES 1 to CES 6) the pH remained within stable limits between 7.1 and 8.5. A drop to 7.1 (CES 2) and 7.4 (CES 3) was observed at higher hydrogen loading. Average volatile fatty acids level between 290 mg L^{-1} and 1,673 mg L^{-1} were monitored and considered within stable conditions as defined by Drosg (2013). The slight increase in acetate and lower concentrations of longer chained

fatty acids indicates a stimulation of the Wood-Ljungdahl pathway (Fukuzaki et al., 1990).

6.3.3 Comparison of in-situ, batch ex-situ and continuous ex-situ methanation

A performance and efficiency comparison of in-situ, ex-situ and continuous methanation at various hydrogen injection levels is illustrated in figure 6.6 and 6.7. A similar behaviour was recognised within all applied upgrading strategies. An increasing MFR and decreasing conversion efficiency can be assumed with rising rates of hydrogen injection. Best results were obtained with the batch ex-situ strategy, exceeding the continuous strategy in methane production performance and efficiency. The highest hydrogen injection rates were imposed on the continuous methanation strategy CES 1 - CES 3 (blue line in figure 6.6). At 73 L H_2 L_{VR}^{-1} d^{-1} hydrogen injection the methane production appeared to plateau. The non-linear characteristic indicates a maximum production rate of the hydrogenotrophic methanogenic archaea for this reactor configuration.

A comparison of the continuous upgrading strategies with and without methane in the feed gas mixture (blue vs. red line in figure 6.6 and 6.7) reflects a distinct difference in methane formation and conversion efficiency at rising hydrogen injecting rates. This was explained by the presence of methane in the introduced gas mixture, consequently lowering the hydrogen partial pressure and thus the level of dissolved hydrogen. In addition, it reduced gas residence time for possible upgrading. A similar correlation was also observed by Martin et al. (2013) using a continuous culture *Methanothermobacter thermautotrophicus* in an ex-situ system. At an MFR of 21 L CH_4 L_{VR}^{-1} d^{-1} the conversion efficiency dropped from pervious 89% (no methane in feed gas) to 62% utilizing a biogas with 70% methane content.

The MFR and efficiency of the in-situ system remains low. The considerably lower production rate is a result of the fixed carbon dioxide quantity released in the anaerobic digestion process at a certain organic loading rate. The efficiency was markedly dependent on the employed diffusing system and only stable at reduced dissolved hydrogen levels using a low performance diffuser.

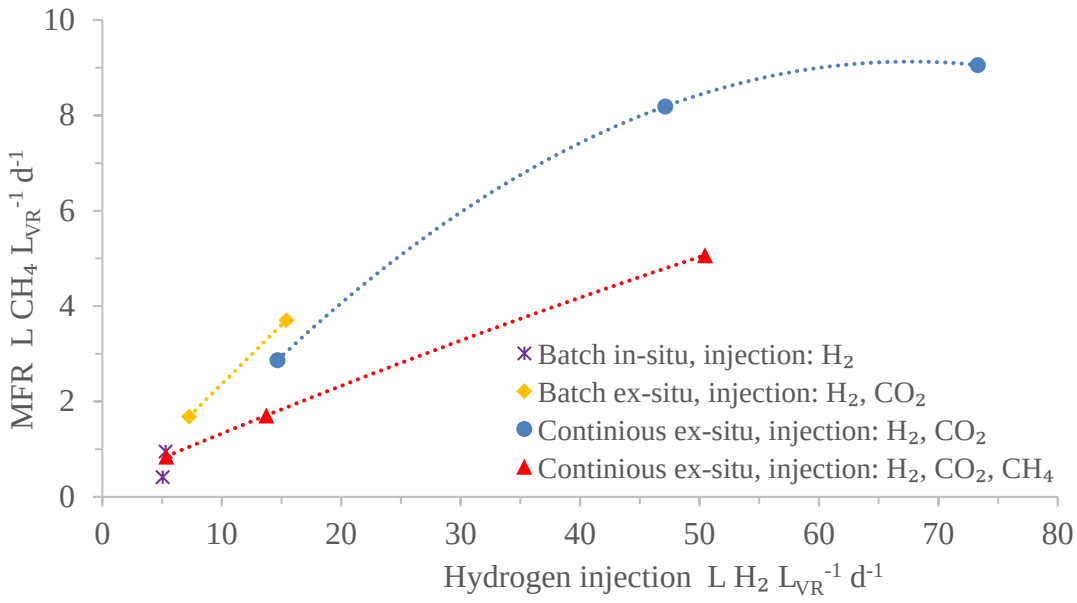

Fig. 6.6. Methane formation rate of in- and ex-situ upgrading strategies displaying performance characteristics (MFR: methane formation rate).

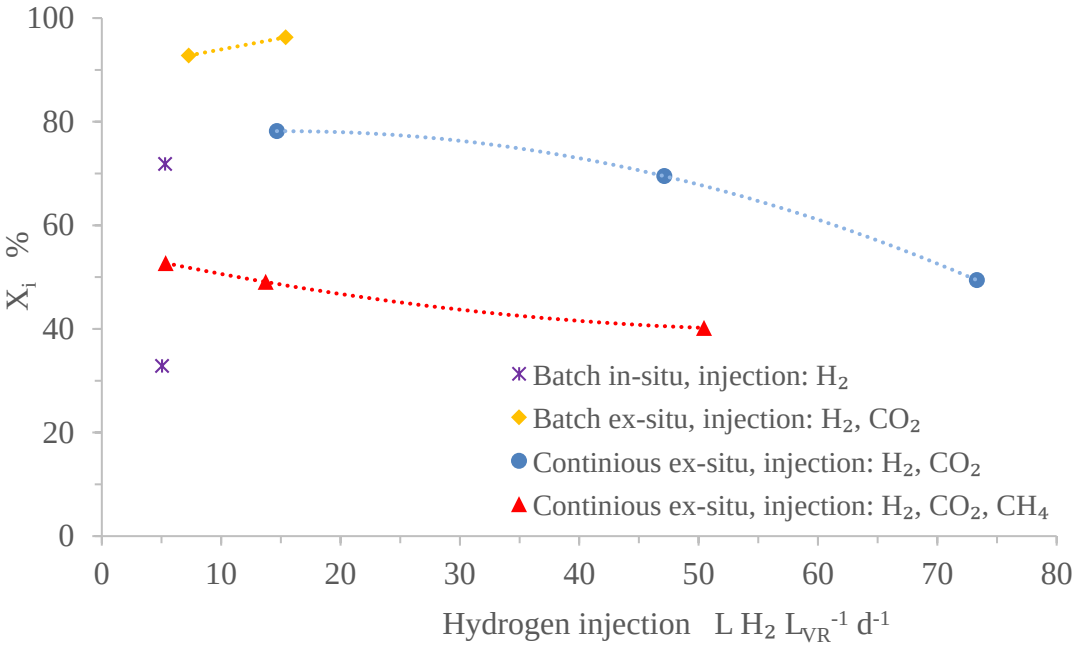

Fig. 6.7. Gas conversion of in- and ex-situ upgrading strategies displaying efficiencies (X_i: gas conversion).

6.3.4 Continuous ex-situ methanation in series

The continuous injection and simultaneous escape of gases reduced the potential conversion efficiencies in the CES systems. A virtual approach to offset the flow of gases bypassing the internal gas recirculation is modelled by arranging three reactors in series. Figure 6.8 illustrates a theoretic model and approach for a full-scale sequential ex-situ methanation unit. The model is based on one operational lab scale ex-situ reactor utilising the findings in CES 2 (stage 1), CES 5 (stage 2) and CES 6 (stage 3). The flow rates and gas concentrations leaving each stage in the model approximately correspond to the quantity and quality entering the next stage.

In the lab the amounts of gases escaping the reactor during the period of CES 2 (corresponds to stage 1, only receiving H_2 and CO_2 at a high rate) were replicated and injected into the reactor for period CES 5 (corresponds to stage 2, receiving H_2, CO_2 and CH_4 at a medium rate). Likewise, the off gas in period CES 5 (stage 2) was replicated and introduced during period CES 6 (corresponds to stage 3, receiving H_2, CO_2 and CH_4 at a low rate). This sequential approach allows conversion of 95% of carbon dioxide into methane; 70% conversion with a methane content of 32% was initially obtained after stage 1. After passing the second stage, the conversion rate increased to 85%, with 61% methane content in the gas mixture. The final conversion in stage 3 pushed the gas conversion to 95%, with a methane concentration of 85%.

Having three reactors in series, the total reactor volume triples as compared to the single reactor in CES 1. The flow rate in CES 1 accounts for approximately 1/3 of the sequential system's flow rate. Thus, the input gas flow per litre reactor volume remains similar comparing both systems. In contrast to the 78% carbon dioxide conversion to methane in the single reactor of CES 1, the three reactors in series were able to attain 95% conversion. A methane content of 85% was obtained at 3.6 L CH_4 L_{VR}^{-1} d^{-1}. This methane formation rate matches the results accomplished in BES 2, yet the methane content falls short to satisfy requirements for gas grid injection.

If only stage 2 and 3 are taken into consideration, this system could also be seen as a biogas upgrading unit with a total hydrogen loading (cumulated average of stage 2 and 3) of 6.9 L H_2 L_{VR}^{-1} d^{-1}. A biogas mixture with 70% methane content at a methane flow rate of 4.1 L CH_4 L_{VR}^{-1} d^{-1} could be elevated to 5.4 L CH_4 L_{VR}^{-1} d^{-1} at a

methane concentration of 85%. The corresponding MFR in stage 2 and 3 is calculated as 1.3 L CH_4 L_{VR}^{-1} d^{-1} with 89% of carbon dioxide conversion.

The results compare to Luo and Angelidaki (2012b) using a biogas with 62.5% methane content retrieving an MFR of 5.3 L CH_4 L_{VR}^{-1} d^{-1} at 90.8% methane concentration in the off gas. At similar hydrogen loading of 6.5 L H_2 L_{VR}^{-1} d^{-1} and 36 - 42% carbon dioxide in the input biogas mixture, Rachbauer et al. (2016) observed carbon dioxide conversion of 96% in a trickle bed system. High performances have been stated by Alitalo et al. (2015) investigating two ex-situ trickle bed reactors in series with a hydrogen flow rate of 25.2 L H_2 L_{VR}^{-1} d^{-1}. Complete consumption of hydrogen was accomplished at gas retention times of 144 hours. The corresponding MFR was 6.4 L CH_4 L_{VR}^{-1} d^{-1}. This compares to twice the performances obtained in this experiment with only 85% methane content in the off gas, yet at a residence time of only 3.3 hours (according to cumulated gas retention times of CES 2, CES 5 and CES 6 in table 6.2 with 0.57 h, 1.14 h and 1.63 h).

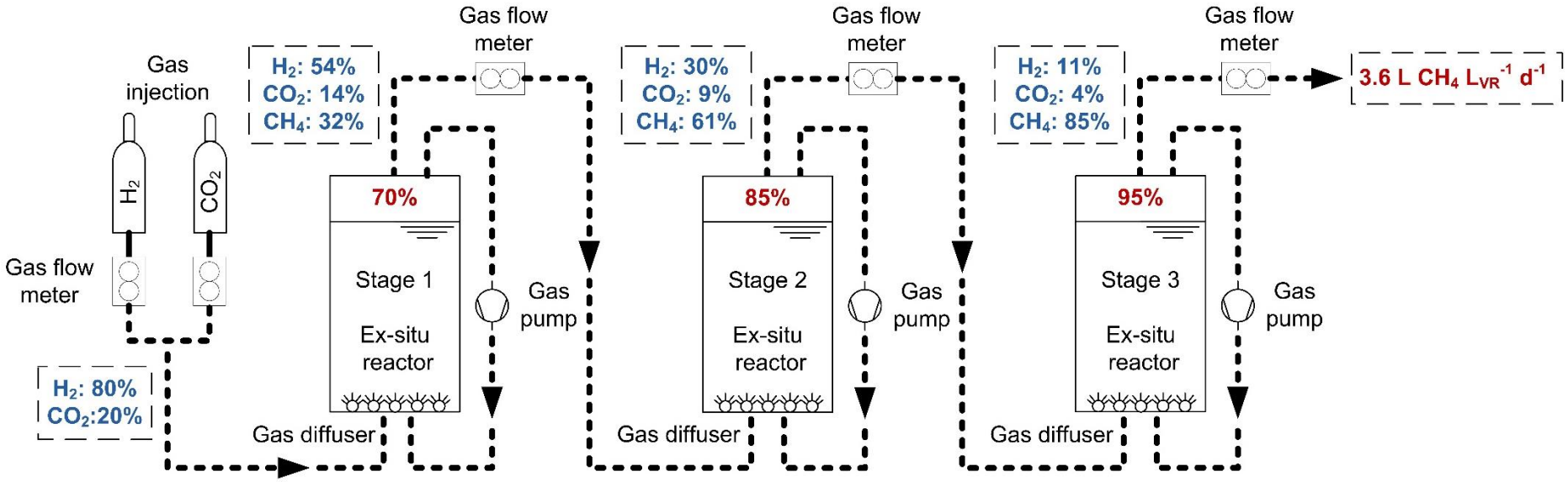

Fig. 6.8. Three stage sequential ex-situ methanation at a methane formation rate of 3.6 L CH_4 L_{VR}^{-1} d^{-1}. The conversion of carbon dioxide to methane corresponds to 70% (after stage 1), 85% (after stage 2) and 95% (after stage 3).

6.3.5 Hybrid concept of sequential in-situ and ex-situ methanation

A general design idea for an upscaled methanation concept is shown in figure 6.9 and compares to a typical biogas plant with 1 MW_{el} power output. The individual results from in and ex-situ experiments were combined to form a hybrid model. The calculation of flow rates, reactor volumes and efficiencies correspond to the findings attained in the laboratory trials BIS 5 (batch in-situ) and CES 6 (continuous ex-situ). A main in-situ methanation digester with 2440 m^3 volume partially upgrades the biogas and is followed by a 610 m^3 ex-situ methanation unit to further enrich the methane content in the biogas.

In this concept, the in-situ methanation digester receives 9.3 tonnes (volatile solids) of grass silage per day for biogas production. This results in an organic loading rate of 3.8 kg VS m^{-3} d^{-1} at a hydraulic retention time of the grass silage of 47 days. A specific biogas yield of 719 m^3 per ton of volatile solids is assumed with a share of 53% methane (Voelklein et al., 2016). The expected quantity of carbon dioxide (338 m^3 t VS^{-1}) from grass silage is matched with an equimolar amount of hydrogen (5.2 m^3 m_{VR}^{-3} d^{-1}) and injected into the in-situ reactor. During the course of the 24-hour period the produced biogas accumulates in the gas storage and is recirculated with the exogenous hydrogen through the in-situ reactor. Hydrogenotrophic methanogens couple the hydrogen with carbon dioxide. 92% of the expected specific methane yield is obtained after the in-situ upgrading at a level of 70% methane content. The high gas conversion is a result of the low MFR predefined by the amounts of carbon dioxide released from grass. After the 24-hour period the gas is transferred into the intermediate gas storage of a triple membrane gas storage system.

The partially upgraded biogas is now continuously withdrawn and introduced into the ex-situ methanation reactor. At a rate of 14.5 m^3 m_{VR}^{-3} d^{-1} the gases pass the ex-situ unit and are further upgraded in a gas recirculation process until 96% of the potential specific methane yield is reached. The biogas escapes the sequential process at a rate of 6434 m^3 of methane per day at a level of 84% methane. The ex-situ reactor only contributes an additional share of 4% to the overall specific methane yield, as at reduced hydrogen/carbon dioxide levels the conversion rate drastically declines. This is in line with observed findings in figure 6.1, figure 6.2 and figure

6.5. This phenomenon is also described in Agneessens et al. (2017) and Mulat et al. (2017).

The proposed model is a first estimation to upscale laboratory findings, still subjected to certain assumptions. For once, equimolar hydrogen to carbon dioxide ratios are assumed in the in-situ process (as compared to BIS 5). Secondly, a stable long-term operation of the in-situ reactor at this efficiency remains to be accomplished. In order to integrate the upgrading strategy into an industrial process, the periodic feeding and upgrading rescheme in the in-situ digester will have to be adjusted to hourly increments. Firstly, to allow for a realistic feeding scenario and secondly to accommodate the gas quantities in the gas storage system. Complete upgrading in this configuration was not obtained. If direct gas grid injection is aspired, the ex-situ unit needs to elevate the methane content to greater than 95%. This could be achieved changing operation conditions to more efficient batch upgrading or by changing the size, configuration or operational pressure of the ex-situ reactor.

If the proposed hybrid system is operated in connection with on-site combined heat and power units, a mixed operation mode of part time upgrading and storage of cheap hydrogen (associated with surplus otherwise curtailed electricity) in the intermediate gas storage appears feasible. The in-situ process would only be operational for periodic instances at times with sufficient hydrogen available.

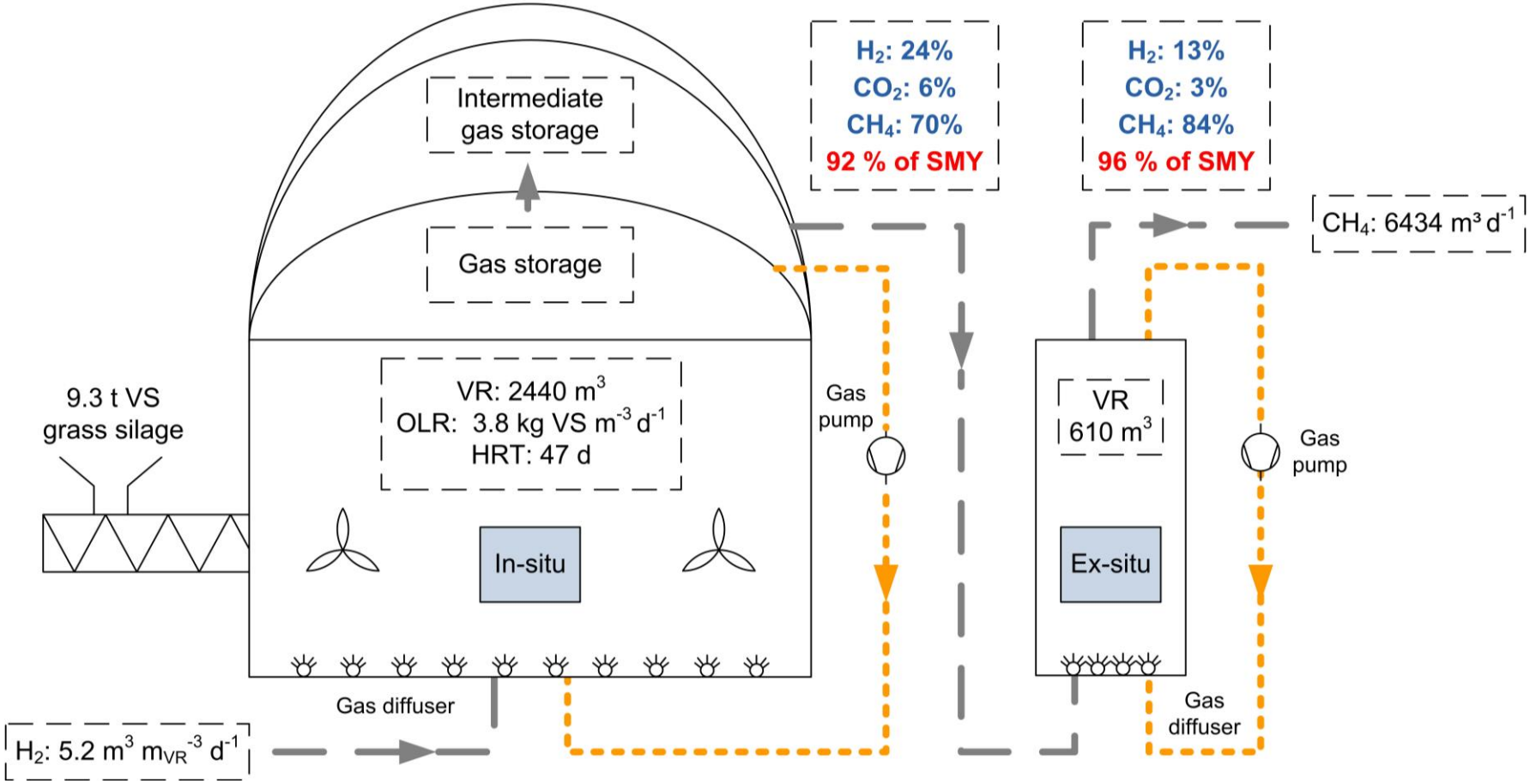

Fig. 6.9. Hybrid concept of sequential in-situ and ex-situ methanation with triple gas storage membrane on top of in-situ digester (SMY: specific methane yield, VR: reactor volume, OLR: organic loading rate, HRT: hydraulic retention time, VS: volatile solids).

In an alternative concept the biogas quantity (6678 m^3 d^{-1}) retrieved from a similar 1 MW digester (2440 m_{VR}^{-3}) fed by 9.3 t VS grass silage per day may be treated in a conventional biogas upgrading facility. The methane (3539 m^3 d^{-1}) is segregated from the biogas and injected into the natural gas grid. The excess carbon dioxide fraction (3139 m^3 d^{-1}) is further utilised exclusively either in a batch ex-situ (described in section 3.2.1) or continuous sequential ex-situ methanation system (described in section 3.4) and coupled with equimolar amounts of external hydrogen to form methane. Based on the MFR data obtained in the lab scale trials of batch ex-situ (BES 2) and continuous ex-situ methanation (CES 2, CES 5, CES 6), a reactor volume of 848 m^3 and 870 m^3 (3 x 290m^3) is required to attain an additional 3014 m^3 CH_4 d^{-1} (at 96% CH_4 content) and 2668 m^3 CH_4 d^{-1} (at 85% CH_4 content) in a batch ex-situ and a continuous sequential ex-situ methanation system, respectively. The cumulated methane yield per day calculates to 6553 m^3 CH_4 d^{-1} for the batch ex-situ and 6207 m^3 CH_4 d^{-1} for the continuous sequential ex-situ methanation concept.

All investigated concepts are capable to upgrade biogas to a level close to or within the boundary acceptable for gas grid injection. A comparison of the required reactor volumes to upgrade biogas in a hybrid model or within a single or sequential system of ex-situ methanation units ranges between 610 m_{VR}^3 and 870 m_{VR}^3. A substantial reduction in reactor size of the ex-situ unit following partially upgraded biogas of the in-situ methanation may be expected but exact volumes remain difficult to predict. The marginal deviation in volume is a result of methane being present in the introduced gas mixture entering the ex-situ unit of the hybrid model, lowering the level of dissolved hydrogen and gas residence time for possible upgrading.

6.4 Conclusion

This study provides insights into biological methanation strategies. A general correlation between increasing hydrogen injection, elevated methane formation and diminishing conversion rates was established for all applied strategies. The presence of methane in the upgrading biogas markedly reduced gas conversion rates compared to similar hydrogen loading without methane. The challenge for in-situ methanation remains to ensure a balanced system, with adequate levels of hydrogen in solution to allow both, acetogenic and hydrogenotrophic microbes to coexist. In general, below

carbon dioxide levels of 9%, conversion of carbon dioxide to methane drastically diminishes. Thus, connecting in-situ or ex-situ units in series may provide a more favourable pathway as compared to individual systems. A concept of a hybrid model combining in- and ex-situ methanation in full scale suggests an alternative to conventional upgrading systems.

6.5 Supplementary data

All standard conditions mentioned in chapter 6 refer to standard temperature at 273K and standard pressure at 1013mbar.

Importance of Kla:

The phase boundary interface is the crucial element to provide efficient gas liquid mass transfer. Any increase in k_La for instance by smaller bubble size, enlarged contact surface, elevated gas retention or immediate dissolution (membranes), proportionally enhances the quantities of gases dissolved into liquid until maximum solubility is reached (figure 6.2). Several gas injection methods such as hollow fibre membranes, gas diffusers and electrochemical methods have been described in the scientific literature (Angelidaki et al., 2018; Bassani et al., 2016; Kraakman et al., 2011; Lecker et al., 2017). In addition, increased system pressure improves solubility of gases in liquid and reduces bubble size; smaller bubbles are less buoyant and possess a diminished upflow potential. Thereby the ratio of surface to volume is drastically elevated, further enhancing the phase boundary contact area (Lecker et al., 2017). Overall, reducing the bubble size during gas injection is a pivotal factor to extend gas retention and gas to liquid transfer. Similarly, gas recirculation (Alitalo et al., 2015; Bassani et al., 2016; Kougias et al., 2017; Luo et al., 2012a) or for example recirculation of liquid in a trickle bed reactor facilitates and enhances gas liquid contact (Burkhardt et al., 2015; Rachbauer et al., 2016; Strübing et al., 2017; Ullrich et al., 2018).

Chapter 7: Conclusions and recommendations

7.1 Chapter overview

The thesis set out to explore integrated biogas systems and optimise the technology of biogas production and upgrading. The conclusions and possible solutions to the objectives given in Chapter 1.3 are presented in this chapter. Overall and detailed conclusions synthesising the major findings of this thesis are identified. Recommendations, final remarks, future research and possible developments based on the content of this study complete this thesis.

7.2 Thesis conclusions with respect to the initial thesis objectives

The thesis successfully demonstrates the optimisation potential in novel and existing digestion systems. Its various studies sought to explore and promote pathways to conduct anaerobic digestion at elevated organic loading rates and high specific methane yields, while maintaining short substrate retention and still attaining favourable volumetric methane production rates, ideally at a final level suitable for gas grid injection. The key contributors to achieve those objectives and derive overall conclusions are listed as follows:

Maximise possible biogas quantities per unit substrate input (SMY)

- Pre-treatment by a two-stage digestion system separating fermentation stages of acidification and methanation generates optimum conditions for microbial communities and increases specific methane yields.
- Digestion at elevated temperature accelerates degradation kinetics; biogas yields increase and full biomethane potential is reached at reduced substrate retention.

Increase possible loading (OLR)

- Elevated temperature levels facilitate microbial activity and beneficial viscosity properties; accelerated degradation improves mixing conditions and enables higher organic loading.
- Supplementation of trace elements at adequate levels allows stable digestion and favours an increase in loading rate.

Reduce necessary retention time (HRT)

- Hydrolysis in a two-stage digestion system solubilises substrate and provides immediate precursors for methanogenesis shortening overall substrate retention time.
- Elevation of process temperature stimulates a more rapid degradation and higher biomethane yields at short substrate retention.

Improve reactor utilisation (VMP)

- Reactor utilisation corelates with retention time and loading rates; elevated loading and reduced retention time improves volumetric methane production rates.
- Elevated temperature levels compensate for short substrate retention and enhance reactor utilization.
- Increased hydrogen addition to biological methanation systems boosts volumetric methane production.

Enrich methane concentrations and attain a biomethane meeting gas grid injection standards

- Two stage digestion of food waste releases major quantities of hydrogen sulphide and carbon dioxide during hydrolysis; a biogas rich in methane is obtained in the downstream methane reactor.
- Addition of hydrogen to an in-situ and ex-situ biological methanation system; carbon dioxide is reduced to methane by hydrogenotrophic methanogenic archaea yielding methane concentrations satisfying requirements for gas grid injection.

The detailed conclusions for each chapter of the thesis are as follows:

Assessment of increasing loading rate on two-stage digestion of food waste

- Variations in loading rate impact possible solubilisation of substrate in the first stage.
- Highest solubilisation was achieved at an organic loading rate of 15 g VS L^{-1} d^{-1}.

- Low hydrogen formation in the first stage resulted in minimal energy in the hydrolysis gas.
- More than 99% of the total energy value in biogas originated from the second stage.
- Upstream hydrolysis facilitated much shorter retention times and higher loading rates while increasing methane concentration and yield.
- Methane yield was more dependent on reactor configuration and retention time rather than organic loading rate.
- The two-stage system yielded up to 23% more methane than the single-stage system in this setup.
- The two-stage system produced up to 404 L CH_4 kg VS^{-1} or 15.1 MJ kg VS^{-1}.
- The methane content of the biogas increased by 14% to 71% in the two-stage system as compared to single-stage digestion.

Role of trace elements in single- and two-stage digestion of food waste at high organic loading rates

- Food waste lacked essential nutrients for stable anaerobic digestion.
- Single- and two-stage reactor performance failed after exceeding an organic loading rate of 2.0 g VS L^{-1} d^{-1} without TE supplementation under mesophilic conditions.
- Reactor failure was characterised by pH, VFA/TIC, VFA concentrations exceeding limits considered stable and reduced SMYs.
- TE addition of Co, Fe, Mo, Ni and Se restored a stable process.
- Supplementation of TE did not elevate specific methane yield but allowed an increase in loading to 5 g VS L^{-1} d^{-1}.
- Upstream release of hydrogen sulphide potentially improves bioavailability of TE; however the two-stage system did not show any better resilience to nutrient deficiency than the single-stage system.

Increased loading rates and specific methane yields facilitated by digesting grass silage at thermophilic temperatures rather than mesophilic

- Thermophilic grass digestion enabled higher loading and superior methane yields as compared to mesophilic digestion.

- The resilience at thermophilic temperature at high loading rates was attributed to the beneficial viscosity characteristics of increased temperature, trace element addition and improved mixing conditions.
- Elevated pH in thermophilic (as compared to mesophilic) digestion restricts increased VFA concentration to its more dissociated (unprotonated) state; high VFA concentrations at higher pH with associated buffering capacity are less harmful to the cell membrane of the methanogenic archaea, as compared to a reactor system close to failure at lower pH (such as in mesophilic reactors).
- Retention times of 25 days and loading rates of 7 g VS L^{-1} d^{-1} were feasible with TE supplementation at thermophilic temperature conditions.
- Decreased retention time at enhanced loading rates reduced gas yield.
- Optimum performance was identified at a loading rate of 4 g VS L^{-1} d^{-1} and 46 days retention time, achieving 86% of the maximum theoretical SMY.

Biological methanation: Strategies for in-situ and ex-situ upgrading in anaerobic digestion

- Increasing hydrogen injection caused elevated methane formation (expressed in L CH_4 L_{VR}^{-1} d^{-1}) and diminishing conversion rates in all applied strategies; a maximum MFR of 3.7 L CH_4 L_{VR}^{-1} d^{-1} at 96% methane content was feasible ex-situ.
- In-situ methanation requires a balanced system with adequate levels of hydrogen in solution to allow both, acetogenic and hydrogenotrophic microbes to coexist; short-term maximum methane productivity of 2.5 L CH_4 L_{VR}^{-1} d^{-1} was obtained in-situ.
- Below carbon dioxide levels of 9%, conversion of carbon dioxide to methane drastically diminishes.
- Connecting in-situ or ex-situ units in series provides a more favourable pathway as compared to individual single systems.
- A concept of a hybrid model combining in- and ex-situ methanation in full scale suggests an alternative to conventional upgrading systems.

7.3 Recommendations

The thesis successfully demonstrates optimisation strategies in state-of-the-art digestion systems. The cost of biogas production and upgrading can be reduced by implementing novel technology into existing biogas infrastructure. In theory, an ideal biogas plant continuously delivers maximum substrate throughput and methane yields to facilitate peak reactor utilisation, either for CHP use or gas grid injection. As a recommendation of this thesis, such a system could possibly comprise a pre-acidifying hydrolysis reactor, attached to a digester at elevated temperatures stabilised by trace elements and followed by an ex-situ methanation unit.

The two-stage system allows high loadings at short retention times while maintaining excellent substrate degradation leading to higher biogas yields from the same amount of substrate. The upstream solubilisation of COD enables the utilisation of a wide and more complex substrate spectrum. A retention time of 2-4 days at an OLR of 15 g VS L^{-1} d^{-1} is recommended in the upstream hydrolysis reactor to effectively acidify and break down macromolecules into precursors for the methanogens in the second reactor. Longer retention times only marginally contribute to a higher degree of acidification. This digester choice allows feeding upon arrival on site and conservation of highly degradable substrate (such as food waste) in the first reactor; this reduces upfront aerobic storage losses typically found in conventional waste treating facilities. In this scenario, the first reactor may function as both a pre-treatment and storage system for feedstock. This approach essentially decouples the closely linked main process steps of substrate delivery and feeding from methane production.

The off-gas of the hydrolysis reactor may be separated from the biogas produced in the downstream methane reactor. It comprises significant quantities of hydrogen sulphide and thus reduces expenditures on biogas desulphurisation treatments. Furthermore, the upstream segregation of hydrogen sulphide in the hydrolysis reactor mitigates precipitation of trace metals. Therefore, it potentially increases the resilience of the downstream methane formation process to a deficiency in nutrients and favours the associated bioavailability of these required elements. At these intensified conditions additional trace element supplementation is recommended to attain optimum levels in the digestate further stabilising the methane formation

process. The level of trace elements in the digestate should range between 0.05-10 mg L^{-1} for Co, 5-500 mg L^{-1} for Fe, 0.0272-5 mg L^{-1} for Mo, 0.035-10 mg L^{-1} for Ni and 0.056-0.2 mg L^{-1} for Se to sustain stable fermentation.

The downstream methane production can be controlled by a variable feeding rate of pre-acidified substrate. A pulse feeding regime and the associated temporary increase in gas production can facilitate power output to coincide with daily peak electricity prices or complement existing sources of renewable electricity generation. The retention time in the second reactor depends on the substrate kinetics and associated revenue or procurement costs of the substrate. It should remain in the second reactor between 12 and 46 days at an OLR between 5 and 7 g VS L^{-1} d^{-1}. The recommended thermophilic temperature level further stimulates microbial activity, facilitates rapid degradation, reduces viscosity properties of the digestate and therefore provides superior mixing conditions.

A close monitoring of pH, COD, VFA, alcohols, gas composition and flow rate in the first hydrolysis reactor and pH, trace element concentration, VFA, VFA/TIC, NH_4 levels, gas composition and flow rate in the second methane reactor is advised to establish reactor specific operational data and recognise deviations from the norm. In case the process shows signs of overload, it is recommended to reduce the feeding rate or ultimately introduce alkalinity to induce immediate reactor recovery.

The biogas from the acidification reactor consists mainly of carbon dioxide resulting in a biogas with enhanced methane content in the downstream methane reactor. If the energy vector for biogas is biomethane, it is recommended to utilise the hydrolysis gas separately (for example methanation processes) or remove the hydrogen sulphide in an aerobic filter and release the carbon dioxide into the atmosphere. The upstream partial segregation of carbon dioxide facilitates biogas rich in methane in the second reactor. An increase of methane concentrations by an average of 14% to levels of 71% is realistic. Thus, final biogas upgrading is less energy intensive leading to a reduction in associated overall capital and operational costs.

A mismatch between demand and production from fluctuating sources such as wind or photovoltaic may be offset by demand driven electricity sourced from biogas CHP. Moreover, it is suggested to interconnect biogas and biological power to gas into existing energy systems to facilitate a higher penetration of variable renewable

energy. Additional, cheap or otherwise curtailed electricity from intermittent renewable sources is suggested to be utilised in an electrolyser to produce hydrogen in order to facilitate ex-situ biogas upgrading to biomethane. The obtained hydrogen has positive effects on the methanogenic process and is advised to be injected at equimolar levels into an ex-situ methanation unit. At a recommended rate of 15 L H_2 L_{VR}^{-1} d^{-1} it is coupled with carbon dioxide from the biogas or hydrolysis process. Theoretically (if the initial biogas composition was 50% CH_4 and 50% CO_2) the methane production could almost double with carbon dioxide being fully removed and thus facilitating a biomethane ultimately satisfying gas grid injection standards.

As an alternative, a combined hybrid concept of in-situ methanation, followed by an ex-situ methanation unit suggests another upgrading approach. It is recommended to ensure a balanced in-situ system, with adequate levels of hydrogen in solution to allow both, acetogenic and hydrogenotrophic microbes to coexist. The interconnection of biogas and biological power to gas into existing energy systems completes this concept of an integrated biogas systems and enables a change in energy vector from electricity to renewable green decarbonised gas. The upgraded biogas can be stored and withdrawn from the gas grid and utilised for heat, transport and electricity applications.

7.4 Final remarks

In future smart energy systems integrated biogas systems may function as the centrepiece of an interconnected energy system. This will lead to optimised consumption and production of electricity or biomethane on demand while simultaneously changing the energy vector. The obtained performance characteristics of the investigated in-situ and ex-situ methanation strategies show realistic potential to be scaled up to novel cascading upgrading systems. They provide storage capacity for intermittent renewable energies such as wind or photovoltaic within the gas grid. In this scenario, the storage capability of biomethane functions as a "battery" of the electricity grid. Furthermore, the dependency on natural gas imports is reduced, indigenous renewable energy resources are promoted and energy (including for heat and transport) can be decarbonised.

7.5 Future research and developments

Based on the results and conclusions presented in this thesis the following topics have been identified for further research:

1. Assess the benefit of a pre-treating hydrolysis reactor in terms of hydrogen sulphide removal and associated elevation of trace element bioavailability; further investigate the potential as a storage system for feedstock to facilitate demand driven biogas/electricity production.

2. Examine further increases in organic loading rate of a two-stage system at short substrate retention. A substantial increase in loading at short substrate retention facilities cost effective digestion of gate fee associated waste streams.

3. Examine the impact of diffuser units on solubilisation of hydrogen in digestate for methanation processes.

4. Determine long term adequate hydrogen level for stable in-situ methanation. Assess the implications of high viscous digestate on gas residence time, capture of ultra-fine gas bubbles and ultimately on gas to liquid mass transfer.

5. Improve the performance of sequential ex-situ methanation by elevating temperature and pressure levels.

6. Assess the robustness and potential scalability of sequential cascading ex-situ methanation. Propose, price and size a full scale methanation unit based on optimum performance findings at elevated temperature and pressure levels.

References

[1] Agneessens, L.M., Ottosen, L.D.M., Voigt, N.V., Nielsen, J.L., de Jonge, N., Fischer, C.H., Kofoed, M.V.W., 2017. In-situ biogas upgrading with pulse H2 additions: The relevance of methanogen adaption and inorganic carbon level. Bioresour. Technol. 233, 256-263.

[2] Ahring, B.K., 1995. Methanogenesis in thermophilic biogas reactors. Antonie van Leeuwenhoek 67, 91-102.

[3] Alitalo, A., Niskanen, M., Aura, E., 2015. Biocatalytic methanation of hydrogen and carbon dioxide in a fixed bed bioreactor. Bioresour. Technol. 196, 600-605.

[4] Allen, E., Wall, D.M., Herrmann, C., Murphy, J.D., 2016. A detailed assessment of resource of biomethane from first, second and third generation substrates. Renew. Energy 87, Part 1, 656-665.

[5] Amnuaycheewa, P., Hengaroonprasan, R., Rattanaporn, K., Kirdponpattara, S., Cheenkachorn, K., Sriariyanun, M., 2016. Enhancing enzymatic hydrolysis and biogas production from rice straw by pretreatment with organic acids. Industrial Crops and Products 87, 247-254.

[6] Angelidaki, I., Ahring, B.K., 1994. Anaerobic thermophilic digestion of manure at different ammonia loads: Effect of temperature. Water Res. 28, 727-731.

[7] Angelidaki, I., Treu, L., Tsapekos, P., Luo, G., Campanaro, S., Wenzel, H., Kougias, P.G., 2018. Biogas upgrading and utilization: Current status and perspectives. Biotechnol. Adv. 36, 452-466.

[8] Argelier, S., Delgenes, J.-P., Moletta, R., 1998. Design of acidogenic reactors for the anaerobic treatment of the organic fraction of solid food waste. Bioprocess Eng. 18, 309-315.

[9] Banks, C.J., Heaven, S., 2013. 6 - Optimisation of biogas yields from anaerobic digestion by feedstock type, in: Wellinger, A., Murphy, J., Baxter, D. (Eds.), The Biogas Handbook. Woodhead Publishing, pp. 131-165.

[10] Banks, C.J., Zhang, Y., Jiang, Y., Heaven, S., 2012. Trace element requirements for stable food waste digestion at elevated ammonia concentrations. Bioresour. Technol. 104, 127-135.

[11] Bassani, I., Kougias, P.G., Angelidaki, I., 2016. In-situ biogas upgrading in thermophilic granular UASB reactor: key factors affecting the hydrogen mass transfer rate. Bioresour. Technol. 221, 485-491.

[12] Bochmann, G., Montgomery, L., 2013. Storage and pre-treatment of substrates for biogas production, in: Wellinger, A., Murphy, J.D., Baxter, D. (Eds.), The biogas handbook, vol. 52. Woodhead Publishing, Oxford, Cambridge, Philadelphia, New Delhi, pp. 95-96.

[13] Bouallagui, H., Torrijos, M., Godon, J.J., Moletta, R., Ben Cheikh, R., Touhami, Y., Delgenes, J.P., Hamdi, M., 2004. Two-phases anaerobic digestion of fruit and vegetable wastes: bioreactors performance. Biochem. Eng. J. 21, 193-197.

[14] Browne, J.D., Allen, E., Murphy, J.D., 2014. Assessing the variability in biomethane production from the organic fraction of municipal solid waste in batch and continuous operation. Appl. Energy 128, 307-314.

[15] Browne, J.D., Murphy, J.D., 2014b. The impact of increasing organic loading in two phase digestion of food waste. Renew. Energy 71, 69-76.

[16] Burkhardt, M., Busch, G., 2013. Methanation of hydrogen and carbon dioxide. Appl. Energy 111, 74-79.

[17] Burkhardt, M., Koschack, T., Busch, G., 2015. Biocatalytic methanation of hydrogen and carbon dioxide in an anaerobic three-phase system. Bioresour. Technol. 178, 330-333.

[18] Chen, X., Yuan, H., Zou, D., Liu, Y., Zhu, B., Chufo, A., Jaffar, M., Li, X., 2015. Improving biomethane yield by controlling fermentation type of acidogenic phase in two-phase anaerobic co-digestion of food waste and rice straw. Chem. Eng. J. 273, 254-260.

[19] Chinellato, G., Cavinato, C., Bolzonella, D., Heaven, S., Banks, C.J., 2013. Biohydrogen production from food waste in batch and semi-continuous conditions: Evaluation of a two-phase approach with digestate recirculation for pH control. Int. J. Hydrogen Energy 38, 4351-4360.

[20] Climenhaga, M., Banks, C., 2008. Anaerobic digestion of catering wastes: effect of micronutrients and solids retention time. Water Sci. Technol. 57, 687-692.

[21] De La Rubia, M.A., Raposo, F., Rincón, B., Borja, R., 2009. Evaluation of the hydrolytic–acidogenic step of a two-stage mesophilic anaerobic digestion process of sunflower oil cake. Bioresour. Technol. 100, 4133-4138.

[22] Demirel, B., Scherer, P., 2011. Trace element requirements of agricultural biogas digesters during biological conversion of renewable biomass to methane. Biomass Bioenergy 35, 992-998.

[23] Deppenmeier, U., 2002. Redox-driven proton translocation in methanogenic Archaea. Cellular and Molecular Life Sciences CMLS 59, 1513-1533.

[24] Diekert, G., Jaenchen, R., Thauer, R.K., 1980. Biosynthetic evidence for a nickel tetrapyrrole structure of factor F430 from Methanobacterium thermoautotrophicum. FEBS Letters 119, 118-120.

[25] Drosg, B. 2013. Process monitoring in biogas plants. IEA Bioenergy Task.

[26] EC, 2009. Decision No 406/2009/EC of the European Parliament and of the Council of 23 April 2009 on the effort of Member States to reduce their greenhouse gas emissions to meet the Community's greenhouse gas emission reduction commitments up to 2020. Official Journal of the European Union, Brussels, Belgium.

[27] European Commission, 2015. Moving towards a circular economy (Retrieved 03-10-2015). Available from: <http://ec.europa.eu/environment/circular-economy/index_en.htm>.

[28] Fermoso, F.G., Bartacek, J., Jansen, S., Lens, P.N.L., 2009. Metal supplementation to UASB bioreactors: from cell-metal interactions to full-scale application. Science of The Total Environment 407, 3652-3667.

[29] Franke-Whittle, I.H., Walter, A., Ebner, C., Insam, H., 2014. Investigation into the effect of high concentrations of volatile fatty acids in anaerobic digestion on methanogenic communities. Waste Manage. 34, 2080-2089.

[30] Fukuzaki, S., Nishio, N., Shobayashi, M., Nagai, S., 1990. Inhibition of the Fermentation of Propionate to Methane by Hydrogen, Acetate, and Propionate. Appl. Environ. Microbiol. 56, 719-723.

[31] Guneratnam, A.J., Ahern, E., FitzGerald, J.A., Jackson, S.A., Xia, A., Dobson, A.D.W., Murphy, J.D., 2017. Study of the performance of a thermophilic biological methanation system. Bioresour. Technol. 225, 308-315.

[32] Guo, X.M., Trably, E., Latrille, E., Carrère, H., Steyer, J.-P., 2010. Hydrogen production from agricultural waste by dark fermentation: A review. Int. J. Hydrogen Energy 35, 10660-10673.

[33] Gustavsson, J., Shakeri Yekta, S., Karlsson, A., Skyllberg, U., Svensson, B.H., 2011. Bioavailability and chemical forms of Co and Ni in the biogasprocess: an evaluation based on sequential and acid volatile sulfide extractions. Linköping University. Department of Thematic Studies, Water and Environmental Studies.

[34] Gustavsson, J., Shakeri Yekta, S., Sundberg, C., Karlsson, A., Ejlertsson, J., Skyllberg, U., Svensson, B.H., 2013. Bioavailability of cobalt and nickel during anaerobic digestion of sulfur-rich stillage for biogas formation. Appl. Energy 112, 473-477.

[35] Gustavsson, J., Svensson, B., Karlsson, A., 2011. The feasibility of trace element supplementation for stable operation of wheat stillage-fed biogas tank reactors. Water Sci. Technol. 64, 320-325.

[36] Guwy, A.J., Dinsdale, R.M., Kim, J.R., Massanet-Nicolau, J., Premier, G., 2011. Fermentative biohydrogen production systems integration. Bioresour. Technol. 102, 8534-8542.

[37] Herrmann, C., FitzGerald, J., O'Shea, R., Xia, A., O'Kiely, P., Murphy, J.D., 2015. Ensiling of seaweed for a seaweed biofuel industry. Bioresour. Technol. 196, 301-313.

[38] Jiang, Y., Banks, C., Zhang, Y., Heaven, S., Longhurst, P., 2018. Quantifying the percentage of methane formation via acetoclastic and syntrophic acetate oxidation pathways in anaerobic digesters. Waste Management 71, 749-756.

[39] Karakashev, D., Batstone, D.J., Angelidaki, I., 2005. Influence of environmental conditions on methanogenic compositions in anaerobic biogas reactors. Applied and Environmental Microbiology 71, 331-338.

[40] Karlsson, A., Einarsson, P., Schnürer, A., Sundberg, C., Ejlertsson, J., Svensson, B.H., 2012. Impact of trace element addition on degradation efficiency of volatile fatty acids, oleic acid and phenyl acetate and on microbial populations in a biogas digester. J. Biosci. Bioeng. 114, 446-452.

[41] Karlsson, A., Vallin, L., Ejlertsson, J., 2008. Effects of temperature, hydraulic retention time and hydrogen extraction rate on hydrogen production from the

fermentation of food industry residues and manure. Int. J. Hydrogen Energy 33, 953-962.

[42] Kida, K., Shigematsu, T., Kijima, J., Numaguchi, M., Mochinaga, Y., Abe, N., Morimura, S., 2001. Influence of Ni2+ and Co2+ on methanogenic activity and the amounts of coenzymes involved in methanogenesis. J. Biosci. Bioeng. 91, 590-595.

[43] Koch, K., Wichern, M., Lübken, M., Horn, H., 2009. Mono fermentation of grass silage by means of loop reactors. Bioresour. Technol. 100, 5934-5940.

[44] Kougias, P.G., Treu, L., Benavente, D.P., Boe, K., Campanaro, S., Angelidaki, I., 2017. Ex-situ biogas upgrading and enhancement in different reactor systems. Bioresour. Technol. 225, 429-437.

[45] Kraakman, N.J.R., Rocha-Rios, J., van Loosdrecht, M.C.M., 2011. Review of mass transfer aspects for biological gas treatment. Appl. Microbiol. Biotechnol. 91, 873.

[46] Kumar, G., Bakonyi, P., Periyasamy, S., Kim, S.H., Nemestóthy, N., Bélafi-Bakó, K., 2015. Lignocellulose biohydrogen: Practical challenges and recent progress. Renewable and Sustainable Energy Reviews 44, 728-737.

[47] Lecker, B., Illi, L., Lemmer, A., Oechsner, H., 2017. Biological hydrogen methanation – A review. Bioresour. Technol. 245, 1220-1228.

[48] Lemmer, A., Vintiloiu, A., Preißler, D., Bastam, C., Bäuerle, L., Oechsner, H., Mathies, E., Ramhold, D., 2010. Untersuchungen zum Einsatz von Mineralstoffen in Biogasanlagen. Gülzower Fachgespräche 35, 83-84.

[49] Li, J., Zheng, G., He, J., Chang, S., Qin, Z., 2009. Hydrogen-producing capability of anaerobic activated sludge in three types of fermentations in a continuous stirred-tank reactor. Biotechnol. Adv. 27, 573-577.

[50] Linke, B., Mähnert, P., 2005. Biogasgewinnung aus Rindergülle und nachwachsenden Rohstoffen-Einfluss der Belastung des Fermenters. Agrartechnische Forschung 11.

[51] Liu, R., Hao, X., Wei, J., 2016. Function of homoacetogenesis on the heterotrophic methane production with exogenous H2/CO2 involved. Chem. Eng. J. 284, 1196-1203.

[52] Liu, X., Li, R., Ji, M., Han, L., 2013. Hydrogen and methane production by co-digestion of waste activated sludge and food waste in the two-stage

fermentation process: Substrate conversion and energy yield. Bioresour. Technol. 146, 317-323.

[53] Luo, G., Angelidaki, I., 2013a. Co-digestion of manure and whey for in situ biogas upgrading by the addition of H2: process performance and microbial insights. Appl. Microbiol. Biotechnol. 97, 1373-1381.

[54] Luo, G., Angelidaki, I., 2013b. Hollow fiber membrane based H(2) diffusion for efficient in situ biogas upgrading in an anaerobic reactor. Appl. Microbiol. Biotechnol. 97, 3739-44.

[55] Luo, G., Angelidaki, I., 2012b. Integrated biogas upgrading and hydrogen utilization in an anaerobic reactor containing enriched hydrogenotrophic methanogenic culture. Biotechnol. Bioeng. 109, 2729-2736.

[56] Luo, G., Johansson, S., Boe, K., Xie, L., Zhou, Q., Angelidaki, I., 2012a. Simultaneous hydrogen utilization and in situ biogas upgrading in an anaerobic reactor. Biotechnol. Bioeng. 109, 1088-1094.

[57] Luo, G., Xie, L., Zhou, Q., Angelidaki, I., 2011. Enhancement of bioenergy production from organic wastes by two-stage anaerobic hydrogen and methane production process. Bioresour. Technol. 102, 8700-8706.

[58] Luo, G., Xie, L., Zou, Z., Wang, W., Zhou, Q., Shim, H., 2010. Anaerobic treatment of cassava stillage for hydrogen and methane production in continuously stirred tank reactor (CSTR) under high organic loading rate (OLR). Int. J. Hydrogen Energy 35, 11733-11737.

[59] Mackie, R.I., Bryant, M.P., 1981. Metabolic Activity of Fatty Acid-Oxidizing Bacteria and the Contribution of Acetate, Propionate, Butyrate, and CO(2) to Methanogenesis in Cattle Waste at 40 and 60°C. Appl. Environ. Microbiol. 41, 1363-1373.

[60] Mähnert, P., 2007. Kinetik der Biogasproduktion aus nachwachsenden Rohstoffen und Gülle, Humboldt-Universität zu Berlin. Landwirtschaftlich-Gärtnerische Fakultät.

[61] Mähnert, P., Heiermann, M., Linke, B., 2005. Batch-and semi-continuous biogas production from different grass species. Agric. Eng. Int.s: CIGR Journal 7, manuscript EE 05 010.

[62] Martin, M.R., Fornero, J.J., Stark, R., Mets, L., Angenent, L.T., 2013. A single-culture bioprocess of Methanothermobacter thermautotrophicus to

upgrade digester biogas by CO2 -to-CH4 conversion with H2. Archaea 2013, 157529.

[63] Massanet-Nicolau, J., Dinsdale, R., Guwy, A., Shipley, G., 2013. Use of real time gas production data for more accurate comparison of continuous single-stage and two-stage fermentation. Bioresour. Technol. 129, 561-567.

[64] Massanet-Nicolau, J., Dinsdale, R., Guwy, A., Shipley, G., 2015. Utilising biohydrogen to increase methane production, energy yields and process efficiency via two stage anaerobic digestion of grass. Bioresour. Technol. 189, 379-383.

[65] McEniry, J., Crosson, P., Finneran, E., McGee, M., Keady, T., O'Kiely, P., 2013. How much grassland biomass is available in Ireland in excess of livestock requirements? Irish J. Agric. Food. Res., 67-80.

[66] Moestedt, J., Nordell, E., Shakeri Yekta, S., Lundgren, J., Martí, M., Sundberg, C., Ejlertsson, J., Svensson, B.H., Björn, A., 2016. Effects of trace element addition on process stability during anaerobic co-digestion of OFMSW and slaughterhouse waste. Waste Manage. 47, 11-20.

[67] Mulat, D.G., Mosbæk, F., Ward, A.J., Polag, D., Greule, M., Keppler, F., Nielsen, J.L., Feilberg, A., 2017. Exogenous addition of H2 for an in situ biogas upgrading through biological reduction of carbon dioxide into methane. Waste Manage. 68, 146-156.

[68] Murphy, J.D., McKeogh, E., 2004. Technical, economic and environmental analysis of energy production from municipal solid waste. Renew. Energy 29, 1043-1057.

[69] Murphy, J.D., Power, N.M., 2009. An argument for using biomethane generated from grass as a biofuel in Ireland. Biomass Bioenergy 33, 504-512.

[70] Murphy, J.D., Power, N.M., 2006. A technical, economic and environmental comparison of composting and anaerobic digestion of biodegradable municipal waste. J. Environ. Sci. Health., Part A 41, 865-879.

[71] Myszograj, S., Stadnik, A., Płuciennik-Koropczuk, E., 2018. The Influence of Trace Elements on Anaerobic Digestion Process. 28, 105.

[72] Nges, I.A., Björn, A., Björnsson, L., 2012. Stable operation during pilot-scale anaerobic digestion of nutrient-supplemented maize/sugar beet silage. Bioresour. Technol. 118, 445-454.

[73] Nizami, A.-S., Murphy, J.D., 2010. What type of digester configurations should be employed to produce biomethane from grass silage? Renew. Sustainable Energy Rev. 14, 1558-1568.

[74] Nizami, A.S., Orozco, A., Groom, E., Dieterich, B., Murphy, J.D., 2012. How much gas can we get from grass? Appl. Energy 92, 783-790.

[75] Nordell, E., Nilsson, B., Nilsson Påledal, S., Karisalmi, K., Moestedt, J., 2016. Co-digestion of manure and industrial waste – The effects of trace element addition. Waste Manage. 47, 21-27.

[76] Nordmann, W., 1977. Die Überwachung der Schlammfaulung. KA-Inform. Betr. Pers. Beil. Korr. Abw. 3, 77.

[77] O'Shea, R., Wall, D.M., McDonagh, S., Murphy, J.D., 2017. The potential of power to gas to provide green gas utilising existing CO2 sources from industries, distilleries and wastewater treatment facilities. Renew. Energy 114, 1090-1100.

[78] O'Shea, R., Wall, D., Murphy, J.D., 2016. Modelling a demand driven biogas system for production of electricity at peak demand and for production of biomethane at other times. Bioresour. Technol. 216, 238-249.

[79] Orgill, J.J., Atiyeh, H.K., Devarapalli, M., Phillips, J.R., Lewis, R.S., Huhnke, R.L., 2013. A comparison of mass transfer coefficients between trickle-bed, hollow fiber membrane and stirred tank reactors. Bioresour. Technol. 133, 340-346.

[80] Orozco, A.M., Nizami, A.S., Murphy, J.D., Groom, E., 2013. Optimizing the thermophilic hydrolysis of grass silage in a two-phase anaerobic digestion system. Bioresour. Technol. 143, 117-125.

[81] Ortner, M., Rachbauer, L., Somitsch, W., Fuchs, W., 2014. Can bioavailability of trace nutrients be measured in anaerobic digestion? Appl. Energy 126, 190-198.

[82] Ortner, M., Rameder, M., Rachbauer, L., Bochmann, G., Fuchs, W., 2015. Bioavailability of essential trace elements and their impact on anaerobic digestion of slaughterhouse waste. Biochem. Eng. J. 99, 107-113.

[83] Pobeheim, H., Munk, B., Lindorfer, H., Guebitz, G.M., 2011. Impact of nickel and cobalt on biogas production and process stability during semi-

continuous anaerobic fermentation of a model substrate for maize silage. Water Res. 45, 781-787.

[84] Qiang, H., Lang, D.-L., Li, Y.-Y., 2012. High-solid mesophilic methane fermentation of food waste with an emphasis on Iron, Cobalt, and Nickel requirements. Bioresour. Technol. 103, 21-27.

[85] Rachbauer, L., Voitl, G., Bochmann, G., Fuchs, W., 2016. Biological biogas upgrading capacity of a hydrogenotrophic community in a trickle-bed reactor. Appl. Energy 180, 483-490.

[86] Rittmann, S., Seifert, A., Herwig, C., 2015. Essential prerequisites for successful bioprocess development of biological CH4 production from CO2 and H2. Crit. Rev. Biotechnol. 35, 141-151.

[87] Savvas, S., Donnelly, J., Patterson, T., Dinsdale, R., Esteves, S.R., 2017. Closed nutrient recycling via microbial catabolism in an eco-engineered self regenerating mixed anaerobic microbiome for hydrogenotrophic methanogenesis. Bioresour. Technol. 227, 93-101.

[88] Schmidt, T., Nelles, M., Scholwin, F., Pröter, J., 2014. Trace element supplementation in the biogas production from wheat stillage – Optimization of metal dosing. Bioresour. Technol. 168, 80-85.

[89] Seifert, A.H., Rittmann, S., Herwig, C., 2014. Analysis of process related factors to increase volumetric productivity and quality of biomethane with Methanothermobacter marburgensis. Appl. Energy 132, 155-162.

[90] Seppälä, M., Paavola, T., Lehtomäki, A., Rintala, J., 2009. Biogas production from boreal herbaceous grasses – Specific methane yield and methane yield per hectare. Bioresour. Technol. 100, 2952-2958.

[91] Shen, F., Yuan, H., Pang, Y., Chen, S., Zhu, B., Zou, D., Liu, Y., Ma, J., Yu, L., Li, X., 2013. Performances of anaerobic co-digestion of fruit & vegetable waste (FVW) and food waste (FW): Single-phase vs. two-phase. Bioresour. Technol. 144, 80-85.

[92] Singh, A., Nizami, A.-S., Korres, N.E., Murphy, J.D., 2011. The effect of reactor design on the sustainability of grass biomethane. Renew. Sustainable Energy Rev. 15, 1567-1574.

[93] Smyth, B.M., Murphy, J.D., O'Brien, C.M., 2009. What is the energy balance of grass biomethane in Ireland and other temperate northern European climates? Renew. Sustainable Energy Rev. 13, 2349-2360.

[94] Strübing, D., Huber, B., Lebuhn, M., Drewes, J.E., Koch, K., 2017. High performance biological methanation in a thermophilic anaerobic trickle bed reactor. Bioresour. Technol. 245, 1176-1183.

[95] Thamsiriroj, T., Nizami, A.S., Murphy, J.D., 2012. Why does mono-digestion of grass silage fail in long term operation? Appl. Energy 95, 64-76.

[96] Thauer, R.K., Kaster, A.-K., Seedorf, H., Buckel, W., Hedderich, R., 2008. Methanogenic archaea: ecologically relevant differences in energy conservation. Nature Reviews Microbiology 6, 579.

[97] Uemura, S., 2010. Mineral requirements for mesophilic and thermophilic anaerobic digestion of organic solid waste. Int. J. Environ. Res., 33-40.

[98] Ullrich, T., Lindner, J., Bär, K., Mörs, F., Graf, F., Lemmer, A., 2018. Influence of operating pressure on the biological hydrogen methanation in trickle-bed reactors. Bioresour. Technol. 247, 7-13.

[99] VDI, V.D.I., 2006. 4630: Fermentation of organic materials, characterisation of the substrate, sampling, collection of material data, fermentation tests. Verein Deutscher Ingenieure (VDI), editor. VDI Handbuch Energietechnik. Berlin: Beuth Verlag GmbH, 44-59.

[100] Voelklein, M.A., Jacob, A., O' Shea, R., Murphy, J.D., 2016a. Assessment of increasing loading rate on two-stage digestion of food waste. Bioresour. Technol. 202, 172-180.

[101] Voelklein, M.A., O' Shea, R., Jacob, A., Murphy, J.D., 2017. Role of trace elements in single and two-stage digestion of food waste at high organic loading rates. Energy 121, 185-192.

[102] Voelklein, M.A., Rusmanis, D., Murphy, J.D., 2016. Increased loading rates and specific methane yields facilitated by digesting grass silage at thermophilic rather than mesophilic temperatures. Bioresour. Technol. 216, 486-493.

[103] Waechter, M., 2012. Tabellenbuch der Chemie, Weinheim: Wiley-VCH.

[104] Wall, D.M., Allen, E., O'Shea, R., O'Kiely, P., Murphy, J.D., 2016. Investigating two-phase digestion of grass silage for demand-driven biogas

applications: Effect of particle size and rumen fluid addition. Renew. Energy 86, 1215-1223.

[105] Wall, D.M., Allen, E., Straccialini, B., O'Kiely, P., Murphy, J.D., 2014a. The effect of trace element addition to mono-digestion of grass silage at high organic loading rates. Bioresour. Technol. 172, 349-355.

[106] Wall, D.M., Allen, E., Straccialini, B., O'Kiely, P., Murphy, J.D., 2014. The effect of trace element addition to mono-digestion of grass silage at high organic loading rates. Bioresour. Technol. 172, 349-355.

[107] Wall, D.M., Allen, E., Straccialini, B., O'Kiely, P., Murphy, J.D., 2014b. Optimisation of digester performance with increasing organic loading rate for mono- and co-digestion of grass silage and dairy slurry. Bioresour. Technol. 173, 422-428.

[108] Wall, D.M., McDonagh, S., Murphy, J.D., 2017. Cascading biomethane energy systems for sustainable green gas production in a circular economy. Bioresour. Technol. 243, 1207-1215.

[109] Wall, D.M., O'Kiely, P., Murphy, J.D., 2013. The potential for biomethane from grass and slurry to satisfy renewable energy targets. Bioresour. Technol. 149, 425-431.

[110] Ward, A.J., Hobbs, P.J., Holliman, P.J., Jones, D.L., 2008. Optimisation of the anaerobic digestion of agricultural resources. Bioresour. Technol. 99, 7928-7940.

[111] Xie, S., Lawlor, P.G., Frost, J.P., Hu, Z., Zhan, X., 2011. Effect of pig manure to grass silage ratio on methane production in batch anaerobic co-digestion of concentrated pig manure and grass silage. Bioresour. Technol. 102, 5728-5733.

[112] Yirong, C., Heaven, S., Banks, C.J., 2014. Effect of a trace element addition strategy on volatile fatty acid accumulation in thermophilic anaerobic digestion of food waste. Waste Biomass Valorization 6, 1-12.

[113] Yirong, C., Zhang, W., Heaven, S., Banks, C.J., 2017. Influence of ammonia in the anaerobic digestion of food waste. Journal of Environmental Chemical Engineering 5, 5131-5142.

[114] Zhang, L., Jahng, D., 2012. Long-term anaerobic digestion of food waste stabilized by trace elements. Waste Manage. 32, 1509-1515.

[115] Zhang, L., Ouyang, W., Lia, A., 2012. Essential Role of Trace Elements in Continuous Anaerobic Digestion of Food Waste. Procedia Environ. Sci. 16, 102-111.

[116] Zhang, W., Wu, S., Guo, J., Zhou, J., Dong, R., 2015. Performance and kinetic evaluation of semi-continuously fed anaerobic digesters treating food waste: Role of trace elements. Bioresour. Technol. 178, 297-305.

[117] Zhang, Y., Zhang, Z., Suzuki, K., Maekawa, T., 2003. Uptake and mass balance of trace metals for methane producing bacteria. Biomass Bioenergy 25, 427-433.

[118] Zhang, Y., Zhang, Z., Suzuki, K., Maekawa, T., 2003. Uptake and mass balance of trace metals for methane producing bacteria. Biomass and Bioenergy 25, 427-433.

[119] Zhou, X., Meile, L., Kreuzer, M., Zeitz, J.O., 2013. The Effect of Saturated Fatty Acids on Methanogenesis and Cell Viability of Methanobrevibacter ruminantium. Archaea 2013, 106916.

Appendix A. Laboratory analysis methods

Analysis of trace elements

All metal elements except selenium were analysed according to DIN EN ISO 11885 with inductively coupled plasma optical emission spectrometry (ICP-OES); selenium was determined according to DIN EN ISO 17294-2 (E29) with inductively coupled plasma mass spectrometry (ICP-MS).

Analysis of VFA/TIC ratio

VFA/TIC (ratio of volatile fatty acids to buffering capacity) was measured according to the Nordmann-method using 0.1 N sulphuric acid (Nordmann, 1977); a two point titration method (endpoints 5.0 pH and 4.4 pH) used as a guide in assessing the stability of the anaerobic digestion process. The titration has been facilitated by a Titronic Universal Automatic Titrator. Ratios below 0.3 are indicative of a stable process (Drosg, 2013).

Analysis of sCOD

Soluble chemical oxygen demand (sCOD) was determined using Hach Lange cuvette tests (LCK 914) and evaluated by a DR3900 Hach Lange Spectrophotometer. Samples were centrifuged at 15,000 rpm for 10 minutes prior to testing.

Analysis of ammonia

Total ammoniacal nitrogen (TAN) were analysed using Hach Lange cuvette tests (LCK 313). The concentration of ammonia in the solution was measured using a Hach-Lange DR3900 spectrophotometer.

Analysis of pH

The pH value was measured using a pH meter (Jenway 3510) and calibrated before usage.

Analysis of volatile and total solids

The total solids and volatile solids were determined according to Standard Methods 2540 G. The TS contents were determined by drying the samples at 105 °C for 24 h. VS contents were analysed by burning the dried samples two hours at 550 °C.

Biogas flow

Biogas flow from each reactor was measured by using a water displacement mechanism. A certain amount of gas passes through a tipping mechanism, displaces the volume of water in a pre-defined chamber till it floats and releases the gas. Every release generates a digital impulse, which represents the displaced gas volume in the chamber. The volume of the gas chamber was validated by establishing means of 10 consecutive syringe strokes, considering only the actual volume of gases entering the chamber. The measured biogas volume was adjusted to the volume at standard temperature (273K) and pressure (1013mbar).

Gas flows were also measured by using a Ritter drum type gas meter TG5/5 and digital mass flow meters Voegtlin compact regulator GCR. The measured gas volume was adjusted to the volume at standard temperature (273 K) and pressure (1013 mbar).

Elemental analysis

Elemental analysis samples were analysed in triplicate for C, H, N and O with an elemental analyser using a thermal conductivity detector (Exeter Analytical, CE 440 Model). The samples were analysed in accordance with the SOP provided by the manufacturer Exeter Analytical. The C/N ratio of samples was calculated as the elemental carbon content divided by the elemental nitrogen content.

Gas chromatographic analysis of biogas composition

Biogas composition was analysed for O_2, N_2, CH_4, H_2 and CO_2 using a gas chromatograph (Hewlett Packard HP6890) equipped with a dual column system comprising a Hayesep Q and Molsieve 13x (Mesh range 80-100). The injected gas volume was 1 μL with a split ratio of 10:1. The injector temperature was set at 200 °C. Argon was used as the carrier gas at a constant flow of 15 mL min^{-1}. The inlet is maintained at 80 ^{0}C. The column temperature was initially maintained at 60 °C for 4 min. The slope of the temperature gradient was 10 ^{0}C min^{-1} until reaching 80 ^{0}C. The oven was maintained at 80 ^{0}C for 4.5min. The gases entered a thermal conductivity detector (TCD) detector operating at 250 ^{0}C at a reference flow

of 30 mL min^{-1}. Certified gas standards were employed for the standardization of hydrogen, methane and carbon dioxide, based on a calibration forced through zero.

Gas chromatographic analysis of volatile fatty acid, lactic acid and alcohols

The concentrations of individual volatile fatty acids were analysed with gas chromatography (Hewlett Packard HP6890) using a Nukol^{TM} fused silica capillary column (30 m × 0.25 mm × 0.25 μm) and a flame ionization detector. Hydrogen was used as a carrier gas. The inlets were heated to 200 ^{0}C. Sample sizes of 10 μL were injected. The oven starts with a temperature of 75 ^{0}C (maintained for 1 minute). It is further raised by 16 ^{0}C min^{-1} to reach 185 ^{0}C at 7.88 min; this marks the end of the run. Solutes exiting the column during the run enter the FID detector (250 ^{0}C). Three standard solutions containing 50, 250, 500 and 1000 mg l^{-1} of acetic, propionic, (iso-) butyric, (iso-valeric) acids were used for VFA calibration. A standard solution was run within every sampling array to cross validate results.

Lactic acid and ethanol were determined by high performance liquid chromatography (HPLC) using an Agilent 1200 HPLC system with a refractive index detector. An Agilent Hi-Plex H 300x7.7mm Column is used with 0.01N H_2SO_4 as the elution fluid, at a flow rate of 0.6ml/min. The temperature of the column is maintained at 65°C. 20 μL of sample was injected.